

https://dspace.org/

The atmospheric nitrogen budget over the South African Highveld

Ferguson, Kirsten Sheena

2010-03-15T10:28:33Z
http://hdl.handle.net/10539/7677

Downloaded from a DSpace repository. https://dspace.org/

School of Geography, Archaeology and Environmental Studies
University of the Witwatersrand, Johannesburg

THE ATMOSPHERIC NITROGEN BUDGET OVER THE SOUTH AFRICAN HIGHVELD

Kirsten Sheena Ferguson
Student number: 0314298G

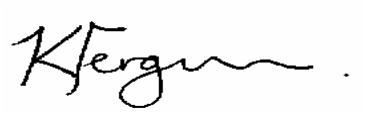
Supervisors: Dr Stuart Piketh
Dr Kristy Ross

A dissertation submitted to the Faculty of Science, University of the Witwatersrand, in fulfilment of the requirements for the degree of Master of Science

Johannesburg, September 2009

DECLARATION

I declare that this dissertation is my own unaided work. It is being submitted for the degree of Master of Science in the School of Geography, Archaeology and Environmental Studies at the University of the Witwatersrand, Johannesburg. It has not been submitted previously for any degree or examination in any other university.



(Kirsten Ferguson)

16th day of September 2009

ABSTRACT

Molecular nitrogen is a highly abundant element in the atmosphere; it is stable and not very reactive. Anthropogenic activities have caused greater concentrations of nitrogen-containing compounds that are highly reactive and ultimately toxic. Reactive nitrogen concentrations have become a growing concern on the South African Highveld, with satellite images indicating very high nitrogen dioxide concentrations in the region. This study investigates the nitrogen budget on the Highveld through the analysis of the nitrogen species emitted into the atmosphere on a temporal scale as well as the atmospheric conversion, transport and removal of these species. Data was collected at Elandsfontein monitoring site, which is centrally located on the industrialised Highveld. The formation and interaction of nitric oxide (NO), nitrogen dioxide (NO_2), and nitrate (NO_3) are a major focus in the study. NO_x concentrations are higher in winter (6.5 to 8.5 $\mu g.m^{-3}$) as a result of stable atmospheric conditions. NO_3 concentrations also peak during winter (3.5 to 5.5 $\mu g.m^{-3}$), with a distinct biomass burning peak during July and August. Diurnally, NO_x concentrations indicate a tall-stack industrial source, with concentrations peaking at midday. NO_3 concentrations are higher at night and lower during the day, as during the day the NO_3 radical is rapidly photolysed and nitrates cannot be produced. Case studies indicate that the conversion rate of NO to NO_2 is highly variable as a result of varying atmospheric factors. These rates range from 11% to 59% per hour. Rates of dry deposition of NO, NO_2 and NO_3 are generally higher during winter as a result of higher concentrations and increased atmospheric stability, which prevents transport out of the region. Nitrogen is predominantly deposited as NO_2 throughout the year, except during spring when NO_3 deposition dominates. The total amount of nitrogen deposited to the Mpumalanga Highveld region is in the range of 6.7 to 13.1 kg ha^{-1} yr^{-1}, which is well below the stipulated critical load value. Such deposition therefore does not pose significant threats to the natural environment on the Highveld. Between 4% and 14% of the total emitted nitrogen on the Highveld is deposited to the surface via wet and dry deposition. The remainder stays in the atmosphere and is advected out of the region.

Keywords: *Nitrogen oxides, nitrate, diurnal variations, seasonal variations, atmospheric conversion, deposition.*

PREFACE

Anthropogenic activities have greatly disrupted the natural nitrogen cycle, via the emission of reactive and sometimes toxic nitrogen-containing compounds. Fossil fuel combustion, increased numbers of motor vehicles, domestic coal combustion and agricultural activities are the main contributors to these emissions. Biomass burning is the largest natural disruptor to this cycle. Such disruptions lead to dire impacts on ecosystems and human health (Galloway, 1998; Olivier *et al*., 1998).

In the South African context various small-scale atmospheric nitrogen studies have been conducted. In terms of a large-scale area like that of the Mpumalanga Highveld, a relatively comprehensive understanding of the sulphur budget has been acquired (Igbafe, 2007). Various sulphur deposition studies have also been performed by Zunckel *et al*. over the years. Limited knowledge on nitrogen characterises on the Highveld provide the necessity for further research in the field.

For this study, the atmospheric nitrogen budget on the Mpumalanga Highveld was evaluated. The specific aims of the study include: assessing the atmospheric temporal variations of the different nitrogen species, calculating the rate of conversion of the species in the atmosphere and determining in what form and quantity nitrogen is deposited to the surface on the Highveld.

The site utilised for the study is Elandsfontein monitoring station, which forms part of Eskom's air quality monitoring network. It has been operational since 1983 and various monitoring campaigns have been performed at the site, providing the perfect platform for comparisons with other studies. Elandsfontein is one of the monitoring stations that is involved in the international aerosol campaign known as EUCAARI (European Integrated Project on Cloud Climate and Air Quality Interactions). Other EUCAARI sites are located in India, China and Brazil, which all contain similar instrumentation allowing for comparisons between sites. The overall objective of EUCAARI is to reduce the current uncertainty in the impact of aerosol particles on climate by 50% and to quantify the relationship between anthropogenic aerosol particles and regional air quality.

This dissertation is divided into six chapters. **Chapter one** provides a basis for the study, presenting some background information together with the aims and objectives of the study. **Chapter two** is a literature review providing the basic background information on nitrogen chemistry, sources, transportation, depositional processes as well as environmental and health effects. **Chapter three** presents the data and methodology used in the study. **Chapter four** examines the seasonal and diurnal variations in nitrogen concentrations. The dependence of these concentrations on wind direction is also discussed. **Chapter five** presents the results of the atmospheric conversion and deposition rate calculations. **Chapter six** is the final chapter presenting the pertinent conclusions of the study.

Sections of this dissertation have been presented at the National Association for Clean Air conference held in Nelspruit in October 2008 as well as at various air quality workshops hosted by both Eskom and the Department of Environmental Affairs and Tourism (DEAT).

The author wishes to thank Eskom Sustainability and Innovation for the use of the data from the Elandsfontein air quality monitoring station. Thanks to Eric Lynch, Neil Snow and Anselm Igbafe for the maintenance and calibrations performed at the site during the study period. Extended thanks are given to Dr Kristy Ross, co-supervisor, for her ongoing support, input and assistance with data analysis throughout this study. Many thanks to Dr Stuart Piketh, primary supervisor, for his guidance and opportunities provided throughout the duration of this project. Finally, thank you to Stephen Broccardo, Roelof Burger and other members of the Climatology Research Group for their assistance and input with data analysis and interpretation during the study.

CONTENTS

Declaration i
Abstract ii
Preface iii
Contents v
List of Figures vii
List of tables x
Abbreviations and Acronyms xi
CHAPTER 1: INTRODUCTION 1
1.1 Background 1
1.2. Aims and objectives 2
CHAPTER 2: LITERATURE REVIEW 4
2.1 Atmospheric nitrogen chemistry 4
2.2 Sources 8
2.2.1 Nitrogen oxides 8
2.2.2 Nitrate 9
2.3 Atmospheric transport 10
2.4 Deposition 12
2.5 Environmental and health effects 17
2.5.1 Nitrogen oxides 17
2.5.2 Nitrate 18
2.5.3 Critical loads 18
CHAPTER 3: METHODOLOGY 20
3.1 Sampling site description 20
3.2 Data collection 22
3.2.1 Instrumentation 22
3.2.1.1 Nitrogen oxides and ammonia 22
3.2.1.2 Nitrate 24
3.3 Data analysis 26
3.3.1 Temporal variations 26
3.3.2 Conversion rates 27
3.3.3 Deposition 29
CHAPTER 4: TEMPORAL VARIATIONS 33
4.1 Recorded hourly nitrogen concentrations 33
4.2 Seasonal variations of atmospheric nitrogen 35
4.3 Diurnal variations of atmospheric nitrogen 40
4.4 The dependence of concentrations of nitrogen species on wind direction 49
CHAPTER 5: ATMOSPHERIC CONVERSION AND REMOVAL 57
5.1 Rates of atmospheric conversion 57

5.2 Case studies 60
5.2.1 Background atmospheric pollution levels at Elandsfontein 61
5.2.2 Elevated NO_x concentrations associated with coal-fired power station sources . 63
5.2.3 Elevated NO_x concentrations associated with a petrochemical source 66
5.2.4 Elevated nitrate concentrations associated with a petrochemical source 69
5.3 Deposition 71
5.3.1 Seasonal deposition patterns 71
5.3.2 Total deposition to the Highveld 75
CHAPTER 6: CONCLUSIONS 80
CHAPTER 7: REFERENCES 84

LIST OF FIGURES

Figure 1. Mean tropospheric NO_2 column density for September 2007 to August 2008 derived from GOME-2 (http://joseba.mpch-mainz.mpg.de/no2_nad.htm). 2
Figure 2. The occurrence of absolutely stable layers within the atmosphere over South Africa on no-rain days (Tyson and Preston-Whyte, 2000, 287). 10
Figure 3. Photograph of the monitoring hut containing equipment at Elandsfontein (left); photograph of the surrounding landscape at Elandsfontein (right). 21
Figure 4. Location of Elandsfontein monitoring site on the Mpumalanga Highveld 22
Figure 5. Flow schematic of the TSI 17C NH_3 analyser (Thermo Environmental Instruments, 2000). 23
Figure 6. Photograph of the Ambient Particulate Nitrate Monitor's pulse generator outside view (left) and inside view (right) 24
Figure 7. Schematic of the Rupprecht and Patashnick 8400N nitrate monitor,consisting of a pulse generator and pulse analyzer. 25
Figure 8. Map indicating the delineated area used to determine total deposition to the Highveld. 31
Figure 9. Hourly average NO concentrations plotted together with the 24-hour moving average for Elandsfontein for the period 1 April 2005 to 31 March 2006. 34
Figure 10. Hourly average NO_2 concentrations plotted together with the 24-hour moving average for Elandsfontein for the period 1 April 2005 to 31 March 2006. 34
Figure 11. Hourly average NO_3 concentrations plotted together with the 24-hour moving average for Elandsfontein for the period 1 April 2005 to 31 March 2006. 35
Figure 12. Mean monthly concentration of nitrogen species at Elandsfontein for the period 1 April 2005 to 31 March 2006. 37
Figure 13. Mean monthly NO_2 box and whisker plot for Elandsfontein for the period 1 April 2005 to 31 March 2006. The average, median (white line), 25^{th} percentile (bottom of box), 75^{th} percentile (top of box), maximum (top whisker) and minimum (bottom whisker) concentration values are represented. 37
Figure 14. Mean monthly NO_3 box and whisker plot for Elandsfontein for the period 1 April 2005 to 31 March 2006. The average, median (white line), 25^{th} percentile (bottom of box), 75^{th} percentile (top of box), maximum (top whisker) and minimum (bottom whisker) concentration values are represented. 38
Figure 15. Mean monthly NO_x and O_3 concentrations at Elandsfontein for the period 1 April 2005 to 31 March 2006. 39
Figure 16. Mean hourly concentrations of pollutants at Elandsfontein for the period 1 April 2005 to 31 March 2006. 41
Figure 17. Diurnal box and whisker plot for NO (top) and NO_2 (bottom) for the period 1 April 2005 to 31 March 2006. The average, median (white line), 25^{th} percentile (bottom of box), 75^{th} percentile (top of box), maximum (top whisker) and minimum (bottom whisker) concentration values are represented. 42

Figure 18. Mean hourly concentrations of NO_3 at Elandsfontein for the period 1 April 2005 to 31 March 2006. 43
Figure 19. Mean hourly concentrations of pollutants at Kendal monitoring station for the period 1 April 2005 to 31 March 2006. 44
Figure 20. Mean hourly concentrations of pollutants at Kendal monitoring station during a fresh plume strike on 21 August 2005. 45
Figure 21. Mean hourly NO concentrations for each season during the period 1 April 2005 to 31 March 2006. 46
Figure 22. Mean hourly NO_2 concentrations for each season during the period 1 April 2005 to 31 March 2006. 47
Figure 23. Mean hourly NO_3 concentrations for each season during the period 1 April 2005 to 31 March 2006. 48
Figure 24. Wind rose for Elandsfontein for the period 1 April 2005 to 31 March 2006. 49
Figure 25. Seasonal wind roses for Elandsfontein for summer (December/January/February); autumn (March/April/May); winter (June/July/August) and spring (September/October/November). 50
Figure 26. Pollution roses indicating the maximum NO concentration (top); the median, 25^{th} and 75^{th} percentile NO concentrations (bottom left); and the average NO concentration (bottom right) at Elandsfontein for the period 1 April 2005 to 31 March 2006. 52
Figure 27. Pollution rose indicating the median, 75^{th} percentile and maximum concentrations of NO_2 at Elandsfontein for the period 1 April 2005 to 31 March 2006. 53
Figure 28. Pollution roses indicating the maximum NO_3 concentration (top); the median, 25^{th} and 75^{th} percentile NO_3 concentrations (bottom left); and the average NO_3 concentration (bottom right) at Elandsfontein for the period 1 April 2005 to 31 March 2006. 55
Figure 29. Average hourly concentrations at Elandsfontein on 5 April 2005 when no industrial sources are directly impacting on the region. 61
Figure 30. Pollution roses for Elandsfontein for 5 April 2005 for NO, NO_2 and NO_3. 62
Figure 31. Average hourly concentrations at Elandsfontein on 9 June 2005 when emissions originated from power station sources to the north-west. 63
Figure 32. Three-day back trajectory from Elandsfontein starting at 22:00 on 9 June 2005. 64
Figure 33. Pollution roses indicating maximum NO_2 concentrations (left) and 75^{th} percentile NO_2 concentrations (right) at Elandsfontein for 9 June 2005. 65
Figure 34. Average hourly concentrations at Elandsfontein on 11 April 2005. 66
Figure 35. Pollution roses indicating maximum NO_2 concentrations (left) and 75^{th} percentile NO_2 concentrations (right) at Elandsfontein for 11 April 2005. 67
Figure 36. Three-day back trajectory from Elandsfontein starting at 22:00 on 11 April 2005. 68
Figure 37. Average hourly concentrations at Elandsfontein on 24 July 2005. 69
Figure 38. Three-day back trajectory from Elandsfontein starting at 22:00 on 24 July 2005. 70

Figure 39. Pollution roses indicating maximum NO_3 concentrations (left) and 75th percentile NO_3 concentrations (right) at Elandsfontein for 11 April 2005... 71
Figure 40. Mean monthly dry depositional flux values (calculated using the mean v_d values) at Elandsfontein for the period 1 April 2005 to 31 March 2006..... 73
Figure 41. Box and whisker plot representing dry depositional fluxes of NO (top) and NO_2 (bottom) at Elandsfontein for the period 1 April 2005 to 31 March 2006. The boxes represent flux measurement using the average v_d value. The maximum whisker is the flux measurement using the maximum v_d value and the minimum whisker is the flux measurement using the minimum v_d value. 74
Figure 42. Box and whisker plot representing dry depositional fluxes of NO_3 at Elandsfontein for the period 1 April 2005 to 31 March 2006. The boxes represent flux measurement using the average v_d value. The maximum whisker is the flux measurement using the maximum v_d value and the minimum whisker is the flux measurement using the minimum v_d value.... 75
Figure 43. Annual wet and dry deposition rates at Elandsfontein. Dry deposition rates are calculated using the minimum, average and maximum v_d values from literature..... 76
Figure 44. Percentage of nitrogen deposited during April 2005 to March 2006 based on inferential model calculations using the minimum, average and maximum v_d values from literature..... 78

LIST OF TABLES

Table 1. Deposition velocity values for NO, NO_2 and NO_3 taken from literature for grasslands. 30

Table 2. The distances and directions of the different nitrogen sources surrounding Elandsfontein monitoring site..... 51

Table 3. Calculated rates of conversion of NO to NO_2 at Elandsfontein for various case study days during the period 1 April 2005 to 31 March 2006. O_3 concentrations and temperature are also listed. 58

Table 4. Calculated rates of conversion of NO to NO_2 at Kendal for various case study days during the period 1 April 2005 to 31 March 2006. O_3 concentrations and temperature are also listed 59

Table 5. NO to NO_3 concentration ratios at the source and at Elandsfontein for various case study days during the period 1 April 2005 to 31 March 2006 when NO_3 concentrations are high 60

ABBREVIATIONS AND ACRONYMS

C	Ambient concentration of a pollutant
DEAT	Department of Environmental Affairs and Tourism
F	Deposition flux
$g.mol^{-1}$	Grams per mole
GOME	Global Ozone Monitoring Experiment
H_2S	Hydrogen sulphide
HNO_3	Nitric acid
hPa	Hectopascals
hv	Sunlight
$J.K^{-1}.mol^{-1}$	Energy (in joules) per kelvin per mole
NH_3	Ammonia
NH_4NO_3	Ammonium nitrate
NO	Nitric oxide
NO_2	Nitrogen dioxide
NO_x	Nitrogen oxides (includes NO and NO_2)
NO_3	Nitrate
O_2	Oxygen
O_3	Ozone
$OH^{\cdot}$	Hydroxyl radical
ppb	Parts per billion
ppt	Parts per trillion
R_a	Aerodynamic resistance
R_b	Boundary layer resistance
R_c	Canopy resistance
SCIAMACHY	SCanning Imaging Absorption spectroMeter for Atmospheric CHartographY
SO_2	Sulphur dioxide
$\mu g.m^{-3}$	Micrograms per cubic meter
$\mu eq.l^{-1}$	Microequivalents per litre

VOC	Volatile Organic Compound
$\mathbf{v_d}$	Deposition velocity

CHAPTER 1: INTRODUCTION

This chapter provides a brief background to the study. The key objectives or research questions to be answered are also described.

1.1 Background

Molecular nitrogen is a natural, highly abundant element in the atmosphere, constituting ~78%. It is stable and is not very reactive. It may however oxidise or react with other species in the atmosphere to form reactive, and sometimes toxic, nitrogen-containing compounds. Such compounds may lead to severe health and environmental effects through their transport and deposition to the earth's surface (Galloway *et* al., 1994; Seinfeld and Pandis, 1998; Holland *et al*., 1999).

Nitrogen exists in a balance in nature, but anthropogenic influences are disrupting this natural nitrogen cycle. Such disruptions include: increased fossil fuel combustion resulting in greater nitrogen oxide (NO_x) emissions; and an increased need for food, resulting in higher ammonia (NH_3) emissions from agricultural activities (Galloway, 1998; Olivier *et al*., 1998; Aneja *et al*., 2001; Krupa, 2003).

The South African Highveld is a highly industrialised area home to various industries, coal mines, coal-fired power stations, vehicles and human settlements, which are all responsible for disrupting the nitrogen budget in the region (Held *et al*., 1993, 1996; Freiman and Piketh, 2003). According to satellite retrievals, the South African Highveld region is an area of highly elevated nitrogen dioxide (NO_2) concentrations (Figure 1). Although satellite-based instruments are good at recording trace gas concentrations with fixed spatial and temporal resolutions over large timescales (Toenges-Schuller *et al*., 2006), the area of elevated NO_2 concentration over the Highveld region has been identified as one of the outliers in the satellite data set. This implies uncertainty, where it has been found that field research does not correlate with the satellite data and so further research is required (Toenges-Schuller *et al*., 2006).

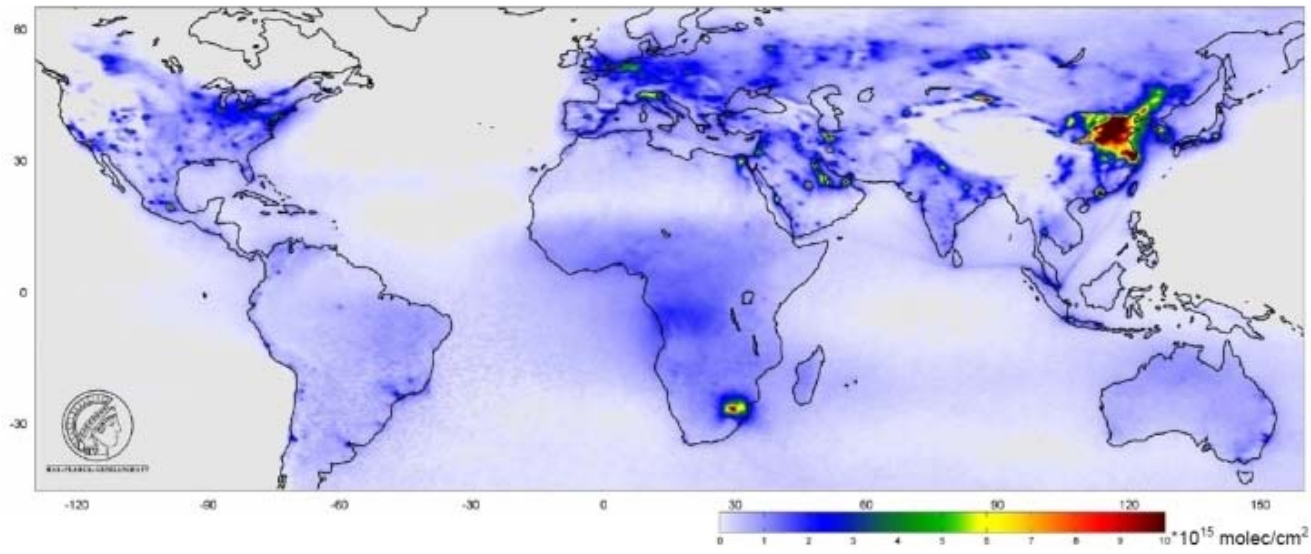


Figure 1. Mean tropospheric NO_2 column density for September 2007 to August 2008 derived from GOME-2 (http://joseba.mpch-mainz.mpg.de/no2_nad.htm).

1.2. Aims and objectives

The main objective of this study is to resolve components of the atmospheric nitrogen budget on the South African Highveld. This is achieved by identifying the major sources of the different nitrogen species in the region as well as the atmospheric transport and deposition of these species.

The main research questions are:

- What are the diurnal and seasonal variations of the different nitrogen species on the Highveld?
- What is the rate of conversion of NO to NO_2 in the atmosphere on the Highveld?
- In what form and quantity is nitrogen deposited to the surface on the Highveld?

****

With the above mentioned objectives in mind, the literature examining the chemistry, sources, deposition and environmental effects of different nitrogen species is presented in the next chapter.

CHAPTER 2: LITERATURE REVIEW

The three nitrogen compounds of interest in this study are NO, NO_2 and NO_3. These compounds are created via a series of chemical reactions in the atmosphere and continue to react with one other, with tropospheric O_3 and with other compounds to create new molecules or break down existing ones. In this chapter, the atmospheric chemistry and sources of the different nitrogen compounds are examined. The atmospheric transport and removal processes of the species are then explained, followed by a description of the environmental and health effects of elevated concentrations of such species in the atmosphere.

2.1 Atmospheric nitrogen chemistry

NO_x (NO + NO_2) is formed when atmospheric nitrogen is oxidised during high temperature combustion (>2000K) and electrical discharges, and by biogenic activity of micro-organisms within soils (Bradshaw *et al*., 2000; Hewitt, 2001; Fenger, 2002; Beirle, 2004; Horri *et al*., 2006). Non-toxic NO is emitted directly into the troposphere via equation 1. Once NO is present in the atmosphere it rapidly oxidises when it comes into contact with O_3 molecules to form toxic NO_2 (equation 2) (Seinfeld and Pandis, 1998; Webb and Hunter, 1998; Atkinson, 2000; Colls, 2002; Fenger, 2002).

$$N_2 + O_2 \rightarrow 2NO \qquad (1)$$

$$NO + O_3 \rightarrow NO_2 + O_2 \qquad (2)$$

Close to a source the NO/NO_2 ratios are relatively high, but as oxidation occurs in the atmosphere, NO_2 becomes the dominant NO_x species (White, 1977; Warneck, 1988; Cocks and Fletcher 1989; Webb and Hunter, 1998). A photochemical equilibrium is established within minutes between NO, NO_2 and O_3 (Lange *et al*., 2001). During the day, NO_2 absorbs UV wavelengths (<400nm) and dissociates back into NO and O_3 (equation 3) establishing

this photochemical equilibrium (Colls, 2002). The rate at which NO converts into NO_2 is highly variable depending on the atmospheric conditions. Laboratory studies conducted by Gertler *et al*. (1984) found NO to NO_2 conversion rates of ~8% per hour. However, these rates are inconclusive as under ambient conditions, oxidation proceeds much slower. Oxidation rates in plumes also differ from those calculated from background or ambient air because there is the possibility of increased catalyst concentrations and rapid reduction of oxidants (such as O_3) within a plume (Hewitt, 2001). Hewitt (2001) found maximum NO to NO_2 conversion rates of ~30% per hour. In a plume however, these rates will be lower as the supply of oxidants decrease via the consumption of O_3.

NO_x is a major precursor for the formation of tropospheric O_3. This O_3 is produced via photolysis when NO_2 and NO are present in the atmosphere (equation 3 and 4). It is generally created during the day, as sunlight is needed to break the bonds of the primary pollutants. NO_x acts as the catalyst for O_3 production when hydrocarbons and CO are oxidized (Murphy *et al*., 1993; Jacob *et al*., 1996; Ryerson *et al*., 1998; Seinfeld and Pandis, 1998; Colls, 2002).

$$NO_2 + hv\ (\lambda < 400nm) \rightarrow NO + O \qquad (3)^1$$

$$O + O_2 + M \rightarrow O_3 \qquad (4)^2$$

O_3 production exhibits a diurnal cycle, with the highest concentrations occurring in the afternoon and the lowest in the early morning. Once O_3 has been formed, it may react with NO in the atmosphere to reform NO_2 (equation 2) (White, 1977; Seinfeld and Pandis, 1998; Atkinson, 2000; Jacob, 2000). This set of cyclical reactions contributes a very small amount to background O_3 concentrations (only a few ppb). In an unpolluted environment these reactions produce low, stable O_3 concentrations, as the O_3 that is produced is instantly consumed by the NO. However in a polluted environment with high NO_2 concentrations, higher O_3 concentrations may be experienced as a secondary pollutant (Colls, 2002).

---

[2] hv represents sunlight; and M represents N_2 or O_2 or another third molecule that absorbs excess vibrational energy (Seinfeld and Pandis, 1998).

NO_x plays a role in the troposphere of regulating the concentration of the hydroxyl radical ($OH^{\cdot}$), a very important atmospheric oxidant (Levine *et al*., 1996; Bradshaw *et al*., 2000; Hewitt, 2001; Tie *et al*., 2003). HNO_3 is a key product of the oxidation of NO_x in the troposphere via the reaction with the $OH^{\cdot}$ radical during the day (equation 5) (Olivier *et al*., 1998; Seinfeld and Pandis, 1998; Jacob, 2000; Hewitt, 2001; Colls, 2002).

$$NO_2 + OH^{\cdot} + M \rightarrow HNO_3 + M \qquad (5)^2$$

NO_x has a very limited tropospheric lifetime (about 1 to 2 days). Equation 5 has a half life of about 23 days, so HNO_3 acts as a store of NO_x, keeping it in the troposphere for longer periods (Seinfeld and Pandis, 1998; Holland *et* al., 1999; Atkinson, 2000; Colls, 2002; Stein and Lamb, 2003; Widory, 2007).

Through further oxidation, NO_2 produces NO_3 particles at night via equation 6 (Orel and Seinfeld, 1977; Wayne *et al*., 1991; Hewitt, 2001; Colls, 2002; Peiró-Garcia and Nebot-Gil, 2003). NO_3 is an important oxidant, and its night time oxidation capacity can be as great as the $OH^{\cdot}$ radical's daytime oxidation capacity (Brown *et al*., 2003a).

$$NO_2 + O_3 \rightarrow NO_3 + O_2 \qquad (6)$$

This is a key reaction in atmospheric chemistry as NO_2 is the dominant NO_x compound, ozone is a highly abundant photochemical oxidant and the reaction occurs rapidly (Peiró-Garcia and Nebot-Gil, 2003). Hov and Isaken (1981) found that this reaction occurs so quickly, that ~80% of the NO_x converts into NO_3 or HNO_3 within three hours (with an initial NO_x concentration of 0.5 ppm at 26°C).

NO_3 may also form as a result of the dissociation of HNO_3 (equation 7). HNO_3 is one of the most water soluble gases in the atmosphere and thus dissociates readily (Orel and Seinfeld, 1977; Wayne *et al*., 1991; Matsumoto and Tanaka, 1996; Seinfeld and

[2] M represents N_2 or O_2 or another third molecule that absorbs excess vibrational energy (Seinfeld and Pandis, 1998).

Pandis, 1998). This reaction is the dominant pathway for daytime NO_3 formation (Seinfeld and Pandis, 1998; Gomez-Moreno *et al*., 2007).

$$HNO_3 \leftrightarrow NO_3^- + H^+ \qquad (7)$$

The stability of NO_3 is in part a function of the pH of the particles. If the pH is suitably low enough, HNO_3 may be re-evaporated (Warneck, 1988). Phase changes of NO_3/HNO_3 are highly temperature dependant. Under high temperatures, fine mode NO_3 is volatilised and gaseous HNO_3 is formed. Under low temperatures, NO_3 is generated and HNO_3 concentrations decrease (Matsumoto and Tanaka, 1996; Hewitt, 2001).

Nitrates are predominantly created at night, when the NO_3 radical may react with organics or other cations, which include NH_3 and volatile organic compounds (VOCs) (Wayne *et al*., 1991; Hewitt, 2001; Peiró-Garcia and Nebot-Gil, 2003). NO_3 has been found to react with alkenes (C_nH_{2n}), aldehydes (O=CH-), terpenes (C_5H_8) and benzenes (C_6H_6) (Warneck, 1988). During the day NO_3 rapidly photolyses via two different pathways (equations 8 and 9) and nitrates cannot be produced (Wayne *et al*., 1991; Seinfeld and Pandis, 1998; Atkinson, 2000).

$$NO_3 + hv\ (\lambda < 700\ nm) \rightarrow NO + O_2 \qquad (8)$$

$$NO_3 + hv\ (\lambda < 580\ nm) \rightarrow NO_2 + O \qquad (9)$$

Nitrates have been found to exhibit a bi-modal size distribution, occurring in both fine and coarse particle mode. Kadowaki (1977) discovered that fine particle mode NO_3 are produced as a result of the photo-oxidation of NO_2 and NH_3 to produce ammonium nitrates (NH_4NO_3), whilst the coarse mode NO_3 are produced mainly by reactions of coarse particles (such as sea salt or soil derived material) and HNO_3 (Kadowaki, 1977; Warneck, 1988; Seinfeld and Pandis, 1998).

NH_4NO_3 aerosols may also be formed via the gas phase reaction of NH_3 and HNO_3 (equation 10) (Orel and Seinfeld, 1977; Wayne *et al*., 1991; Yeatman *et* al., 2001; Chan and Chan, 2004). NH_4NO_3 is unstable and exists in a reversible reaction equilibrium with its

precursors. NH_4NO_3 has been found to be one of the most important atmospheric aerosols, accounting for up to 30% of fine aerosols in polluted urban environments (Dassios and Pandis, 1999; Chan and Chan, 2004).

$$NH_3 + HNO_3 \leftrightarrow NH_4NO_3 \qquad (10)$$

In the absence of HNO_3, NH_3 remains in the troposphere for extended periods of time and reacts slowly with the $OH^{\cdot}$ radical to produce NH_2. This NH_2 may then react with O_3, NO or NO_2 in the atmosphere or become oxidised to NO by HNO_3 (Kadowaki, 1977; Atkinson, 2000; Krupa, 2003; Widory, 2007).

NH_3 may also react with sulphuric acid (H_2SO_4) (equation 11) or hydrochloric acid (HCl) to produce ammonium (NH_4^+) containing aerosols. The rates of these reactions are dependant on the humidity, temperature and acid concentration. Reverse reactions may also occur with HNO_3 and HCl (Benner *et al*., 1991; Tanaka and Matsumoto, 1996; Asman *et al*., 1998; Dassios and Pandis, 1999; Aneja *et al*., 2001; Yeatman *et al*., 2001).

$$NH_3 + H_2SO_4 \rightarrow NH_4HSO_4 + NH_3 \rightarrow (NH_4)_2SO_4 \qquad (11)$$

NH_3 is the most abundant alkaline species in the atmosphere. NH_3 is highly responsible for neutralizing atmospheric acids created from NO_x and SO_2. The reaction product of NH_3 or NH_4^+ with acidic compounds is a key component of rain and aerosols, which occur predominantly in the fine particle size range (< 2.5 μm) (Warneck, 1988; Asman *et al*., 1998; Seinfeld and Pandis, 1998; CENR Air Quality Research Sub Committee, 2000; Aneja *et al*., 2001; Krupa, 2003).

2.2 Sources

2.2.1 Nitrogen oxides

NO_x is produced from both natural and anthropogenic sources. Natural tropospheric NO_x concentrations are around 10 – 20 ppt, but concentrations exceeding 200 ppb can be found in urban areas (Leue *et al*., 2001).

Natural sources include: biomass burning, lightning, biogenic soil emissions and transport from the stratosphere (Warneck, 1988; Jacob *et al*., 1996; Galloway, 1998; Schultz *et al*., 1999; Atkinson, 2000; Leue *et al*., 2001; Horii *et al*., 2005). Anthropogenic sources of NO_x are emissions from motor vehicles, aircraft as well as from fossil fuel burning associated with power stations and industrial activities (Warneck, 1988; Cocks and Fletcher, 1989; Olivier *et al*., 1998; Placet *et al*., 2000; Widory, 2007), which makes up the major constituent of NO_x production (Munger *et al*., 1998; Olivier *et al*., 1998). Concentrations of nitrogen species within combustion plumes, under many meteorological conditions, have been found to be substantially greater than ambient concentrations even after 24 hours of dispersion (Cocks and Fletcher, 1989).

The sources described above provide the high temperature from combustion (or microbial action for soil emissions) which is required for NO_x production (Warneck, 1988; Galloway, 1998; Ryerson *et al*., 2001; Fenger, 2002). In the case of biomass burning, the temperatures of combustion are seldom high enough to create NO_x via oxidation, so the NO_x is mainly a result of the nitrogen content of the fuel (Warneck, 1988).

Lightning is the largest natural source of NO_x, providing high temperatures in excess of 30 000K. According to Lee *et al*. (1997) lightning contributes ~12% of total NO_x emissions globally. For the South African context it has been estimated that lightning contributes ~25% of tropospheric NO_x over the Highveld (Wenig *et al*., 2003). However, estimates may vary, as lightning is a very uncertain source of NO_x and is mainly an upper tropospheric source. These varying estimates pose a major uncertainty in the reactive nitrogen cycle (Lange *et al*., 1998). Brunner *et al*. (1998) observed large scale NO_x plumes downwind of thunderstorms, but there was great uncertainty as to whether this was created by lightning or if it was NO_x lifted from the ground.

2.2.2 Nitrate

Nitrates are aerosols (any solid or liquid particles suspended in the air) that act as a sink for atmospheric NO_x (Kadowaki, 1977; Wayne *et al*., 1991; Seinfeld and Pandis, 1998). They are not emitted into the atmosphere by a direct source, but are secondary aerosols produced

from gas-to-particle conversion (equation 4 and 5) (Kadowaki, 1977; Wayne *et al*., 1991; Seinfeld and Pandis, 1998).

2.3 Atmospheric transport

Transport of nitrogen species within the atmosphere is dependent on the state of the atmosphere and circulation of air. Transport acts vertically as well as horizontally (Garstang *et al*., 1998; Tyson and Preston-Whyte, 2000).

Vertical transport of pollutants is primarily due to deep convection. This convection transports nitrogen emissions from the surface into the upper troposphere (Jacob *et al*., 1996; Bradshaw *et al*., 2000; Savage *et al*., 2004). Vertical motion is eventually inhibited due to the absolutely stable layers found preferentially at ~850hPa (over coastal regions), ~700hPa, ~500hPa and ~300hPa (Figure 2) on no-rain days. These stable layers trap pollutants at lower atmospheric levels and so influence the transport of pollutants over the whole of southern Africa (Cosijn and Tyson, 1996; Garstang *et al*., 1996; Tyson *et al*., 1996b).

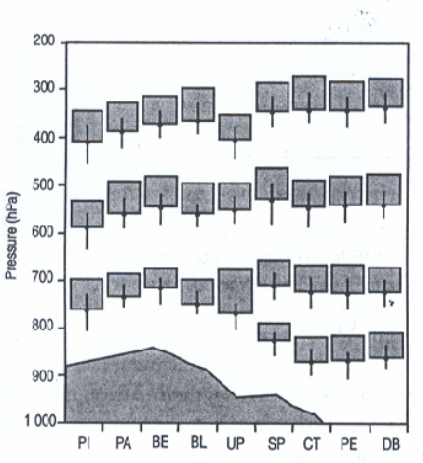


Figure 2. The occurrence of absolutely stable layers within the atmosphere over South Africa on no-rain days (Tyson and Preston-Whyte, 2000, 287).

On a more local scale, like that of the Highveld area, vertical motion and hence dispersion of pollutants is inhibited by surface inversions that form during the night. These inversions are a result of radiational cooling at the surface and are most pronounced just before sunrise. In the presence of sunlight the inversions begin to break down through convective heating and the height of the mixed layer is increased (Tyson *et al*., 1976; Cosijn and Tyson, 1996; Tyson and Preston-Whyte, 2000). On the Highveld, a tall-stack policy has been introduced due to the climatological conditions and poor dispersion in the region. Stacks are generally 200 – 300m tall, allowing pollutants to be dispersed well above the natural surface inversion layer (Scheifinger and Held, 1997).

Atmospheric stability is more pronounced during the winter months. This was evident on the Highveld during an aerosol study performed by Scheifinger and Held (1997), with maximum concentrations occurring during late winter and early spring when the subsidence inversions are at their strongest, limiting the height of the mixed layer. Gomez-Moreno *et al*. (2007) also noted higher NO_3 concentrations in winter as a result of limited atmospheric mixing due to increased stability.

In terms of horizontal transport, local winds may transport pollutants within the vicinity of their source. These include: anabatic and katabatic winds, sea and land breezes, valley and mountain winds, and mountain-plain and plain-mountain winds (Tyson and Preston-Whyte, 2000).

On a larger scale, various synoptic systems affect circulation over the whole of southern Africa. These systems include: continental highs, ridging highs, westerly lows, westerly waves and easterly waves, which transport air and any pollutants contained within over larger distances. On a synoptic scale, some air is transported towards the west coast (to the Atlantic Ocean), but transport is primarily towards the east coast (towards the Indian Ocean) (Garstang *et al*., 1996; Tyson *et al*., 1996a, 1997). This eastward flow is evident as a well defined plume that has been found to eventually pass south of Australia, such that in winter 30% of South African air is found in the Australian vicinity. With weaker westerlies during summer, the occurrence of this plume in the Australian region is less frequent and

more air recirculates and exits towards to equator (Tyson and Preston-Whyte, 2000; Freiman and Piketh, 2003).

Transport associated with continental highs occurs all year round, but with greater frequency during winter. Easterly waves show an annual cycle, peaking in summer and almost never occurring in winter. Transport associated with ridging highs and westerly waves shows little annual variation; however these westerly waves occur with greater frequency during winter on the Highveld (Garstang *et al*., 1996; Tyson *et al*., 1996a, 1996b).

Recirculation is also important in the transport of pollutants and occurs frequently over southern Africa due to the high frequency of anticyclonic circulations (Garstang *et al*., 1996; Tyson *et al*., 1996b, 1997; Freiman and Piketh, 2003). Recirculation occurs when air is transported away from its source and returns in the opposite direction after rotating cyclonically or anticyclonically (Tyson *et al*., 1996a). Recirculation can occur at a number of scales from sub-continental to regional, and an interaction between different scales of wind systems results in further recirculation (Tyson *et al*., 1996a, 1996b, 1997; Tyson and Preston-Whyte, 2000; Freiman and Piketh, 2003).

2.4 Deposition

Anthropogenic sources have greatly increased the concentration of nitrogen containing species in the atmosphere. This in turn has affected the amount of nitrogen that is deposited to the surface. Such deposition severely affects the natural nitrogen status of ecosystems. Although nitrogen acts as a fertilizer, in large amounts it may damage plants and alter ecosystem biodiversity (Meyers *et* al., 1991; Hesterberg *et al*., 1996; Holland *et al*., 1999; Watt *et al*., 2004). In recent times, deposition has become a larger source of nitrogen to aquatic and terrestrial ecosystems than biological nitrogen fixation (Holland *et al*., 1999). Thus, analysis of the deposition of such nitrogen species to the surface determines the impacts on the environment itself (Watt *et al*., 2004).

Atmospheric pollutants and particles are eventually deposited back to the ground via two different depositional processes: dry and wet deposition. Dry deposition is the process whereby atmospheric trace chemicals are transported to the surface by air motion. Dry removal processes include: sedimentation, impaction, diffusion and gravitational settling (Jacob *et al*., 1996; Seinfeld and Pandis, 1998; Bradshaw *et al*., 2000; Wesely and Hicks, 2000; Baumgardner *et al*., 2002; Gao, 2002).

Wet deposition occurs when particles and gases are brought to ground-level via precipitation mechanisms. Wet deposition occurs via precipitation scavenging, where particles are dragged down to ground level via falling precipitation below the cloud base, and within a cloud as part of the cloud droplets, also known as cloud interception (Asman *et al*., 1998, Seinfeld and Pandis, 1998; Bradshaw *et al*., 2000; Baumgardner *et al*., 2002; Gao, 2002). Wet deposition is more prominent downwind of the source where as dry deposition is significant close to the source (Asman *et al*., 1998).

NO_x has a very low solubility, so it is not easily deposited to the ground directly (Asman *et al*., 1998; Seinfeld and Pandis, 1998; Wesley and Hicks, 2000). NO_x is primarily emitted in the form of NO, but in terms of deposition to the surface, NO_2 is the main pathway (Watt *et al*., 2004). However, most deposition occurs after further oxidation, in the form of HNO_3 or as NO_3 aerosols, which are highly soluble and may act as condensation nuclei, transporting nitrogen back to ground level (Fowler *et al*., 1998; Munger *et al*., 1998; Wesley and Hicks, 2000; Horii *et al*., 2005). Such deposition is the main process for the loss of reactive nitrogen from the troposphere (Horii *et al*., 2005).

NO_3^- and NH_4^+ aerosols are deposited via both wet and dry deposition. Fine NO_3 particles are deposited via wet deposition when particles are incorporated in clouds or rain (Fowler *et al*., 1998; Krupa, 2003; Stein and Lamb, 2003). Coarse NO_3 particles are primarily dry deposited via the process of impaction (Warneck, 1988) whilst the smaller NH_4^+ particles are dry deposited as a result of Brownian motion and diffusion (Krupa, 2003). These NH_4^+ aerosols have relatively long atmospheric lifetimes (1 – 15 days) and are thus deposited further downwind (Aneja *et al*., 2001; Krupa, 2003).

Wet deposition is generally measured directly using rainwater samples. However, using everyday rainwater samples can be inaccurate, as the samples are affected by both wet and dry deposition (Zapletal, 1998). To overcome this, an automated sampling bucket is utilised, which is only exposed when a rainfall event occurs. This is achieved via an automated lid that detects the onset of rain and opens and closes accordingly. The chemical content of the rainwater is then analysed by ion chromatography, to determine which ions are in highest concentration (Hesterberg *et al*., 1996; Russell *et al*., 1998; Mphepya *et al*., 2004).

Dry deposition is fairly difficult to determine as it is greatly dependant on the characteristics of the surface that it is deposited to. Rates of deposition to forested canopies will therefore be very different to those to grasslands (Schmitt *et al*., 2005). Rates of dry deposition are very difficult to measure directly, so various indirect methods have been employed to determine such rates in an area. These include eddy correlation, mass balance and gradient techniques. For this study, the inferential method was used. The inferential method has been found to compare well with the other micrometeorological techniques (Meyers *et* al., 1991; Zunckel *et* al., 1996; Brook *et al*., 1997; Watt *et al*., 2004).

The inferential method calculates the dry deposition flux using the atmospheric concentration (C) and the deposition velocity (v_d) of a certain species (equation 12). v_d is described as a parameterization of the rate of transfer of a pollutant from the atmosphere to the receptor surface (Meyers *et al*., 1991; Hesterberg *et al*., 1996; Brook *et al*., 1997; Clarke *et al*., 1997; Asman *et al*., 1998, Wesley and Hicks, 2000; Schmitt *et al*., 2005). Inferential deposition modelling is easily determined provided the meteorological and vegetation conditions in the area are known (Brook *et al*., 1997; Clarke *et al*., 1997). The flux is determined by:

$$F = -v_d C \qquad (12)$$

Both v_d and C are height dependent and the negative sign indicates a downward flux (Seinfeld and Pandis, 1998; Wesley and Hicks, 2000; Baumgardner *et al*., 2002; Gao, 2002;

Marner and Harrison, 2004; Yang *et al*., 2005). v_d is expressed as the reciprocal of a series of resistances:

$$v_d = (Ra + Rb + Rc)^{-1} \qquad (13)$$

Ra represents the aerodynamic resistance, Rb is the boundary layer resistance and Rc is the canopy resistance. v_d involves these three resistances because the process of dry deposition usually involves three stages: the gas being transported from source to receptor (Ra); the transport through the quasi-laminar layer near the receptor surface (Rb); and the pollutant depositing on or being absorbed by the surface (Rc) (Seinfeld and Pandis, 1998; Colls, 2002). Ra and Rb can be calculated using the frictional velocity and wind speed. Rb and Rc are dependant on the characteristics of the surface and the nature of the pollutant (Meyers *et al*., 1991; Hesterberg *et al*., 1996; Zunckel *et al*., 1996; Clarke *et al*., 1997; Seinfeld and Pandis, 1998, Zapletal, 1998).

From a previous nitrogen deposition study performed in the USA using the inferential model calculations, Meyers *et al*. (1991) found that the majority of all the dry deposited nitrogen was in the form of HNO_3. No distinct seasonal depositional cycles of nitrogen were evident and dry deposition was found to contribute between 30% and 50% of total nitrogen deposition in Eastern USA. From a depositional study performed for a grassland in central Switzerland, the rates of dry deposition of nitrogen (15 to 25 kg N ha^{-1} yr^{-1}) were found to be substantially higher than the rates of wet deposition (9 kg N ha^{-1} yr^{-1}) (Hesterberg *et al*., 1996).

Using the inferential model during a depositional study in the Czech Republic, oxidised nitrogen species (NO_y) contributed 52% and reduced nitrogen species (NH_x) contributed 48% to the total dry deposition of nitrogen compounds. It was found that 61% of total nitrogen deposition in the region was attributed to dry deposition (Zapletal, 1998).

On the Highveld, the inferential technique was utilised by Zunckel *et al*. (1996) during a pilot study on sulphur deposition. Specific focus was on SO_2 deposition in the area, using comparisons between winter and summer months. 80% of all sulphur deposited was in the

form of SO_2 in winter and 82% as SO_2 in summer. The rate of dry deposition of sulphur on the Highveld was calculated as 8.22 kg S ha^{-1} yr^{-1}, which was found to exceed the rate of wet deposition in a ratio of approximately 60:40.

More recently, Lowman (2003) utilised the inferential technique to analyse nitrogen deposition to a grassland area and a forested area on the Mpumalanga Highveld. It was calculated that the total amount of dry deposition to the grassland and forest were 7 kg N ha^{-1} yr^{-1} and 21.4 kg N ha^{-1} yr^{-1} respectively. Cloud droplet deposition was also found to be a significant contributor to overall deposition. When wet, dry and cloud droplet deposition are all incorporated, the total amount of deposition to the grassland region was 25 kg N ha^{-1} yr^{-1} and 71.2 kg N ha^{-1} yr^{-1} to the forested area. In both areas, NH_3 was found to contribute the most to dry deposition, followed by HNO_3 and NO_2. Maximum deposition rates were found to occur in summer, with lowest rates in winter. Spring was found to have slightly higher rates than autumn, as a result of biomass burning.

In many of the previous studies when investigating dry deposition using the inferential model, the v_d estimates have much uncertainty and may not be specified correctly. This may be due to changing meteorological, physical, chemical and surface conditions. Due to spatial variability, it is difficult to determine how representative v_d is of nearby locations (Brook et al., 1997; Seinfeld and Pandis, 1998).

Recently, acid deposition has become a major area for concern and it has been found that such deposition has important links with global climate via the impacts on carbon uptake within plants (Horii *et al*., 2005). NO_x oxidation results in the production of acidic species leading to acid deposition (equation 3 and 5). In South Africa, specific acid deposition studies were performed at Amersfoort (an industrialised site in eastern Mpumalanga) and Louis Trichart (a rural site in the Limpopo province). It was found that the concentration of NO_3 in the precipitation at Amersfoort (25 $\mu eq.l^{-1}$) was significantly higher than the concentration at Louis Trichart (8 $\mu eq.l^{-1}$). The NO_3 rainwater concentration was directly proportional to the higher atmospheric NO_x concentration at the industrialised site. NO_3 deposition at both sites was higher during spring as a result of biomass fires in the region at

this time. At Amersfoort deposition in the form of SO_4^{2-} and NO_3 is most significant contributing to ~90% of the rainwater acidity, whilst at Louis Trichart, deposition occurs mainly in the form of organic acids, accounting for up to 50% of the rainwater acidity in the area (Mphepya *et al*., 2004).

2.5 Environmental and health effects

2.5.1 Nitrogen oxides

NO_x most significantly contributes to the formation of tropospheric O_3 (Levine *et al*., 1996; Atkinson, 2000; Jacob, 2000; Aneja *et al*., 2001; Hewitt, 2001). The residence time of NO_x is much shorter than other O_3 precursors (carbon monoxide (CO), VOCs and hydrocarbons) and throughout the troposphere NO_x acts as the rate-limiting precursor for O_3 production (Murphy *et al*., 1993; Schultz *et al*., 1999; Savage *et al*., 2004; Mauzerall *et al*., 2005). Therefore, increased NO_x concentrations can lead to highly elevated tropospheric O_3 concentrations (Munger *et al*., 1998; Seinfeld and Pandis, 1998). Tropospheric O_3 is an important atmospheric oxidant and a major air pollutant, and also acts as a key greenhouse gas. It has implications for humans and the natural environment and has been linked to increased morbidity and mortality rates (Jacob *et al*., 1996; Seinfeld and Pandis, 1998; Horowitz and Jacob, 1999; Schultz *et al*., 1999; Jacob, 2000).

NO_x itself is a significant pollutant as it has several implications for human health. Elevated concentrations may lead to asthma, emphysema, bronchitis, damage to lung tissue and even premature death. NO_x may also lead to biological imbalances and mutations in vegetation; as well as effecting visibility, decreasing regional air quality (Lee *et al*., 1997; Fenger, 2002; Mauzerall *et al*. 2005). NO_x leads to the formation of acid rain via the production of HNO_3. HNO_3 may remain in the troposphere for days or weeks and may be transported great distances by prevailing winds.

Deposition of HNO_3 leads to hazardous implications for ecosystems, resulting in eutrophication which leads to changes in species diversity and degraded water quality

(Galloway *et al*., 1994; Atkinson, 2000; Aneja *et al*., 2001; Hewitt, 2001; Harrison *et al*., 2004; IDAF, 2004; Watt *et al*., 2004).

2.5.2 Nitrate

NO_3 particles cause air pollution; create deteriorations in visibility; severely affect people's health, ecosystems and the natural environment; and contribute to acid rain (Seinfeld and Pandis, 1998; Curtius, 2006; Dore *et al*., 2007; Kai *et al*., 2007). In a natural, pollutant-free environment, rain generally has a pH of 5.6. With the introduction of NO_3, the pH of rain droplets is lowered and acidic water is carried to the ground, which is harmful to ecosystems, acidifies water sources, damages vegetation and damages materials and buildings (Seinfeld and Pandis, 1998). In low concentrations, NO_3 is an essential nutrient for plants; however, at higher concentrations NO_3 can be highly toxic (Aneja *et al*., 2001; Marner and Harrison, 2004; Horii *et al*., 2005).

Aerosols exhibit both a direct and indirect effect on the earth's radiation balance. Direct aerosol effects include scattering and absorption of solar radiation. NO_3 aerosols are effective at light scattering when the particles are large enough. Indirect effects are when aerosols act as cloud condensation nuclei (CCN), contributing to cloud formation and affecting cloud lifetime and albedo (Seinfeld and Pandis, 1998; Harrison, 2004; Curtius, 2006; Reason *et al*., 2006).

2.5.3 Critical loads

Critical loads, as defined by Nilsson and Grennfelt (1988) are ' a quantitative estimate of exposure to one or more pollutants below which significant harmful effects on specified sensitive elements of the environment do not occur according to our present knowledge'. This value is determined based on the vegetation type in the region and the soil characteristics. Globally, the critical load for nitrogen has been set at 15 kg N ha^{-1} yr^{-1} for grasslands and 20 – 30 kg N ha^{-1} yr^{-1} for forests (Grennfelt and Thörnelöf, 1992). The degree to which the critical load is exceeded, determines the severity of the impacts on an ecosystem. Exceedance is defined as the difference between deposition and the critical

load. To calculate the exceedance, the amount and speciation of the nitrogen that is deposited is required (Hesterberg *et al*., 1996; Augustin *et al*., 2005).

Utilising critical loads in deposition studies, aid in the assessment of the possible impacts of atmospheric deposition on the environment. The critical loads approach has been adopted in various regions as a method for controlling pollutant emissions (Bull, 1991; van Tienhoven, 1995; Krupa, 2003; Dore *et al*., 2007).

****

NO, NO_2 and NO_3 are air pollutants leading to various impacts on the environment and human health. NO is emitted directly into the atmosphere via high temperature combustion, where after it oxidises into NO_2 and further oxidises into NO_3. NO_x has both natural and anthropogenic sources, however the latter is of far more concern in recent times. Over southern Africa, transport of such pollutants occurs both vertically due to convection and horizontally on a number of scales ranging from local to synoptic. Removal processes include dry and wet deposition. Wet deposition can be measured directly from rain samples but dry deposition requires further manipulation in the form of an inferential model. Now that the nitrogen literature has been disclosed, the specifics of this study will be discussed in the methodology chapter that follows.

CHAPTER 3: METHODOLOGY

This chapter provides an overview of the sampling site and methods utilised in this study. A description of the instrumentation that was used to measure the various nitrogen species concentration is presented. The data that was collected and used for analysis is discussed and finally, the methods used to calculate atmospheric conversion and removal processes are described.

3.1 Sampling site description

The industrialised Highveld Plateau region in north-eastern South Africa extends across parts of Gauteng, the Free State and Mpumalanga provinces at about 1400 –1700 m above sea level (Scheifinger and Held, 1997; Freiman and Piketh, 2003; Wenig *et al*., 2003). About 70% of the Highveld area is covered by grassland and the rest is utilised for agricultural, industrial and urban activities. The area houses rich coal reserves and the Mpumalanga Highveld is home to eleven coal-fired power stations, which are in close proximity to one another resulting in very high emission densities in the region. The area is also home to heavy industry as well as petrochemical industries in Sasolburg and Secunda (Scheifinger and Held, 1997; Zunckel *et al*., 2004).

Being a highly industrialised area (accounting for ~75% of South Africa's industrial activity) this region accounts for ~90% of South Africa's NO_x emissions (Freiman and Piketh, 2003; Wenig *et al*., 2003). Low-level pollutant emission sources that are also of great concern in the region include: domestic coal burning in informal settlements, combustion in colliery discard dumps and motor vehicles (Scheifinger and Held, 1997).

Eskom's air quality monitoring network consists of a number of ground-based monitoring sites located within industrial areas, alongside major roads, near power stations and in areas not directly affected by emissions. Data from Elandsfontein monitoring station, a site situated in central Mpumalanga was utilised for this study. It is ideally situated in the heart

of this industrialised region, allowing for an intensive study on industrial nitrogen emissions.

Elandsfontein is a supersite which houses various trace gas, particulate and meteorological instruments (Figure 3 (left)). It is positioned at 26°15'09" S and 29°25'17"E at an altitude of 1760m. The landscape is relatively flat with a few rolling hills, and is covered mainly by grasslands (Figure 3 (right)). The open environment allows for effective dispersion and mixing close to the surface.



Figure 3. Photograph of the monitoring hut containing equipment at Elandsfontein (left); photograph of the surrounding landscape at Elandsfontein (right).

The monitoring site is surrounded by various nitrogen emission sources including coal-fired power stations; a petrochemical industry; iron, steel, manganese and vanadium smelters; and domestic coal burning sources (Figure 4). It is situated 25km east of Kriel and Matla power stations, 33km south of Duvha power station and 49km south-east of Kendal power station. The Secunda petrochemical plant is situated 40km south-west of Elandsfontein. Hendrina power station and Arnot power station are 30km and 50 km north-east of Elandsfontein respectively. To the south are: Camden power station which is 78km south-east of Elandsfontein, Majuba power station is 99 km south-south-east and Tutuka is 58km south.

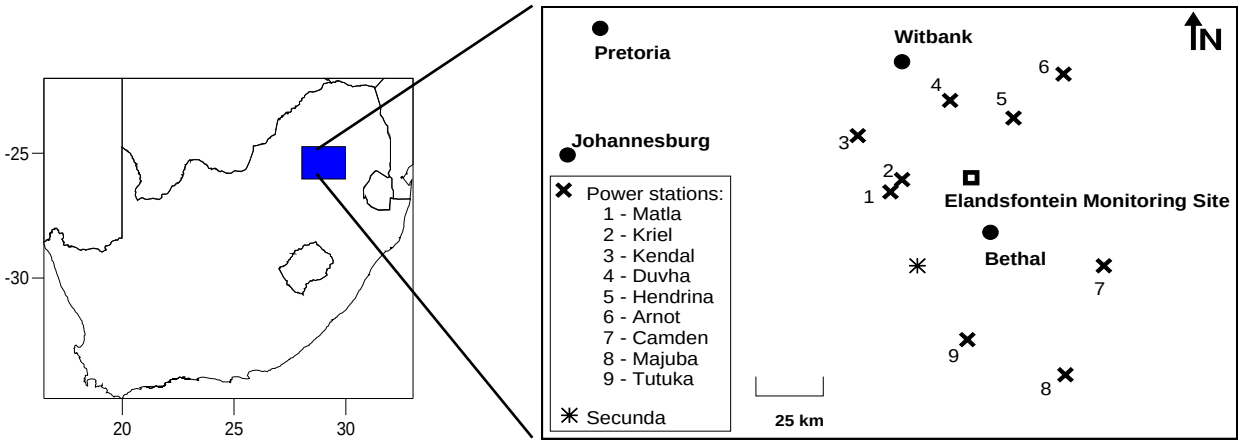


Figure 4. Location of Elandsfontein monitoring site on the Mpumalanga Highveld

3.2 Data collection

Pollutant concentrations and meteorological conditions are continuously recorded at Elandsfontein monitoring site. For this study, hourly concentrations from continuous monitoring for a year from April 2005 to March 2006 were utilised. NO, NO_2, NO_3, SO_2, H_2S, black carbon and O_3 concentration data as well as meteorological data was collected.

3.2.1 Instrumentation

For the measurement of NO_x and NH_3, a TSI Model 17C Chemiluminescence NH_3 analyser was utilised. There were, however, some problems with the NH_3 component of the instrument, so NH_3 concentrations were not recorded and therefore are not analysed in this study. Nitrates were measured using a Rupprecht and Patashnick Series 8400N Ambient Particulate Nitrate Monitor. Ozone concentrations were recorded using a TSI UV Photometric O_3 analyser and meteorological parameters were measured with various meteorological instruments that were mounted on a microwave mast located at the site.

3.2.1.1 Nitrogen oxides and ammonia

The TSI model 17C Chemiluminescence NH_3 analyser is based on the reaction of NO with O_3 (equation 2), using the principle that NO and O_3 react to produce a distinguishing luminescence with a concentration directly proportional to the NO concentration. An external pump draws the sample in, where after it mixes with O_3 in the reaction chamber

via an internal ozonator (Figure 5). The reaction in equation 2 then occurs, creating a characteristic luminescence. When electronically charged NO_2 molecules decay to a lower energy state, a specific light emission is produced. This light emission is detected by a photomultiplier tube, which creates a proportional electronic signal. This signal is then processed and recorded as the NO signal (Warneck, 1988; Bradshaw *et al*., 2000; Thermo Environmental Instruments, 2000).

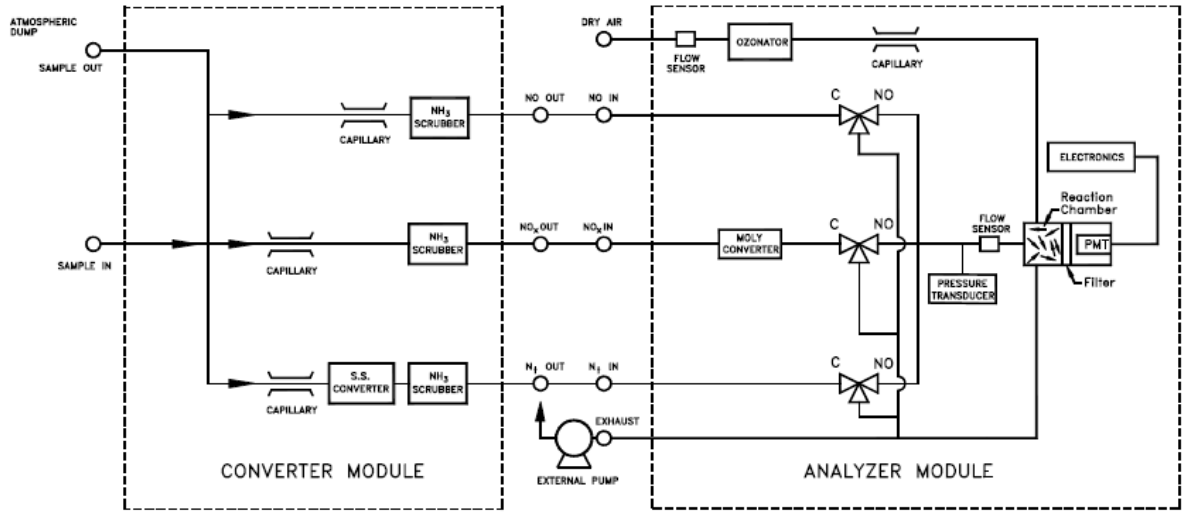


Figure 5. Flow schematic of the TSI 17C NH_3 analyser (Thermo Environmental Instruments, 2000).

In order to measure the NO_x concentration, NO_2 is transformed into NO (in a molybdenum converter heated to 325ºC) before reaching the reaction chamber. When these molecules and the original NO molecules reach the reaction chamber they react with O_3, producing the resultant NO_x concentration reading (Thermo Environmental Instruments, 2000).

To measure the total nitrogen (N_t: NO + NO_2 + NH_3) concentration, all NO_2 and NH_3 are converted to NO in a stainless steel converter which is heated to about 750ºC. In the reaction chamber these molecules (and existing NO molecules) react with O_3, producing the N_t concentration reading. The NO_2 concentration is obtained by subtracting the reading of NO from the reading obtained for NO_x. To determine the NH_3 concentration, the

concentration of NO_x is subtracted from the N_t concentration signal obtained (Thermo Environmental Instruments, 2000).

3.2.1.2 Nitrate

The Rupprecht and Patashnick Series 8400N Ambient Particulate Nitrate Monitor (Figure 6) provides semi-continuous, time resolved measurements of fine particulate matter (PM2.5) mass concentration of ambient particulate nitrates in real time. It measures all forms of inorganic NO_3 in micrograms per cubic meter ($\mu g.m^{-3}$) and computes a new data point every 10 minutes (Rupprecht and Patashnick Co., 2003).



Figure 6. Photograph of the Ambient Particulate Nitrate Monitor's pulse generator outside view (left) and inside view (right).

An inlet system composed of a rain cap, sample line and flexible sheath flow line is used for the sample collection. From here the sample passes through the C3 Pulse Generator for collection, conditioning and flashing (Figure 7). The air sample first passes through a sharp-cut cyclone (to remove the larger particles), then through an activated carbon denuder (to separate out any gaseous material from the particulates) and finally through a critical orifice which then impacts the sample onto a NiChrome flash strip. Those particles that are

not large enough to be detected are grown to larger sizes via humidification through a Nafion tube before impaction. The monitor determines the nitrate concentration by flashing on the NiChrome flash strip. This flashing occurs in a N_2 environment where the flash strip is heated by an electric current from a battery to ~350°C (for about 70 to 90 milliseconds), converting the nitrate in the sample into NO_x. This NO_x that is produced is sent through to the Pulse Analyser for measurement of the gas concentration. The output on the Pulse Analyser is integrated to produce the subsequent NO_3 concentration (Stolzenburg and Herring, 2000; Rupprecht and Patashnick Co., 2003; Harrison *et al*., 2004; Long and McClenny, 2006; Gomez-Moreno *et al*., 2007).

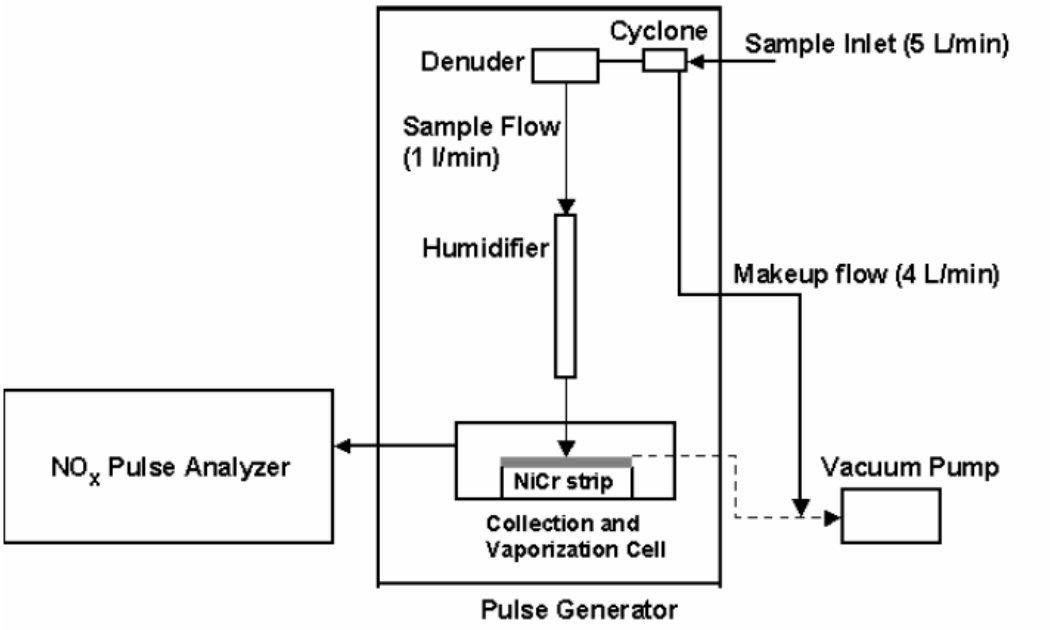


Figure 7. Schematic of the Rupprecht and Patashnick 8400N nitrate monitor,consisting of a pulse generator and pulse analyzer.

The 8400N nitrate monitor is a commercial version of the original prototype produced by Stolzenburg and Herring (2000). Based on a 10 minute monitoring resolution, they found that measurement efficiency was between 95% and 100% for particles > 0.1 μm. Average NO_3 concentrations from this initial study were compared with denuder filter measurements

in three cities and the correlation coefficients were found to be around 0.97 and greater. Data recovery from the instrument was also found to be 97%, with the instrument operating for days, uninterrupted.

There are however some problems encountered when sampling NO_3 aerosols. These include losses of semi-volatile NH_4NO_3 by evaporation; losses due to particle-to-gas conversion during sampling; or nitric acid gas adsorption during sampling. The instrument does attempt to resolve these problems, however minor underestimations in the recorded NO_3 concentrations may result (Stolzenburg and Herring, 2000; Acker *et al*., 2005; Long and McClenny, 2006).

3.3 Data analysis

3.3.1 Temporal variations

NO, NO_2 and O_3 concentration measurements at Elandsfontein are recorded in parts per billion (ppb) and need to be converted into $\mu g.m^{-3}$, to enable a comparison with the particulate nitrate concentration measurements. A simple equation was utilised for this (equation 14), using an average surface pressure of 830hPa and average ambient temperature of 288K (15°C).

$$[\mu g.m^{-3}] = \left(\frac{[ppb] \times \text{Pressure}\,(hPa) \times Molecular\ Weight}{R \div Temperature\,(k)} \right) \div 10 \qquad (14)$$

This equation is derived from the ideal gas equation. R is the gas constant and has a value of $8.314 J.K^{-1}.mol^{-1}$. The molecular weight for each pollutant is calculated by adding the known atomic weight of each individual atom in the molecule. The molecular weight for NO is $30 g.mol^{-1}$, NO_2 is $46 g.mol^{-1}$ and O_3 is $48 g.mol^{-1}$ (Brown et al., 2003b).

Once the concentration in $\mu g.m^{-3}$ is known, then temporal variations for all the pollutants were plotted, in order to have a direct comparison in corresponding units. Box and whisker plots, which are statistical representation methods that indicate the mean, median, 25th and

75^{th} percentile, were also plotted to indicate the measure of spread of the data and to identify any uncertainty in the data sets.

Wind and pollution roses were also generated using one-hour average nitrogen concentrations and wind measurements recorded at Elandsfontein for the 12 month study period; for the different seasons; and for various case study days. In the wind roses, the length of the bar represents the frequency of the wind blowing from a certain direction (with the arcs representing 5% frequency intervals) and the thickness of the bar represents the wind speed. In the pollution roses, the wind frequency is not represented. The length of the bar represents the concentration of the pollutant in question, originating from the direction in which the bar points. The arcs represent concentrations in $\mu g.m^{-3}$. Either the minimum, median, mean, maximum, 25^{th} percentile or 75^{th} percentile concentrations are represented in the pollution roses, allowing for a statistically accurate interpretation of the wind and pollution data.

3.3.2 Conversion rates

Conversion rates of NO to NO_2 were calculated using various case study days when the wind was blowing directly from a power station or industrial source towards Elandsfontein, when high NO_2 concentrations were experienced. To evaluate the rate of conversion, a geometric sequence was used (equation 15), to determine the percentage change of the NO concentration per hour as an air mass travels from its source to the monitoring site.

$$a_n = a_1 r^{n-1} \qquad (15)$$

It was assumed that at the source the ratio of NO to NO_2 is 98:2 (this is known as the initial NO concentration (a_1)). The final concentration (a_n) was calculated as a percentage, based on the ratio of NO to NO_2 concentration recorded at the monitoring site. n is the number of hours taken for an air mass to travel from the source to the receptor. Because the distance between the source and the monitoring site is known, as well as the wind speed during the concentration peak, the time taken for an air mass to travel from the source was calculated using a simple speed-distance-time equation. In equation (15), r is the reduction, which is

the amount that the initial concentration has been reduced from the time it is emitted to the time it is recorded. Since both a_n and a_1 are known in this case, the r value needs to be determined in order to calculate the rate of conversion. Equation (15) was rearranged accordingly to determine r:

$$r = \sqrt[n-1]{\frac{a_n}{a_1}} \qquad (16)$$

For this study, n was relatively low, as the sources are in close proximity to the monitoring site. Therefore, in equation (16), n-1 was not utilised in the calculation, but rather n, as this was not statistically significant. Once r was determined, the conversion rate of NO to NO_2 was calculated via equation (17).

$$\text{Conversion rate (\% per hr)} = (1 - r) \times 100 \qquad (17)$$

Conversion rates for NO to NO_2 were only calculated during the day. This is because without the presence of sunlight, O_3 is unable to be produced and further split up to produce NO_x. Also, any industrial NO_x that is produced at night is trapped above the natural inversion layer. This NO_x would only be detected at the monitoring site much later, after the inversion has dissipated. This would provide an inaccurate indication of the rate of conversion due to the increased residence time in the atmosphere before it is brought to the surface. NO_3 is only created at night, as during the day the NO_3 radical is rapidly photolysed (Wayne *et al*., 1991; Seinfeld and Pandis, 1998; Atkinson, 2000). Any nighttime NO_3 concentration peaks however cannot be of industrial origin, as these emissions are trapped above the inversion layer at night. In determining the NO to NO_3 rates of conversion, the final concentration is known, but the initial concentration is unknown as the plume is not of direct industrial origin. In this case, the NO to NO_3 conversion rates are not calculated as a percentage, but rather the NO to NO_3 ratios at the source and receptor are compared to provide a first step approximation of the rates of conversion.

The calculations for conversion rates described above are based on numerous assumptions. The first assumption is that all the NO_x recorded at Elandsfontein during a NO_2 concentration peak, originates directly from one specific source. This assumes that the NO_x during this peak is not transported from elsewhere and that the initial concentration ratio of $NO:NO_2$ of 98:2 only changes as a result of atmospheric conversion during the transport of the air mass to the monitoring site. Included in this assumption is atmospheric stability, where stable conditions prevail and NO_x is not dispersed upwards. The second assumption is that the rate of conversion of NO to NO_2 is uniform for every hour that the air mass transports downwind. Any outside influences will not speed up or slow down the conversion reaction during transport. A third assumption is that the atmospheric chemistry is conducive to NO_2 formation, with sufficient O_3 available in the atmosphere to allow for the continual formation of NO_2.

3.3.3 Deposition

Deposition is fairly difficult to calculate as it occurs in both wet and dry form. Dry deposition processes are very significant on the Highveld plateau region, as the area receives mostly summer rainfall on average of only 60 days per year (Zunckel *et al*., 1996). Therefore, dry deposition has been the focus for this research. Wet deposition rates were however included in the results and were taken from a study performed by Mphepya in 2002, which investigated the atmospheric deposition characteristics of nitrogen and sulphur species in South Africa.

Rates of dry deposition were calculated using the inferential method, which infers deposition to the surface by calculating the depositional flux (equation 10), utilising the active nitrogen concentration measurements at Elandsfontein along with the deposition velocity (v_d) values taken from literature (Table 1). These values are representative of grassland areas, as the Mpumalanga Highveld is predominantly covered by grassland.

Table 1. Deposition velocity values for NO, NO_2 and NO_3 taken from literature for grasslands.

Species	Deposition velocity (v_d) ($cm.s^{-1}$)	Reference
NO	0 – 1.5	Duyzer *et al.*, 1983
NO	0.016	Seinfeld and Pandis, 1998
NO	0.19	Zapletal, 1998
NO	0.05	Horvath *et al.*, 1998
NO_2	0.05 – 0.56	Wesely *et al.*, 1982
NO_2	0 – 1.5	Duyzer *et al.*, 1983
NO_2	0 – 1.2	Hanson and Lindberg, 1991
NO_2	0.1 – 0.35	Coe and Gallagher, 1992
NO_2	0.11 – 0.24	Hesterberg *et al.*, 1996
NO_2	0.1	Seinfeld and Pandis, 1998
NO_2	0.19	Zapletal, 1998
NO_2	0.27 – 0.34	Watt *et al.*, 2004
NO_3	0.7 – 0.8	Heubert *et al.*, 1988
NO_3	0.2 – 1.2	Hanson and Lindberg, 1991
NO_3	0.12	Hesterberg *et al.*, 1996
NO_3	0.32	Zapletal, 1998

The v_d values in Table 1 range considerably for each of the species. Therefore the average, minimum and maximum v_d values for each of the species were utilised in the inferential model calculations. This resulted in three different sets of flux values, which provide an idea of the uncertainty or the range of possible depositional flux values.

The resultant minimum, average and maximum fluxes that were calculated from this inferential method provide an idea of the rate of deposition of the nitrogen species to the

surface in micrograms per cubic metre per centimetre per second. This was calculated for each month of the year to provide a seasonal depositional signal. Using these monthly flux values, a dry depositional flux value for the whole industrialised Highveld region for one year was calculated in terms of kilograms of nitrogen deposited per hectare per year. This was then added to the total wet deposition flux value taken from Mphepya's study in 2002, producing a total nitrogen flux value to the Highveld for the entire study period. For this purpose the industrialised Highveld region is delineated as a rectangular area that ranges from: just west of Delmas in the west to just east of Ermelo in the east; and just north of Middelburg in the north to south of Standerton (just south of Majuba power station) in the south (Figure 8). This delineated region covers an area of ~ 3 420 000 ha.

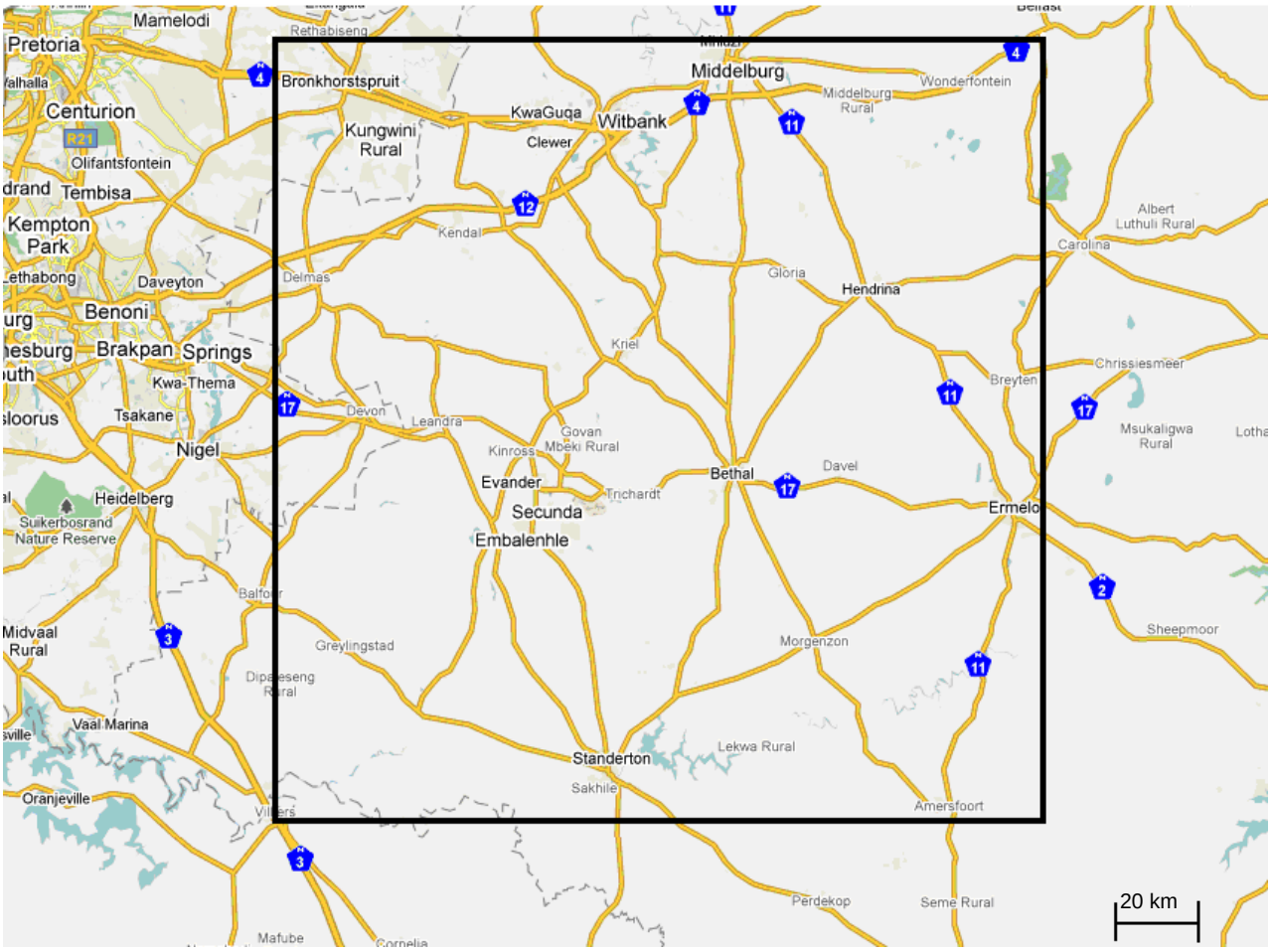


Figure 8. Map indicating the delineated area used to determine total deposition to the Highveld.

****

The results from this field campaign will be presented in the following two chapters. The atmospheric temporal variations of the different nitrogen species will be discussed. Thereafter, the conversion rates of NO to NO_2 as well as the atmospheric removal processes will be investigated.

CHAPTER 4: TEMPORAL VARIATIONS

Seasonal and diurnal variations in the concentrations of the nitrogen species at Elandsfontein are investigated in this section. The affect of meteorological conditions on these variations is also analysed.

4.1 Recorded hourly nitrogen concentrations

The hourly concentration data recorded at Elandsfontein is presented in Figure 9, Figure 10 and Figure 11. From this data a high level of variability in the NO and NO_2 concentrations is evident. There are no distinct monthly patterns in NO and NO_2 concentrations. These values however, clearly indicate that NO_x emissions definitely contribute to air pollution on the Highveld throughout the year. The high peaks in concentration may indicate direct impacts from sources within the vicinity of the monitoring site. Hourly NO_3 concentrations are a lot less variable and indicate seasonal trends with concentrations peaking during late winter and early spring. This peak in concentration correlates well with the seasonal patterns in the monthly average concentration data which will be presented in the next section.

To establish baseline concentration values at Elandsfontein, a 24-hour moving average is applied which smoothes out the data and aids in identifying the underlying trends. The NO moving average data still indicates variability, but some trends are discernable. Slightly higher concentrations during the winter months are evident. The NO_2 moving average data however, still indicates a high amount of variability, with only one discernable peak during March.

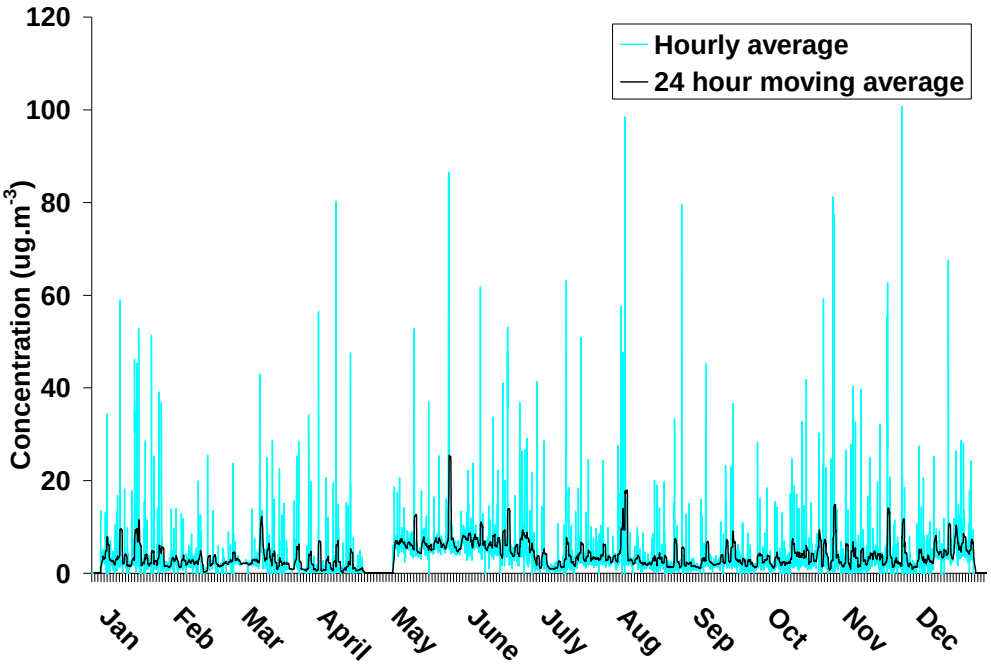


Figure 9. Hourly average NO concentrations plotted together with the 24-hour moving average for Elandsfontein for the period 1 April 2005 to 31 March 2006.

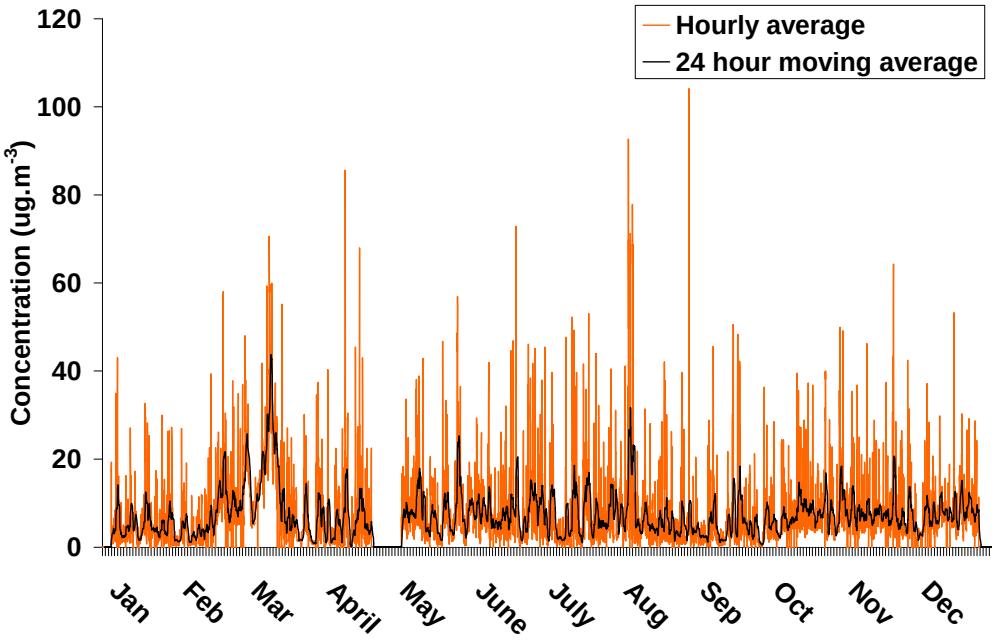


Figure 10. Hourly average NO_2 concentrations plotted together with the 24-hour moving average for Elandsfontein for the period 1 April 2005 to 31 March 2006.

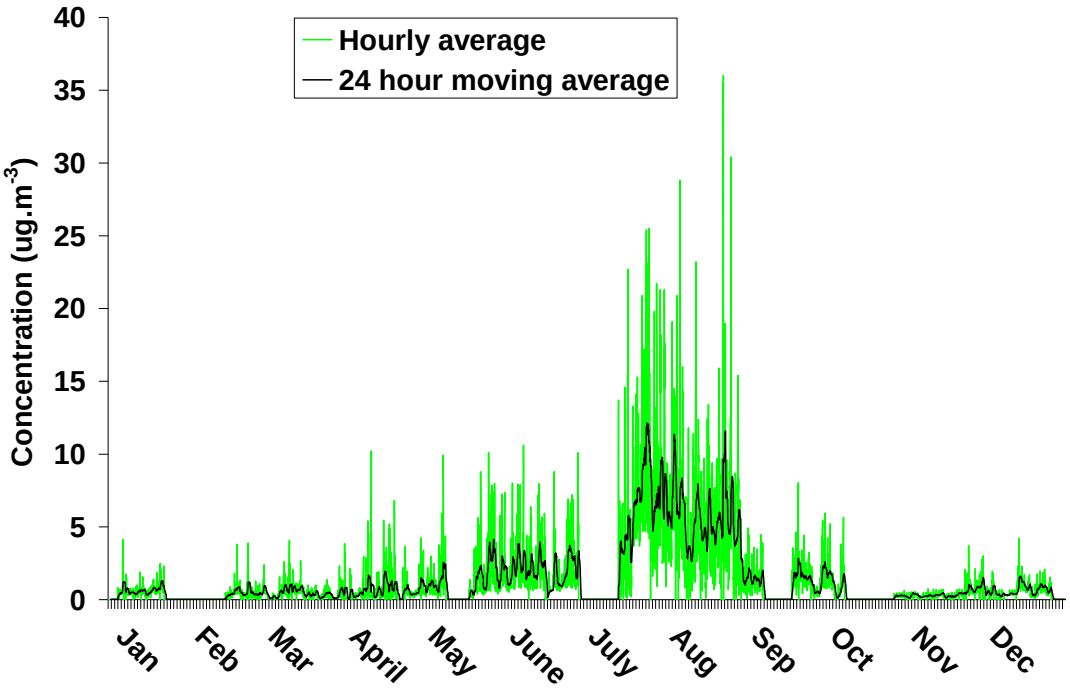


Figure 11. Hourly average NO_3 concentrations plotted together with the 24-hour moving average for Elandsfontein for the period 1 April 2005 to 31 March 2006.

4.2 Seasonal variations of atmospheric nitrogen

NO concentrations peak during early winter (Figure 12), with no other significant trends. The prevalent westerly and north-westerly airflow transports NO directly from the power station sources in the westerly sector that are in close proximity to the monitoring site. This winter peak may also be a result of stable atmospheric conditions, limiting the amount of upward mixing. The lower NO concentrations during April are probably a result of more frequent easterly winds. There are no industrial sources located east of Elandsfontein, so emissions from low-level domestic or vehicular sources may impact at this time.

NO_2 indicates variable concentrations from month to month, with lower concentrations during January, April and September. Highest NO_2 concentrations occur during winter as a result of very stable atmospheric conditions, limiting the amount of atmospheric dilution. The median, maximum, 25^{th} and 75^{th} percentile concentrations are all highly variable throughout the year (Figure 13). Mean and median NO_2 concentrations follow the same

general trend, with slightly higher mean values than the median values. Both the mean and median NO_2 concentrations peak during March. During this month the inter-quartile range of the data is far larger than any other time of the year, which suggests an episode of high NO_x concentrations which in turn raised the average and median values. This therefore may not represent long term seasonal trends.

NO_3 concentrations are relatively low throughout the year, but show a marked peak during July and August (Figure 12). This peak could be a result of no rainfall as well as stable atmospheric conditions leading to accumulation in the region. This is very similar to what was found by Scheifinger and Held (1997) during a study on the Highveld. The peak in August however, is probably augmented by biomass burning emissions in the region at this time. These biomass fires produce high concentrations of NO_x as a result of the high nitrogen content of the fuel. NO_2 concentrations during this time are also expected to be at a maximum as a result of this biomass burning. However, NO_2 readily oxidises due the high occurrence of O_3 in the atmosphere (Figure 15) to produce higher NO_3 concentrations. During May and June, when NO and NO_2 concentrations peak, NO_3 concentrations remain low. Dominant north-westerly flow transports emissions from Kendal, Kriel and Matla power stations. As these sources are at a relatively close distance to Elandsfontein, there is insufficient time for NO_3 to form and hence the higher NO and NO_2 concentrations.

In the box and whisker plot (Figure 14), NO_3 concentrations indicate less variability than the NO_2 dataset. The measure of spread of the data is far greater during July and August compared to the rest of the year. During July and August the median lies closer to the 25^{th} percentile indicating that the distribution of data is skewed to some extent. Maximum, average and median concentrations all peak during August as a result of higher NO_3 emissions from biomass burning. This August peak in NO_3 concentration coincides with a peak in the maximum NO_2 concentration, which is also a result of biomass burning emissions that further oxidise to produce elevated NO_3 concentrations.

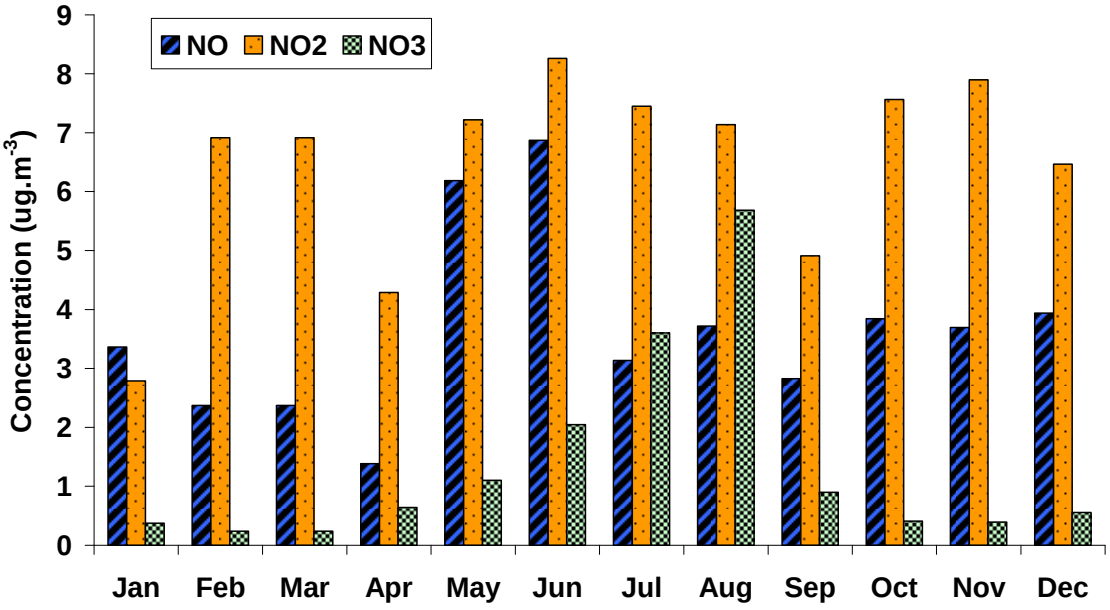


Figure 12. Mean monthly concentration of nitrogen species at Elandsfontein for the period 1 April 2005 to 31 March 2006.

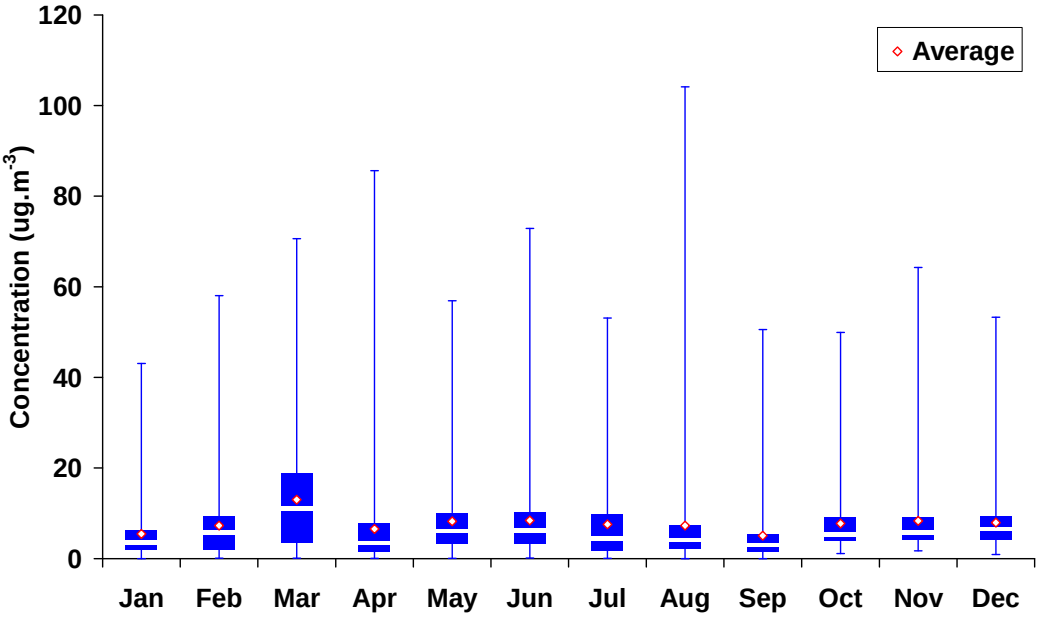


Figure 13. Mean monthly NO_2 box and whisker plot for Elandsfontein for the period 1 April 2005 to 31 March 2006. The average, median (white line), 25th percentile (bottom of box), 75th percentile (top of box), maximum (top whisker) and minimum (bottom whisker) concentration values are represented.

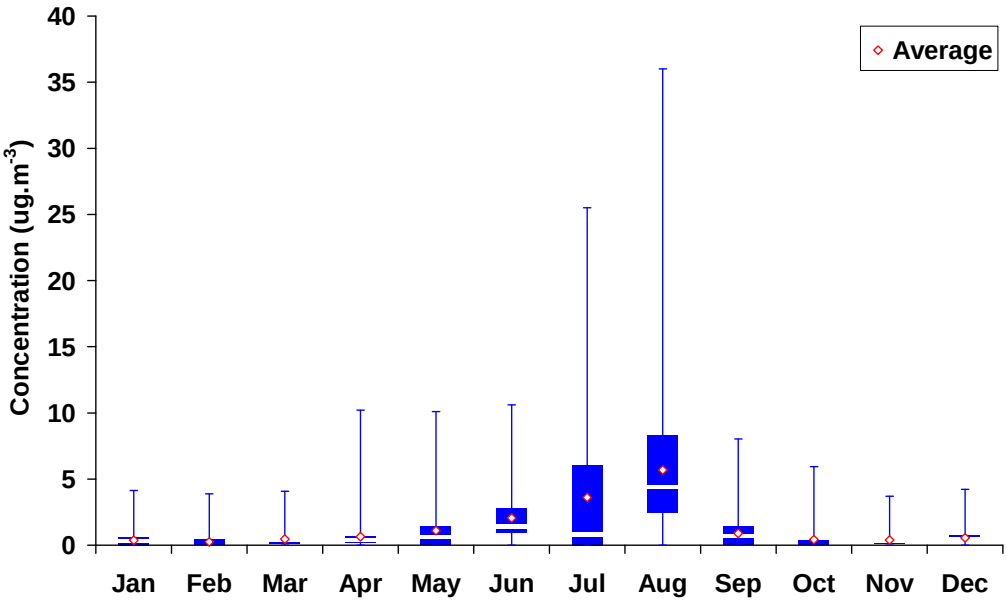


Figure 14. Mean monthly NO_3 box and whisker plot for Elandsfontein for the period 1 April 2005 to 31 March 2006. The average, median (white line), 25th percentile (bottom of box), 75th percentile (top of box), maximum (top whisker) and minimum (bottom whisker) concentration values are represented.

To investigate the NO_x chemistry in the region on a seasonal basis, the O_3 concentration is plotted together with the NO_x concentration (Figure 15). O_3 concentrations are at a minimum in April and October and peak during winter as a result of higher NO_2 concentrations which in the presence of sunlight, react to form O_3. High O_3 concentrations during August are a result of biomass burning in the region, which produces high concentrations of O_3 precursors.

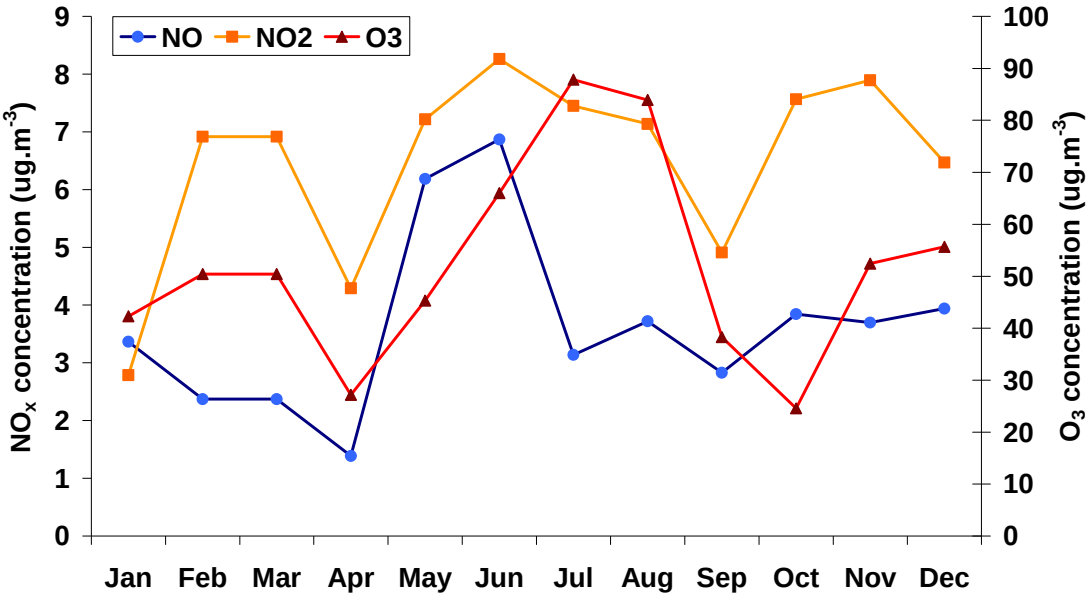


Figure 15. Mean monthly NO_x and O_3 concentrations at Elandsfontein for the period 1 April 2005 to 31 March 2006.

4.3 Diurnal variations of atmospheric nitrogen

Diurnally, NO and NO_2 concentrations are low during the night and peak around midday (Figure 16). This is a result of surface inversions which develop at night. Industrial stacks are 200 – 300 m in height and emit pollutants well above this natural inversion. Pollutants are unable to move to the surface at night. After sunrise, convective mixing is initiated and the surface inversion breaks down, allowing pollutants to be transported to ground level, hence the increase in concentrations at this time. NO_2 is not directly emitted from the stacks, but is created via the oxidation of NO. NO and NO_2 are trapped above the inversion at night and are both brought to the surface during the day. O_3 concentrations are low at night and peak during the day when both NO_2 and sunlight are available. The diurnal trends in concentration however do not reflect the expected NO_x–O_3 photochemical behaviour. During the O_3 peak, there is not a major drop in NO_2 concentration, so it can be assumed that some of the O_3 was transported into the area or that NO_2 is continually forming. This continual NO_2 formation is evident at 12:00 when the rate of increase in O_3 concentration slows down as NO_2 continues to form and its concentration peaks. There is also a disproportionate amount of O_3 produced in the atmosphere in relation to the amount of NO_2 that is available. This may be due to the fact that not all of the O_3 is a direct result of NO_2 dissociation. O_3 also exists at background levels of ~40µg.m^{-3}.

Median NO and NO_2 concentrations indicate little variability throughout the day and unlike the average concentrations, are not that significantly higher at midday (Figure 17). The highest inter-quartile ranges of NO are experienced between 11:00 and 15:00 and of NO_2 between 11:00 and 17:00. The median in both cases is much closer to the 25th percentile, indicating that the data during these times is skewed to some degree.

To aid in confirming that the NO_x emissions recorded at Elandsfontein are predominantly a result of industrial sources, black carbon and SO_2 are also plotted in Figure 16. From the major peak in SO_2 at midday, it is assumed that these emissions are from an industrial source. There are no peaks in SO_2 and black carbon concentrations during peak traffic times in the morning or evening, confirming that the emissions monitored at Elandsfontein do not originate from motor vehicles or domestic coal fires in the region.

NO_3 concentrations increase at night and are lower during the day (Figure 18). This is because during the day the NO_3 radical is rapidly photolysed and nitrates cannot be formed.

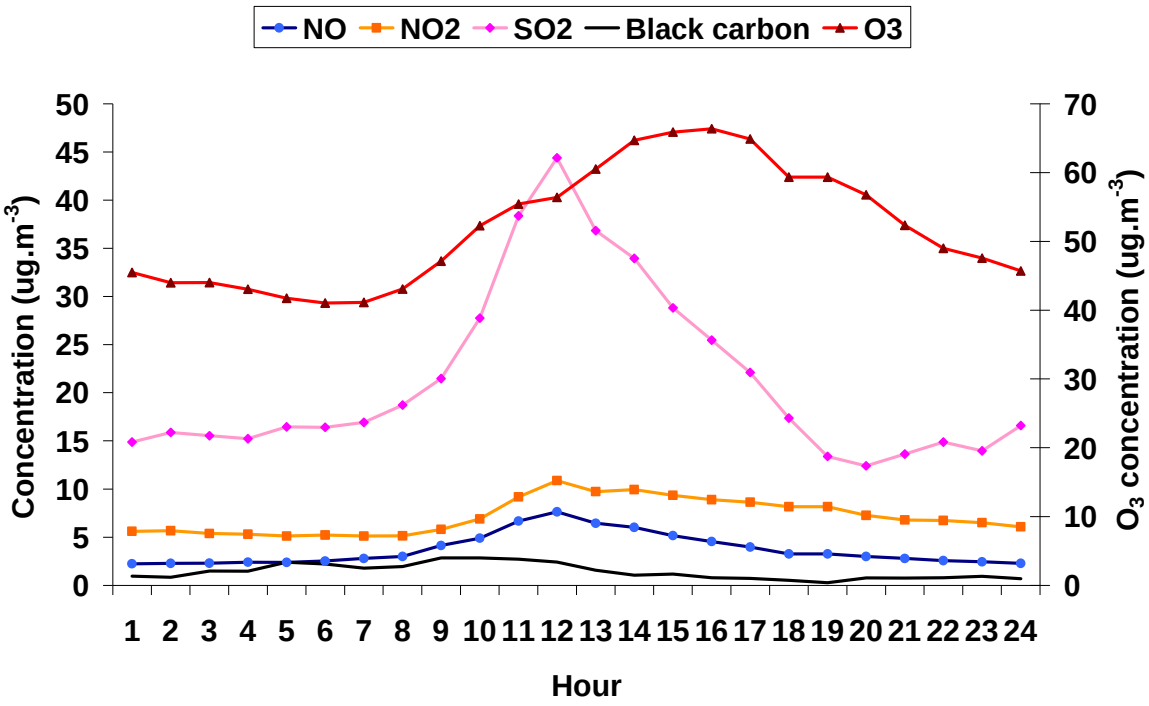


Figure 16. Mean hourly concentrations of pollutants at Elandsfontein for the period 1 April 2005 to 31 March 2006.

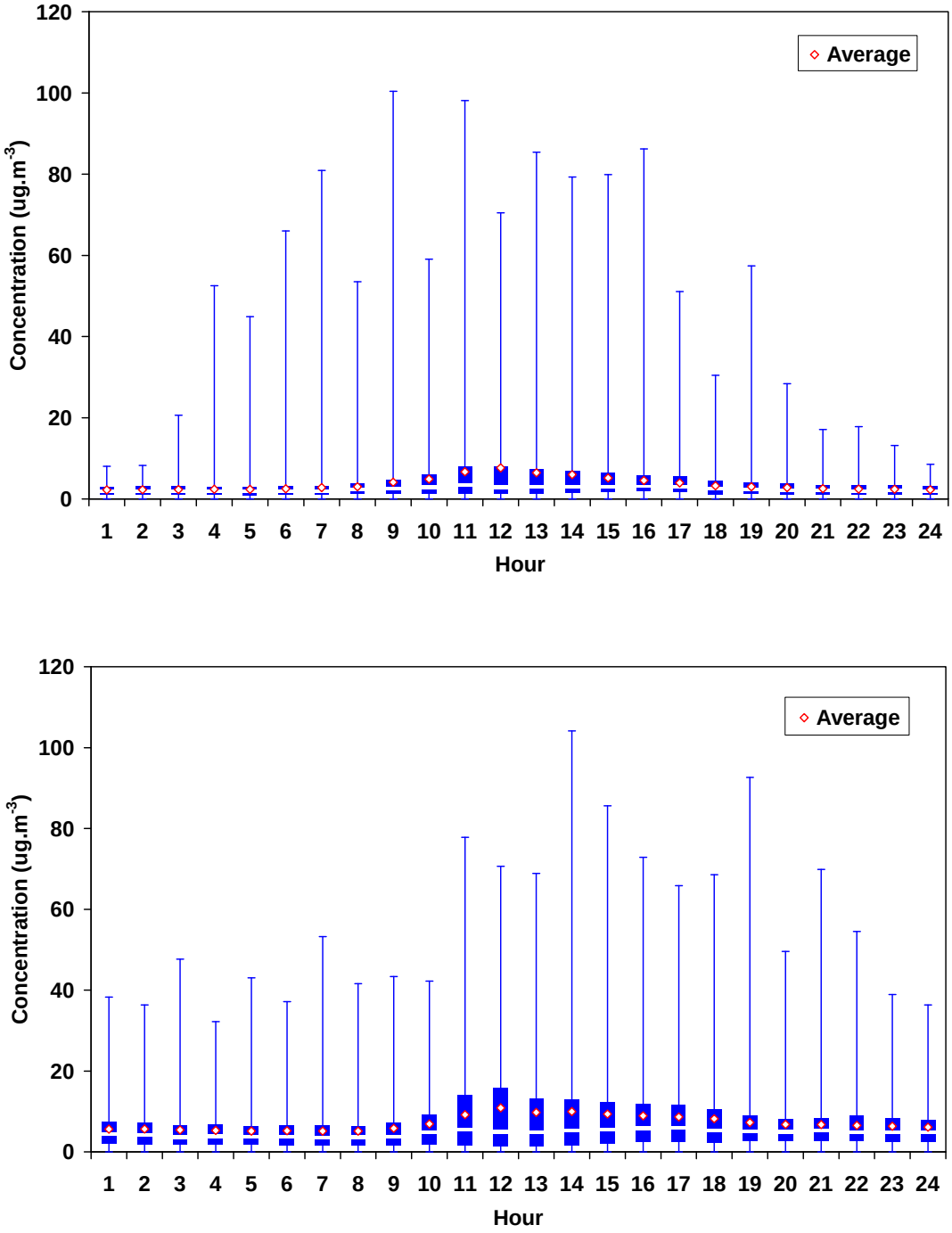


Figure 17. Diurnal box and whisker plot for NO (top) and NO_2 (bottom) for the period 1 April 2005 to 31 March 2006. The average, median (white line), 25th percentile (bottom of box), 75th percentile (top of box), maximum (top whisker) and minimum (bottom whisker) concentration values are represented.

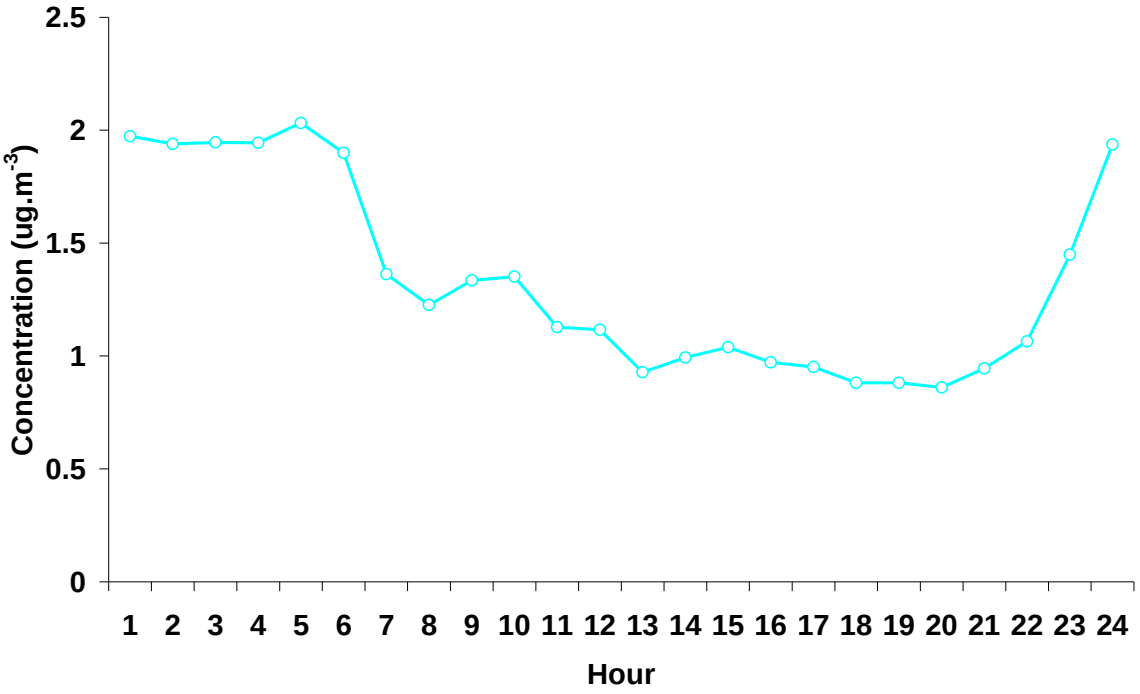


Figure 18. Mean hourly concentrations of NO_3 at Elandsfontein for the period 1 April 2005 to 31 March 2006.

Kendal monitoring station is situated two kilometres directly downwind of Kendal power station, providing a clear industrial source signature. Data from Kendal monitoring station is also plotted (Figure 19) in order to provide confirmation that the measurements at Elandsfontein predominantly reflect the influence of industrial sources. NO and SO_2 concentrations peak at midday, just as they do at Elandsfontein. NO_2 concentrations are lower during this peak, as a result of limited transport time between the source and receptor for NO to oxidise into NO_2. This may also be a result of O_3 formation, as NO_2 is used up in the formation of O_3 during the afternoon. O_3 is also not directly emitted from Kendal and O_3 concentrations gradually increase after sunrise, reaching a maximum after the direct plumes from Kendal have been dispersed.

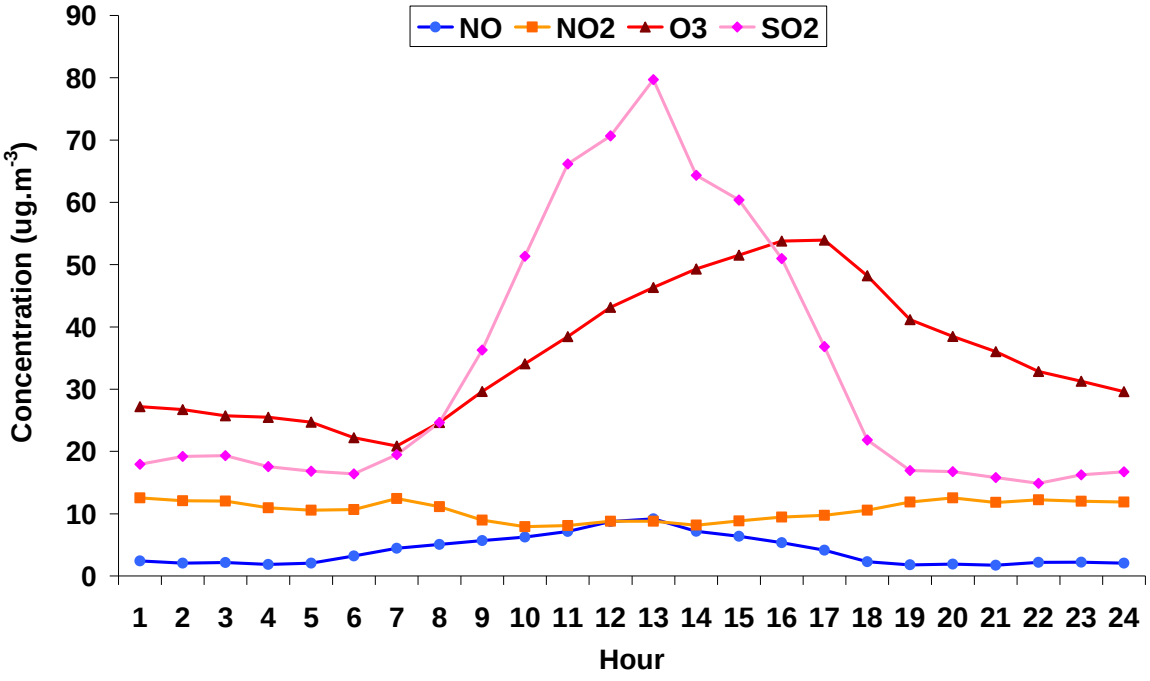


Figure 19. Mean hourly concentrations of pollutants at Kendal monitoring station for the period 1 April 2005 to 31 March 2006.

During a fresh plume strike at Kendal monitoring site on 21 August 2005 (Figure 20), NO and SO_2 concentrations once again peak at midday, but at a more concentrated level as less dilution has occurred. NO_2 concentrations are lower than NO concentrations during this

peak due to limited oxidation time. O_3 concentrations decrease in the plume as a result of NO_2 formation, to such a degree that there is a proportionate amount of NO_2 produced compared to the amount of O_3 consumed. O_3 is also not directly emitted from the source. After the plume has passed, O_3 concentrations increase and reach a maximum in the late afternoon, just as in Figure 19. This direct plume strike case study provides a classic tall stack signature. This underlying pattern is visible in the Elandsfontein data (Figure 19), providing further evidence of tall stack sources at the site.

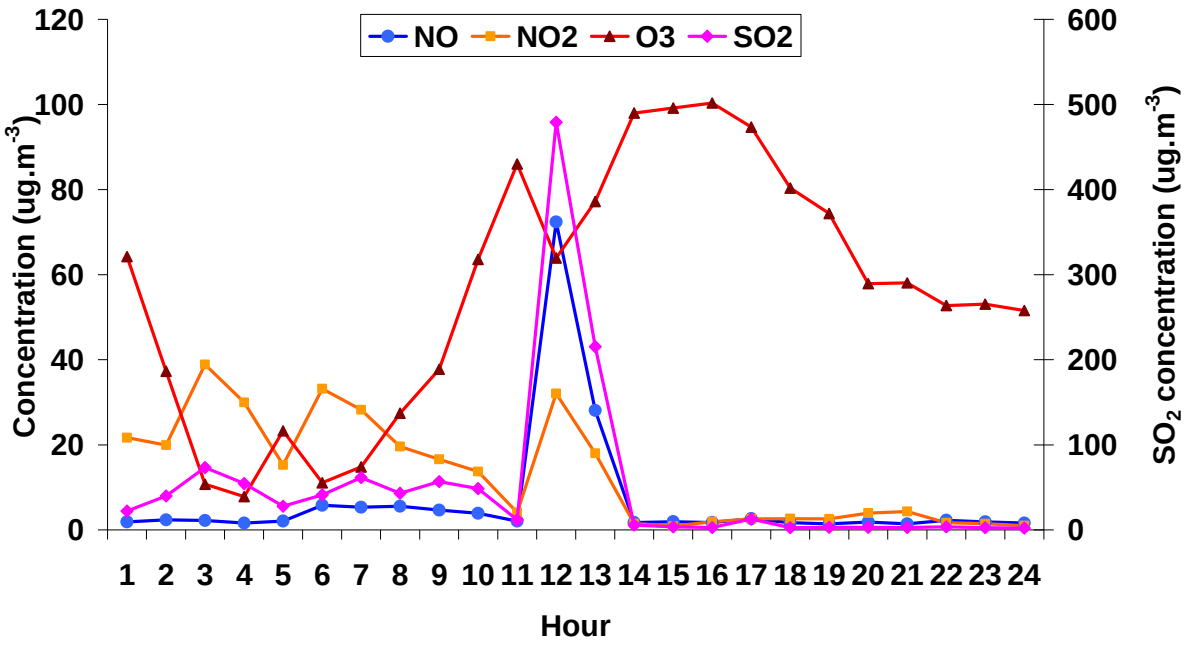


Figure 20. Mean hourly concentrations of pollutants at Kendal monitoring station during a fresh plume strike on 21 August 2005.

Seasonally, diurnal variations of NO at Elandsfontein indicate the overriding influence of tall stack sources with concentrations in summer, autumn and winter peaking at midday (Figure 21). Winter concentrations are higher than the other seasons as a result of stable anticyclonic circulation, limiting the amount of dispersion before plumes are brought to the ground; a higher demand for power associated with more coal combustion (Terblanche *et al*., 1993); as well as north-westerly airflow, transporting NO emissions directly from the power station sources to Elandsfontein. Autumn and spring concentrations are slightly lower than the winter situation; however the spring peak is between 09:00 and 10:00 unlike the other midday peaks. This earlier peak may be a result of biomass burning plumes that are not dispersed upwards as a result of surface inversions that have not yet dissipated.

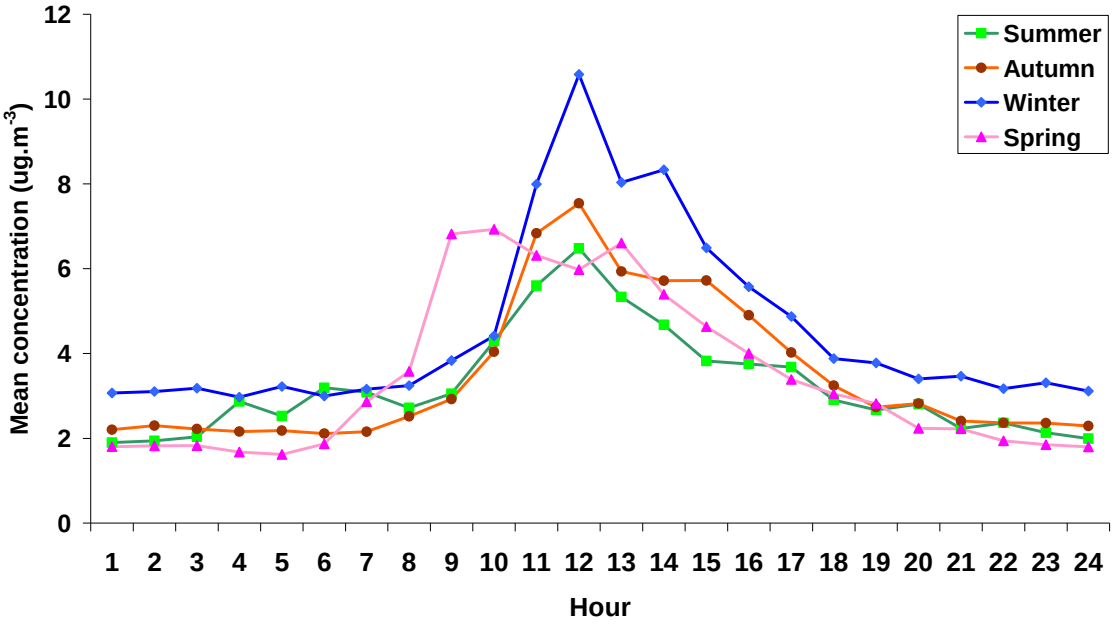


Figure 21. Mean hourly NO concentrations for each season during the period 1 April 2005 to 31 March 2006.

NO_2 concentrations are slightly higher than NO concentrations throughout the year. NO_2 concentrations peak at midday in summer, winter and autumn just as NO does (Figure 22). NO_2 concentrations are low at night and gradually start to increase after sunrise, when air becomes well mixed, transporting industrial NO_2 to the ground. During spring, the peak in concentration occurs at 13:00 unlike the 09:00 to 10:00 peak in the NO dataset. Between 09:00 and 10:00 however, the spring concentrations are higher than during the rest of the year as a result of biomass burning emissions that have not yet dispersed upwards.

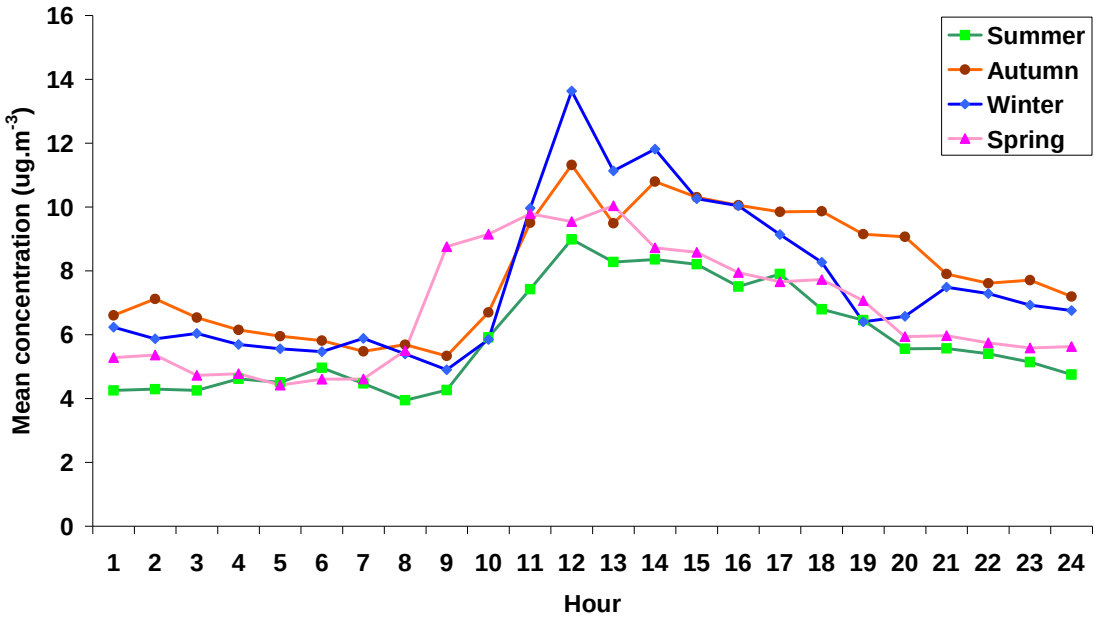


Figure 22. Mean hourly NO_2 concentrations for each season during the period 1 April 2005 to 31 March 2006.

The seasonal diurnal variations for particulate nitrates are very different to the diurnal signature of NO and NO_2 (Figure 23). All seasons indicate lower daytime concentrations, as during the day NO_3 rapidly photolyses and nitrates cannot be produced (Wayne *et al*., 1991; Seinfeld and Pandis, 1998; Atkinson, 2000). Summer, autumn and spring concentrations are low and remain below 1µg.m^{-3} the entire day. Winter concentrations indicate a unique signature. Higher night-time concentrations (around 6µg.m^{-3}) are experienced with a drop to around 2.5µg.m^{-3} during the day. Overall, the winter concentrations are much higher than

the rest of the year, as a result of atmospheric accumulation due to stable conditions and no rainfall at this time.

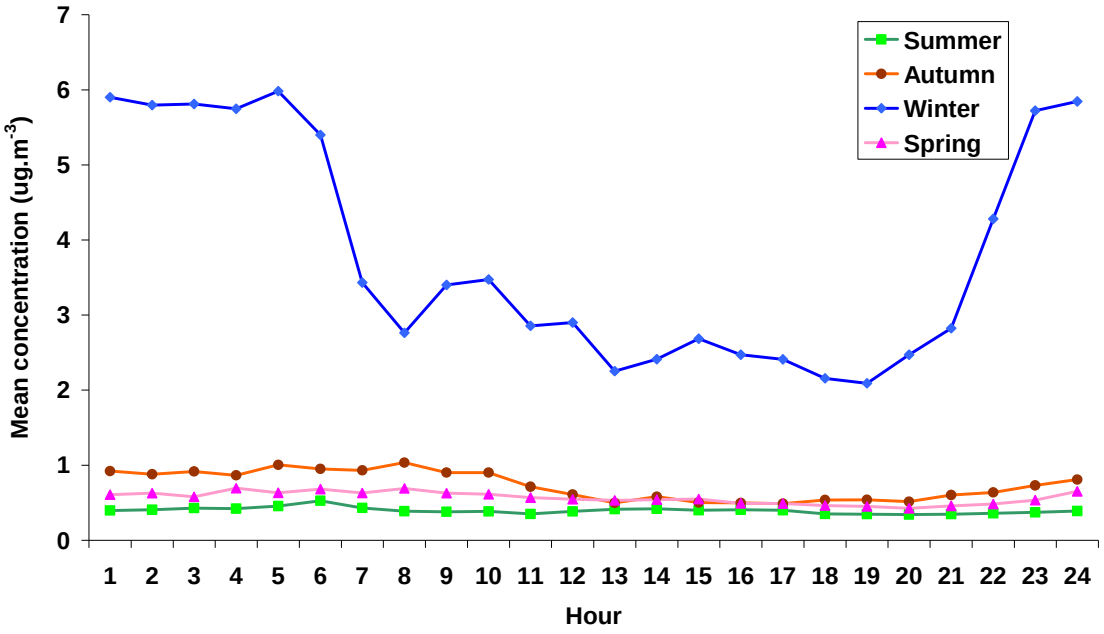


Figure 23. Mean hourly NO_3 concentrations for each season during the period 1 April 2005 to 31 March 2006.

4.4 The dependence of concentrations of nitrogen species on wind direction

The recorded concentrations of nitrogen species are highly dependant on the dominant wind direction. Winds may blow from a specific sector most of the time, however if nitrogen sources are not present in that region, concentrations will remain low.

For the entire study period, winds at Elandsfontein are predominantly between 2 and 6 $m.s^{-1}$ (Figure 24) with winds greater than 6 $m.s^{-1}$ and less than 2 $m.s^{-1}$ occurring less than 30% of the time. Winds are predominantly from the north-north-westerly sector (~30% of the time) and the easterly sector (~28% of the time).

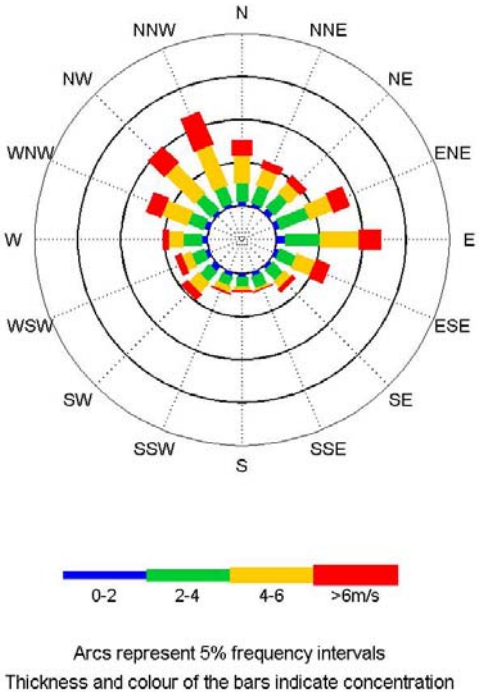


Figure 24. Wind rose for Elandsfontein for the period 1 April 2005 to 31 March 2006.

Seasonally, wind direction patterns change significantly as a result of changing synoptic conditions (Figure 25). During summer easterly winds are dominant as a result of easterly waves, with winds blowing from this sector more than 40% of the time. During winter, winds from the north-westerly sector associated with anticyclonic circulation, are more

frequent. These winds blow for more than 30% of the time. During autumn and spring, both easterly and north-westerly airflow occur.

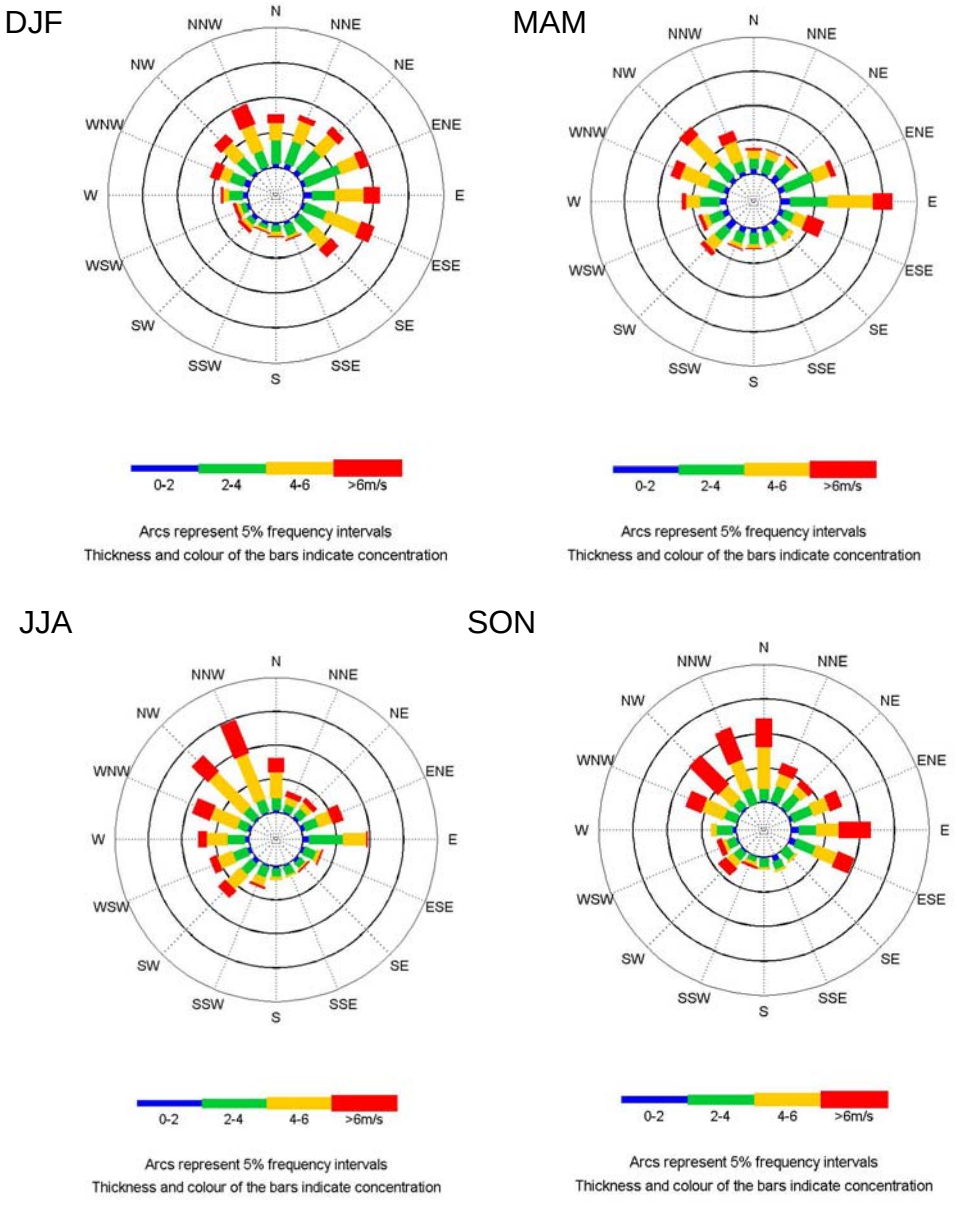


Figure 25. Seasonal wind roses for Elandsfontein for summer (December/January/February); autumn (March/April/May); winter (June/July/August) and spring (September/October/November).

The direction and distance of the various nitrogen emission sources relative to Elandsfontein monitoring site are presented in Table 2. These values, together with the location map in Figure 4, aid in the interpretation of the pollution rose data that follows.

Table 2. The distances and directions of the different nitrogen sources surrounding Elandsfontein monitoring site.

Source	Distance from Elandsfontein (km)	Direction from Elandsfontein
Kendal power station	50	WNW
Kriel and Matla power station	25	W
Duvha power station	33	NNW
Hendrina power station	30	NNE
Arnot power station	51	NE
Tutuka power station	59	S
Secunda petrochemical plant	40	SW

NO and NO_2 concentrations at Elandsfontein are higher when associated with winds from the north-north-westerly and westerly sectors (Figure 26 and Figure 27). It is most likely that this NO_x originates from four power stations located in these sectors that are only 25 to 50km from the monitoring site. Maximum NO concentrations peak at about 100µg.m^{-3} and are slightly higher than the maximum NO_2 concentrations which peak around 65µg.m^{-3}. Highest maximum concentrations of both species are experienced when the wind blows from the north-north-westerly sector, directly from the area where Duvha power station is situated. Average concentrations are highest in association with westerly flow from Kriel and Matla power stations (Figure 26). Average concentrations peak at around 10 to 11 µg.m^{-3} for both NO and NO_2. These high concentrations originating from the westerly sector may also be augmented by industrial and vehicular emissions that are transported from the Ekhuruleni area to the west of Elandsfontein.

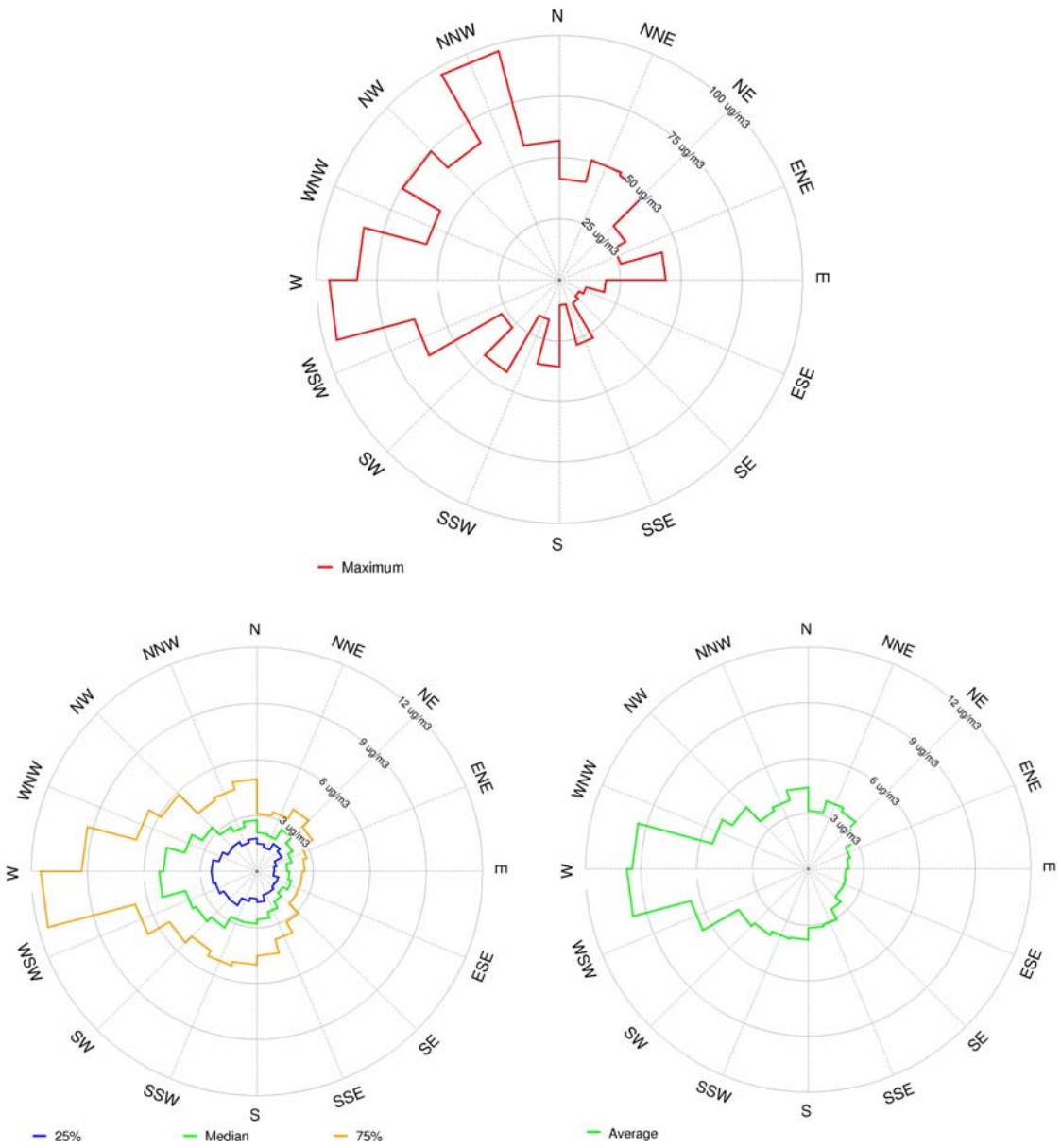


Figure 26. Pollution roses indicating the maximum NO concentration (top); the median, 25th and 75th percentile NO concentrations (bottom left); and the average NO concentration (bottom right) at Elandsfontein for the period 1 April 2005 to 31 March 2006.

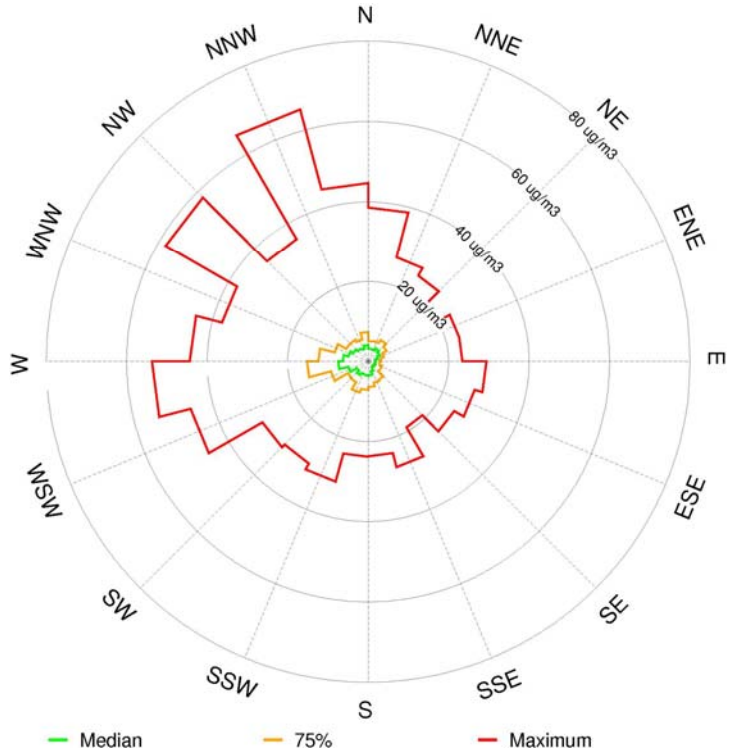


Figure 27. Pollution rose indicating the median, 75th percentile and maximum concentrations of NO_2 at Elandsfontein for the period 1 April 2005 to 31 March 2006.

Average, median, maximum, 25th and 75th percentile NO_3 concentrations at Elandsfontein all peak in association with winds from the north-north-westerly and south-westerly sectors (Figure 28). Although nitrates are secondary pollutants and are not directly emitted into the atmosphere, these elevated concentrations are associated with NO_x emission sources that are located far enough from Elandsfontein to allow for sufficient oxidation for NO_3 production. Using an average NO_2 to NO_3 oxidation rate of between 0.1 to 12%.h^{-1} calculated during a previous power station plume study (Forrest *et al*., 1981) together with the average wind speed (1.5 m.s^{-1}), the resultant time taken for NO_2 to convert into NO_3 is between 1.5 to 2.5 hours (depending on which source is used in the calculation). Therefore, all of the NO_x sources are located at a sufficient distance from Elandsfontein to allow for substantial NO_3 concentrations to be recorded at the monitoring station. These sources include a petrochemical plant to the south-west in Secunda and Kriel, Matla, Kendal and Duvha coal-fired power stations in the north-westerly sector. The area to the south-west

most probably contains the dominant NO_3 source as the median, 75th percentile and average concentrations are the highest from this direction. Peaks in the maximum NO_3 concentration are also experienced in association with airflow from the north-east and east-north-east. These peaks may be associated with Hendrina and Arnot power stations located north-east of Elandsfontein.

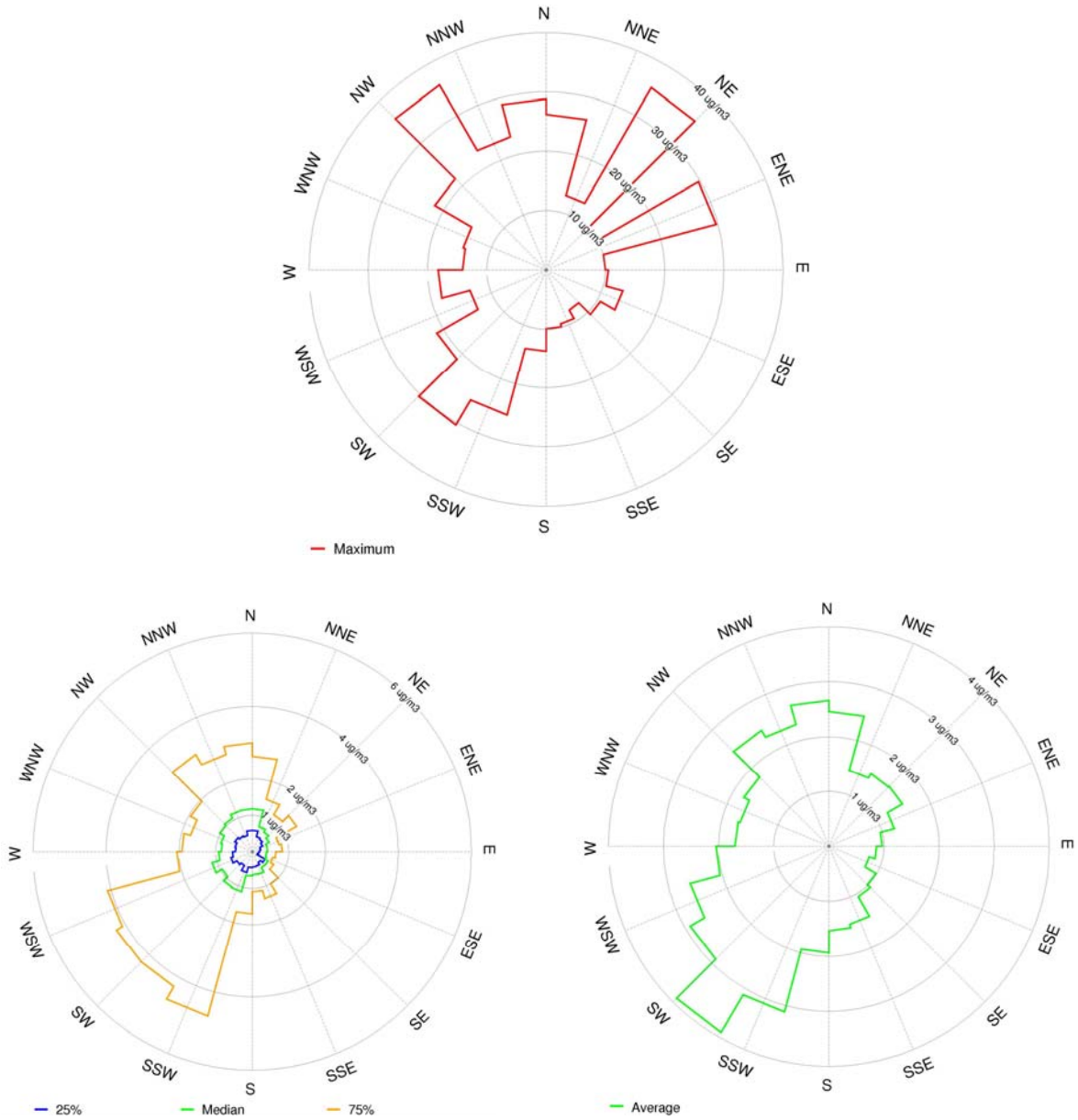


Figure 28. Pollution roses indicating the maximum NO_3 concentration (top); the median, 25th and 75th percentile NO_3 concentrations (bottom left); and the average NO_3 concentration (bottom right) at Elandsfontein for the period 1 April 2005 to 31 March 2006.

In comparison with the NO and NO_2 pollution roses, NO_3 concentrations peak in association with south-westerly and north-north-westerly flow whereas NO_x concentrations only peak when the wind blows from a westerly or north-north-westerly direction. NO_x

does originate from sources to the south-west (or else NO_3 would not form), however in comparison with sources in the westerly sector this concentration is not that significant. NO_3 concentrations do not peak significantly in association with westerly flow, as the power station sources in this sector are too close to Elandsfontein to allow for sufficient oxidation time for NO_3 to form. Air mass recirculation is a major transport pathway for aerosols over southern Africa. The variation in the concentration distribution of NO_3 measured at Elandsfontein may not only be a result of local nitrogen emissions, but may also be associated with long range transport as a result of recirculation (Tyson *et al*., 1996b; Freiman and Piketh, 2003).

****

> NO, NO_2 and NO_3 all exhibit higher concentrations during winter, especially NO_3. This is due to no rainfall at this time of the year as well as increased atmospheric stability leading to accumulation of particles in the atmosphere. Diurnally, NO and NO_2 concentrations peak at midday and decrease during the night, clearly indicating tall stack industrial sources. NO_3 concentrations show a reverse diurnal signature with higher concentrations at night. This is due to photolysis which prevents nitrate formation during the day. The highest concentrations of NO and NO_2 are associated with power station sources to the west and north-north-west of the monitoring site. NO_3 concentrations are highest in association with winds from the south-west, which transport NO_x emissions directly from Secunda. Now that an understanding of the temporal behaviour of the nitrogen species has been gained, the atmospheric reactions, conversions and removal processes will be examined in the following chapter.

CHAPTER 5: ATMOSPHERIC CONVERSION AND REMOVAL

In this chapter the rate of conversion of NO to NO_2 in the atmosphere on the Highveld is investigated in order to gain further understanding of atmospheric nitrogen chemistry. Rates of deposition of the nitrogen species on the Highveld are also examined; as such removal processes provide an indication of how ecosystems may be affected by increased nitrogen concentrations.

5.1 Rates of atmospheric conversion

Six case study days have been selected, when the NO_2 concentrations are relatively high and the wind is blowing directly from an industrial source to the Elandsfontein monitoring site. These criteria are selected as they provide an idea of where an airmass originated from and hence the rate of conversion can be calculated based on the distance between the source and the receptor. The results of the NO to NO_2 conversion rate calculations using equations (16) and (17) are displayed in Table 3. O_3 concentrations and ambient temperature are also shown in order to determine whether these parameters have any effect on the rate of conversion on a given day. NO_2 conversion rates are only calculated for daytime conditions since sunlight is needed for O_3 formation and break-up.

Rates of conversion of NO to NO_2 range from 11% to 59% per hour (Table 3). It is observed that the higher the concentration of O_3, the higher the NO to NO_2 conversion rate. This may be due to the fact that the more O_3 that is available for oxidation, the greater the capacity for NO_2 formation. It is also evident that the ambient temperature does not directly affect the rate of conversion.

Table 3. Calculated rates of conversion of NO to NO_2 at Elandsfontein for various case study days during the period 1 April 2005 to 31 March 2006. O_3 concentrations and temperature are also listed.

Date	Time	Source	Time from source to receptor (hrs)	NO to NO_2 ($\%.hr^{-1}$)	O_3 conc. ($\mu g.m^{-3}$)	Temp. (° C)
11 April 2005	12:00 – 13:00	Secunda	6.5	21.27	55.49	21.85
11 April 2005	14:00 – 17:00	Kriel/ Matla	3.9	29.78	32.11	22.2
27 May 2005	11:00 – 13:00	Kendal	4.19	10.67	12.06	16.67
27 May 2005	15:00 – 18:00	Kendal	4.64	15.09	1.3	19.0
9 June 2005	11:00 – 12:00	Kriel/ Matla	1.18	33.5	25.2	17.9
7 August 2005	11:00 – 13:00	Kriel/ Matla	3.32	17.13	46.81	19.37
7 August 2005	15:00 – 18:00	Duvha	3.71	34.62	110.81	23.6
30 August 2005	13:00 – 15:00	Duvha	1.59	43.23	141.74	24.67
22 November 2005	09:00 – 14:00	Kriel/ Matla	1.19	47.15	70.16	25.43
11 March 2006	10:00 – 12:00	Kendal	3.43	33.82	59.51	21.63
11 March 2006	13:00 – 17:00	Kriel/ Matla	1.62	59.45	86.35	24.54

The conversion rate values in Table 3 range quite significantly. These values do however correspond well with the maximum NO to NO_2 conversion rate of 30% per hour calculated by Hewitt (2001). Gertler et al. (1984) however found much lower conversion rates of around 8% per hour. Calculating conversion rates is very challenging, as they are based on numerous assumptions. These assumptions include: that all the NO and NO_2 comes from one specific source; and that the rate of conversion is uniform for each hour that the air mass transports downwind. Other factors that need to be considered when calculating conversion rates are: dispersion in the region, stability, transport from other areas, regional atmospheric chemistry and time of day.

To provide a comparison of conversion rates at a close proximity to a source to those further away, conversion rates of NO to NO_2 from Kendal power station are calculated from data collected approximately 2 km from the power station at Kendal monitoring site (Table 4). NO to NO_2 conversion rates at Kendal monitoring station range from 66 % to 94 % per hour. These rates are a lot higher than those calculated for Elandsfontein because the conversions rates decrease exponentially with time. The rates are more rapid initially when there are higher NO concentrations and slow down as the air mass travels further from the source.

Table 4. Calculated rates of conversion of NO to NO_2 at Kendal for various case study days during the period 1 April 2005 to 31 March 2006. O_3 concentrations and temperature are also listed

Date	Time	Source	Time from source to receptor (hrs)	$NO:NO_2$ ($\%.hr^{-1}$)	O_3 conc. ($\mu g.m^{-3}$)	Temp. (° C)
10 May 2005	14:00 – 16:00	Kendal	1.18	66.34	53.13	25.37
4 July 2005	15:00 – 17:00	Kendal	2.52	69.94	51.97	20
8 July 2005	12:00 – 16:00	Kendal	0.32	91.2	53.74	24.94
18 July 2008	17:00 – 18:00	Kendal	0.38	94.36	-	18.9
21 August 2005	12:00 – 13:00	Kendal	0.11	92.61	70.55	25.35
13 October 2005	11:00 – 14:00	Kendal	0.11	90.08	71.09	32.82

Conversion rates of NO to NO_3 are not easily calculated as NO_3 only forms at night. A peak in NO_3 concentration at night is not related to an industrial plume. This is because the plumes are trapped above the natural inversion layer at night and are not detected at the monitoring site. Any peaks during the night can be attributed to aged industrial plumes or plumes from non-industrial NO_x sources that are close to the surface. In order to gain some understanding of the conversion of NO to NO_3, conversion rate percentages are not depicted, but rather the source and receptor concentration ratios of NO to NO_3 when recorded NO_3 concentrations are high during the day (Table 5).

Table 5. NO to NO_3 concentration ratios at the source and at Elandsfontein for various case study days during the period 1 April 2005 to 31 March 2006 when NO_3 concentrations are high

Date	Time	Source	Time from source to receptor	NO:NO_3 ratio at the source	NO:NO_3 ratio at Elandsfontein
9 May 2005	17:00 – 19:00	Tutuka	5.8	100:0	0.73:1
31 May 2005	09:00 – 11:00	Duvha	1.67	100:0	1.9:1
7 June 2005	09:00 – 12:00	Duvha	1.55	100:0	2.3:1
26 June 2005	09:00 – 10:00	Kriel/ Matla	2.34	100:0	0.94:1
24 July 2005	09:00 – 11:00	Tutuka	5.9	100:0	0.3:1
24 July 2005	14:00 – 16:00	Secunda	3.06	100:0	0.42:1

The case studies in Table 5 all represent the possibility that the high NO_3 concentrations on these days originate from NO_x emissions from industrial sources. The peaks in NO_3 concentration occur during the day, after the inversions have dissipated and air can be transported to the ground. Although the NO_3 radical is photolysed during the day, these nitrates that are recorded are already in aerosol form having reacted with other cations during the night and do not become photolysed. NO_2 concentrations peak at the same time as NO_3 concentrations in all case studies. This may indicate that the NO_3 originates from the same tall stack industrial NO_x sources or that if these species originate from low-level emission sources in the region, the rate of conversion of NO_2 to NO_3 occurs very rapidly.

5.2 Case studies

Case studies are presented below for specific days when emissions were transported directly from non-industrialised and industrialised areas. The case studies provide further insight into diurnal variations and specific conversion rates of the species from various point sources.

5.2.1 Background atmospheric pollution levels at Elandsfontein

A situation when no direct emission sources are impacting on the monitoring site occurs on 5 April 2005. Concentrations of all pollutants are variable and low throughout the day with no distinct peaks (Figure 29). There is a slight peak in NO_2 concentrations (very small – only 2 $\mu g.m^{-3}$) in the early evening between 17:00 and 19:00. This peak corresponds with a peak in black carbon concentrations. SO_2 concentrations are low and do not peak at this time, confirming that the source of the higher NO_2 and black carbon concentrations is not a result of motor vehicles or domestic coal burning in the area. There is a prevalent easterly wind blowing at ~4$m.s^{-1}$. Various agricultural plots are located just east of Elandsfontein, so it can be assumed that the slightly higher NO_2 and black carbon concentrations at this time may be a result of local domestic biomass fires. During the NO_2 peak, O_3 and NO concentrations decrease slightly as they are used up in the process of NO_2 formation. NO_3 concentrations are low and are only slightly higher at night.

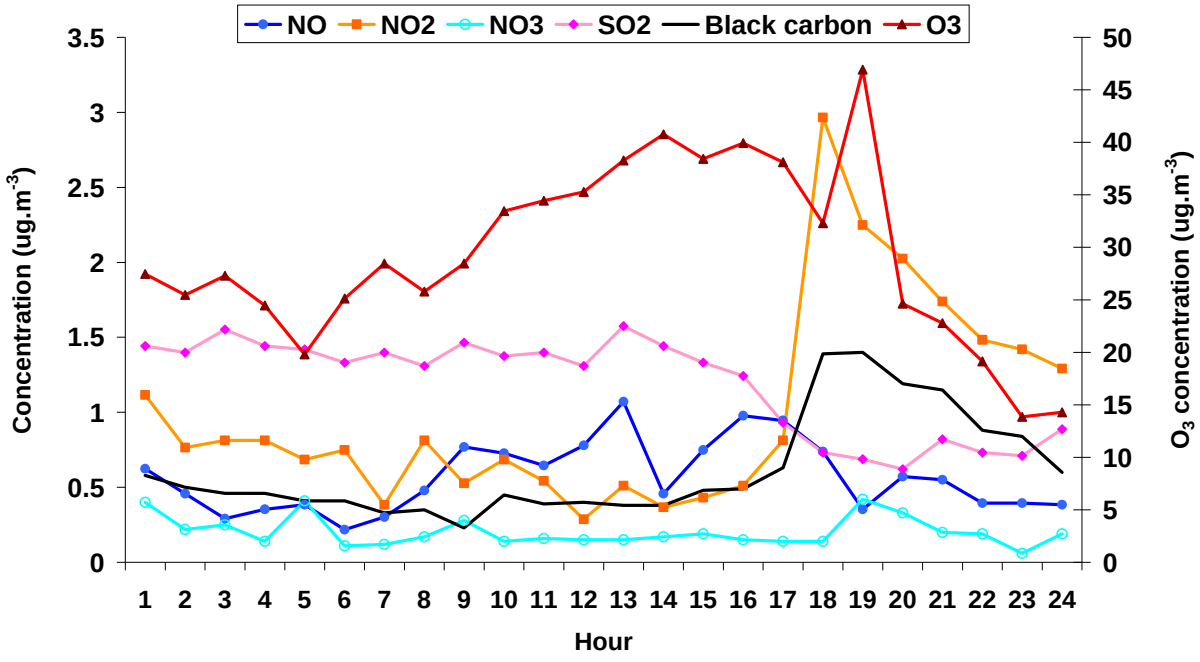


Figure 29. Average hourly concentrations at Elandsfontein on 5 April 2005 when no industrial sources are directly impacting on the region.

For this day, pollution roses indicate easterly winds (Figure 30). No industrial sources are located east of Elandsfontein. Concentrations of all three nitrogen species are very low – below 3µg.m^{-3}. This case study provides a signature of what background emissions in the area would be like without the impact of any direct industrial sources.

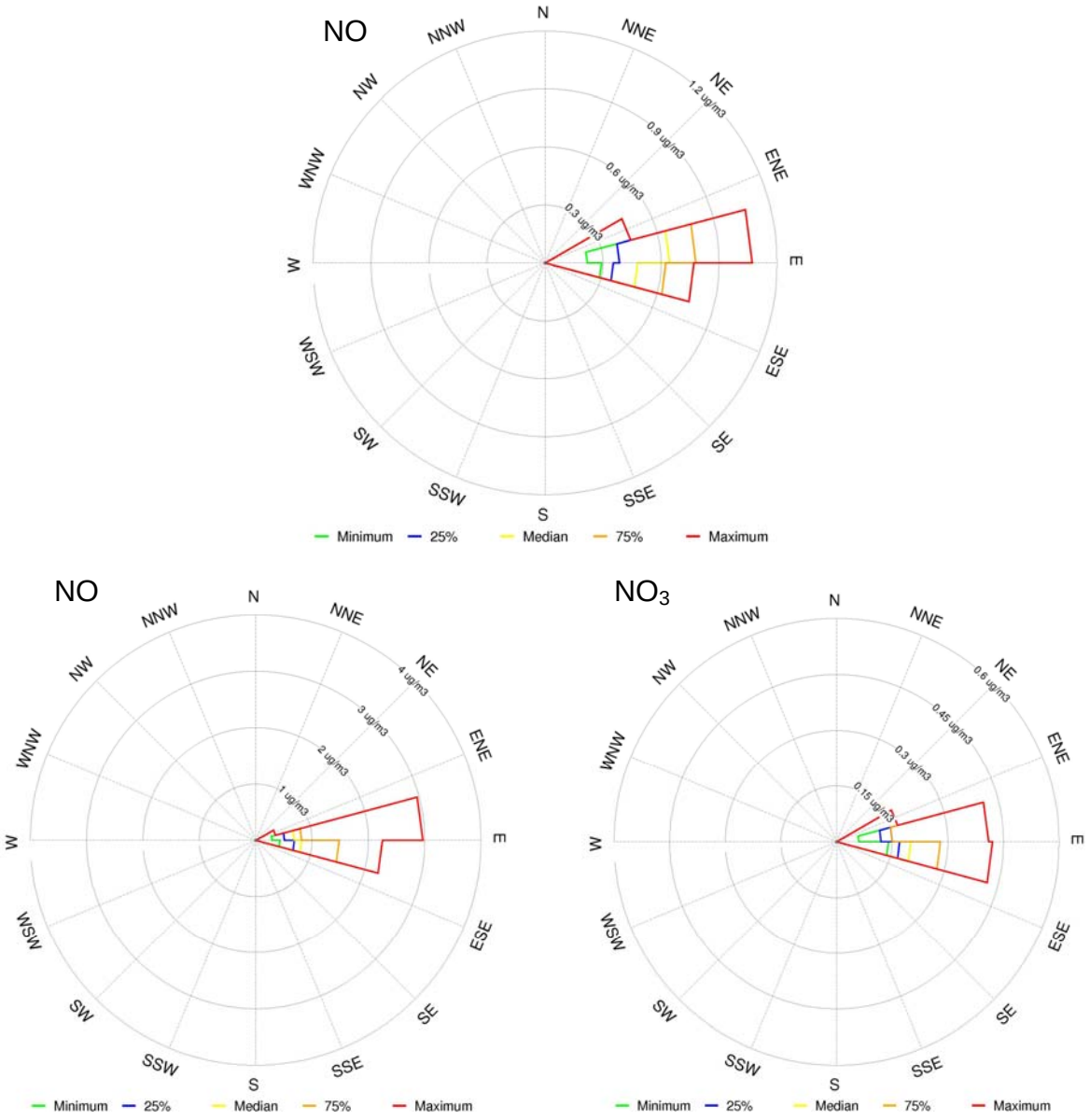


Figure 30. Pollution roses for Elandsfontein for 5 April 2005 for NO, NO_2 and NO_3.

5.2.2 Elevated NO_x concentrations associated with coal-fired power station sources

On 9 June 2005, the diurnal concentrations of NO_x and SO_2 clearly indicate a tall-stack industrial source with concentrations peaking around midday (after surface inversions have dissipated) and diminishing at night (Figure 31). A sharp drop in O_3 concentration occurs at midday, which is highly unusual. This decrease strongly reflects the occurrence of a direct plume impact at the site. Background O_3 is used up in the reaction to produce NO_2 and O_3 is also not directly emitted from the source. A second minor industrial peak in NO_x and SO_2 is experienced between 15:00 and 17:00. This peak is not of vehicular or domestic origin, due to the low black carbon concentration as well as dominant airflow from Kriel and Matla. A slight morning peak in SO_2, NO_2 and black carbon (between 08:00 and 10:00) suggest the influence of domestic coal burning. Airflow is from the west-south-west at this time, transporting emissions from the Thubelihle township situated just outside the town of Kriel, 12km from Elandsfontein.

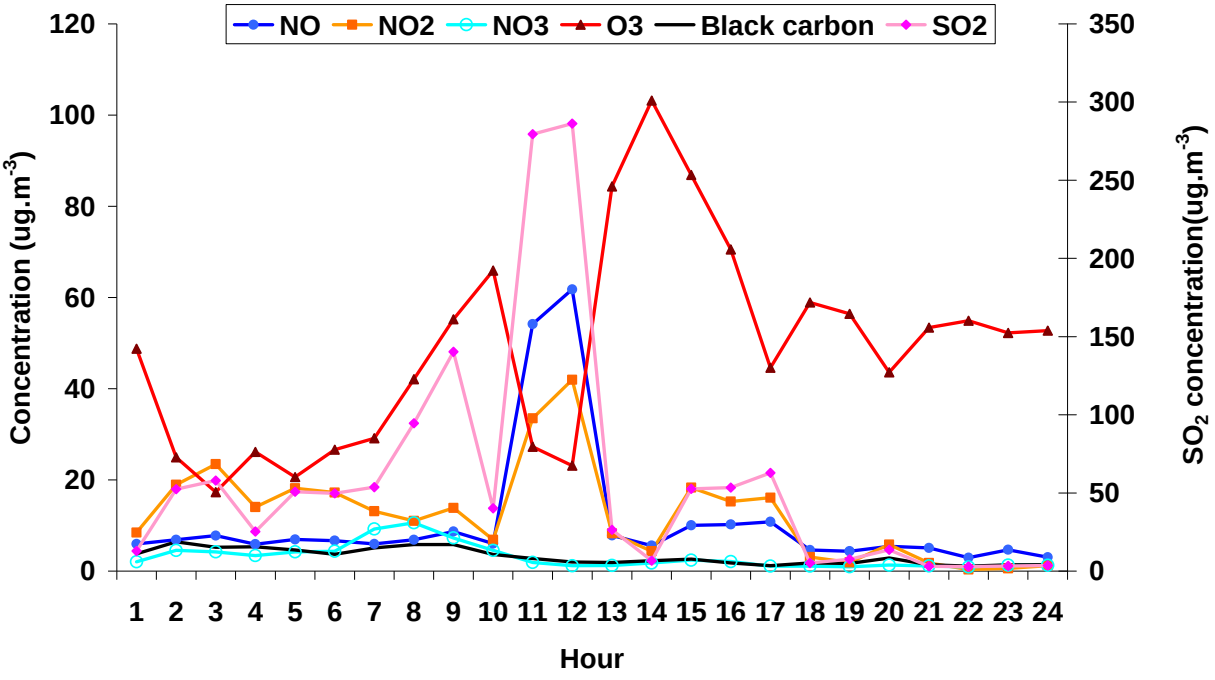


Figure 31. Average hourly concentrations at Elandsfontein on 9 June 2005 when emissions originated from power station sources to the north-west.

Both the trajectory analysis (Figure 32) and the pollution roses (Figure 33) suggest that the high NO_x concentrations on this day originate from Kriel, Matla and Kendal power stations to the west of Elandsfontein. Utilising the midday plume in the conversion calculations and assuming that the NO_2 originated from these power station sources, the average rate of conversion of NO to NO_2 is 34% per hour (wind speed 6m.s^{-1}, distance from source 25km).

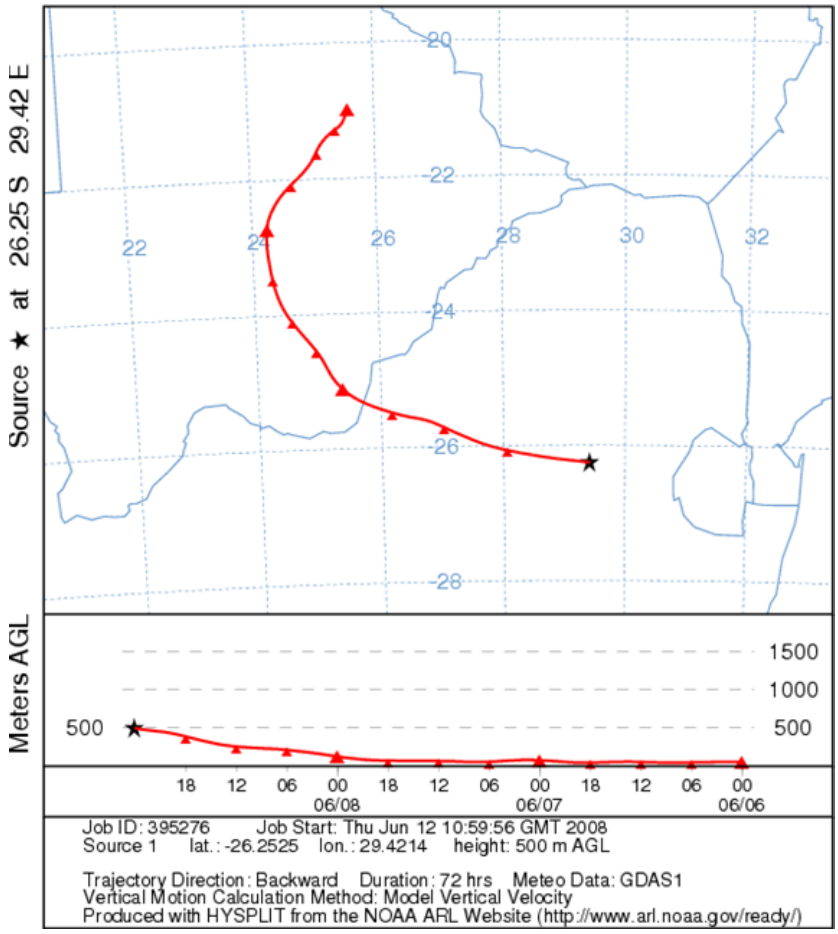


Figure 32. Three-day back trajectory from Elandsfontein starting at 22:00 on 9 June 2005.

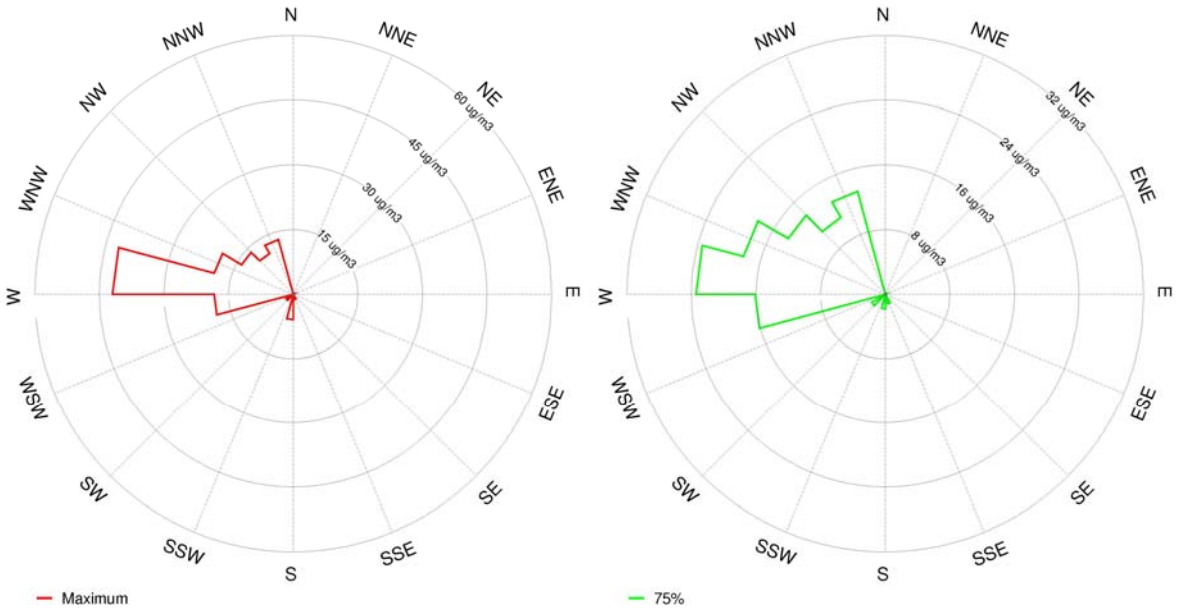


Figure 33. Pollution roses indicating maximum NO_2 concentrations (left) and 75th percentile NO_2 concentrations (right) at Elandsfontein for 9 June 2005.

5.2.3 Elevated NO_x concentrations associated with a petrochemical source

On 11 April 2005 higher NO_x and SO_2 concentrations during the day once again indicate a tall stack source (Figure 34). O_3 concentrations remain high during the day as a result of available precursors and sunlight. During the NO_x peak, O_3 concentrations decrease to 0µg.m^{-3} as O_3 is used up in the production of NO_2 (O_3 is also not emitted directly into the atmosphere from the source). At the time of the plume impact at Elandsfontein the ratio of NO to NO_2 is approximately 1, which indicates to a certain extent that the plume has been aged somewhat. On this day, the average conversion rate of NO to NO_2 is between 21% and 30% per hour (wind speed 0.9 to 2.2 m.s^{-1}, distance from source 40km).

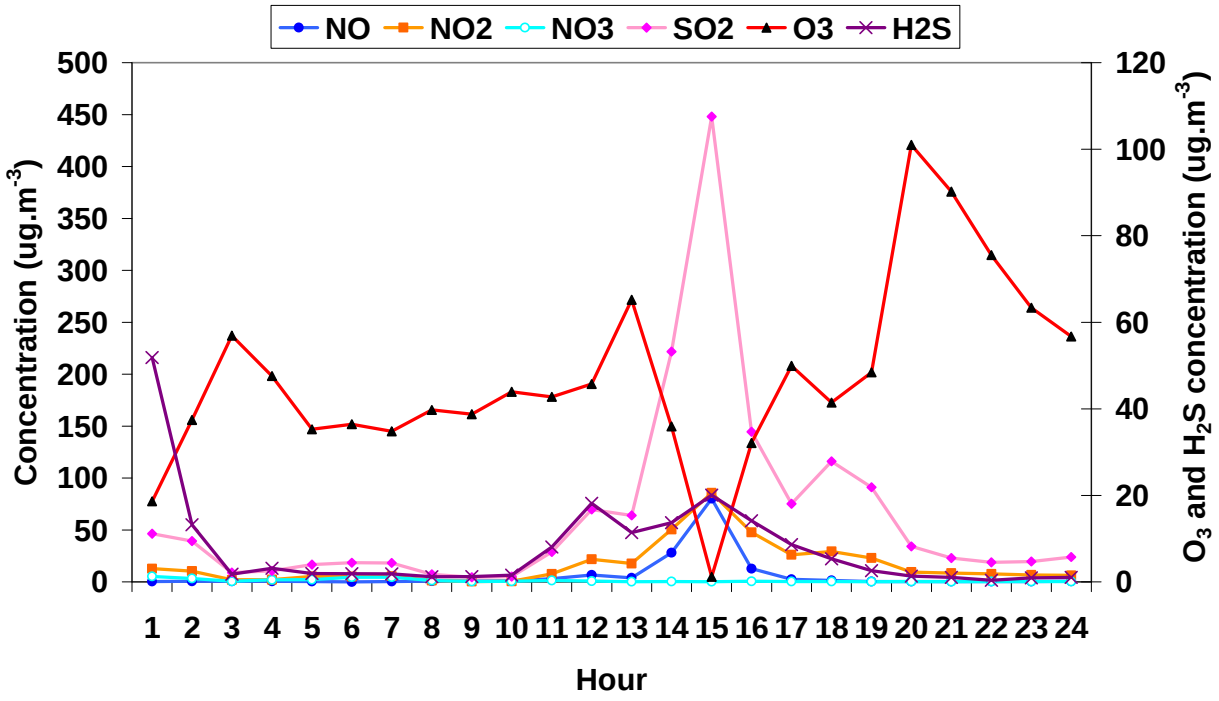


Figure 34. Average hourly concentrations at Elandsfontein on 11 April 2005.

The pollution roses for 11 April 2005 indicate that the highest NO_2 concentrations are associated with flow from Kriel, Matla and Kendal power stations (Figure 35). The pattern in the SO_2 concentrations however, does not reflect a typical power station plume impact. The concentrations start to increase at 10:00 and reach a maximum between 13:00 and

17:00. The elevated concentrations (between 50 and 100 µg.m^{-3}) remain over the station until 20:00. The H_2S concentrations spike at the same time as the other pollutants. H_2S is a primary emission from the Secunda plant (Cardoso *et al*., 1997). The trajectory analysis for 11 April 2005 confirms that the high concentrations during the day may originate from Secunda in the south-west (Figure 36). This trajectory depicts upper level airflow (at 500m above ground level), whereas the pollution roses indicate surface airflow. The higher concentrations may then be associated with the period of upper level anticyclonic stability, resulting in south-westerly transport of industrial emissions from Secunda towards Elandsfontein. This period of anticyclonic stability over the Highveld is also conducive to the accumulation of pollution between 10:00 and 20:00.

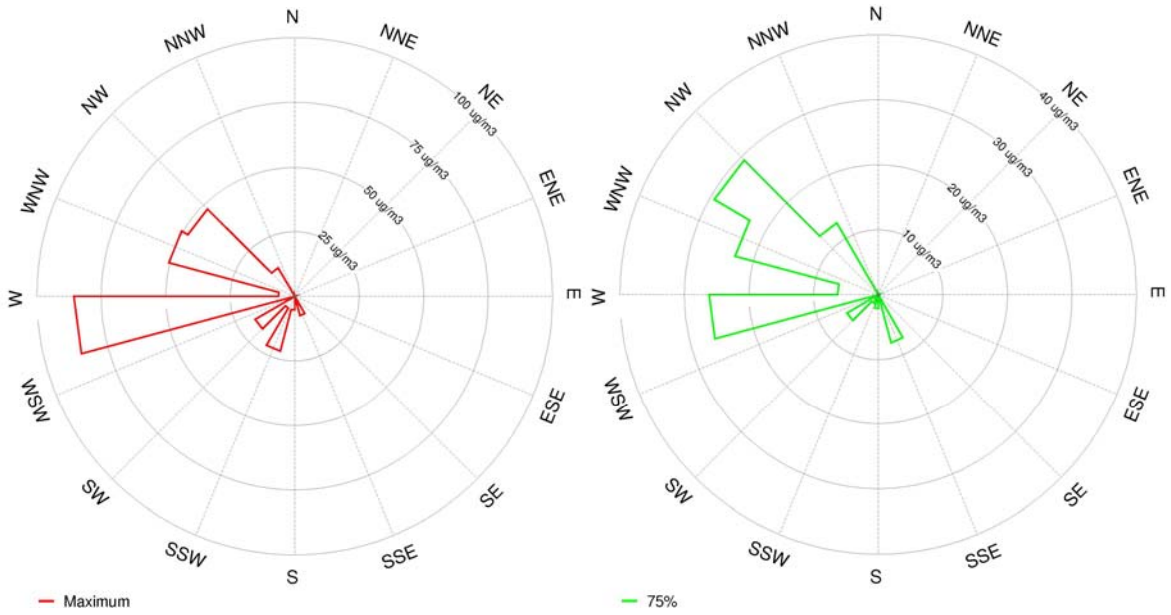


Figure 35. Pollution roses indicating maximum NO_2 concentrations (left) and 75th percentile NO_2 concentrations (right) at Elandsfontein for 11 April 2005.

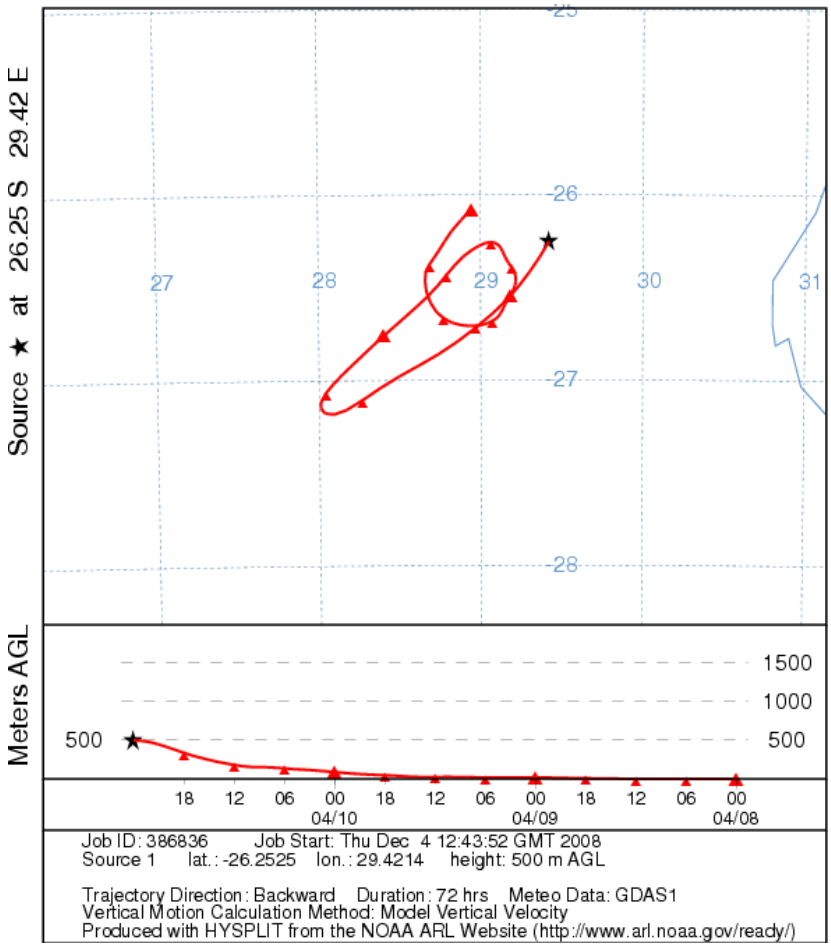


Figure 36. Three-day back trajectory from Elandsfontein starting at 22:00 on 11 April 2005.

5.2.4 Elevated nitrate concentrations associated with a petrochemical source

This case study differs to the others, indicating higher NO_3 concentrations during the day, as a result of industrial emissions. This enables comparisons of the ratios of NO to NO_3 at the source and receptor, providing a first step approximation of rates of conversion.

On 24 July 2005 NO, NO_2 and SO_2 once again provide an industrial signal, peaking during the day (Figure 37). NO_3 concentration peaks coincide with NO_x and SO_2 concentration peaks at 10:00 and between 14:00 and 16:00. These peaks are associated with industrial emissions that are transported to the ground after the inversion breaks down. NO_3 concentrations are high at this time and are in the form of nitrate aerosols, which do not photolyse during the day like their NO_3 radical counterparts. The ratio of NO to NO_3 at the source is 100:0, as no NO_3 is directly emitted. As oxidation occurs as well as reactions with cations, the NO_3 concentration increases and the average NO to NO_3 ratio on this day is 0.35:1.

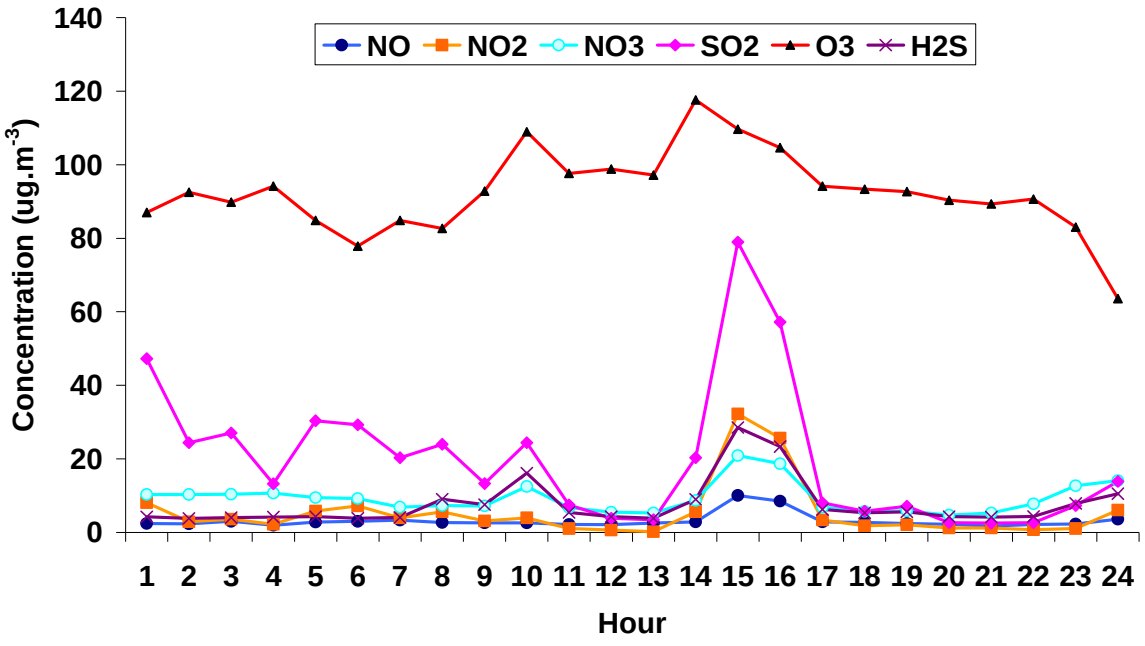


Figure 37. Average hourly concentrations at Elandsfontein on 24 July 2005.

The elevated H_2S concentrations in the plume indicate that these pollutants are of petrochemical origin. South westerly airflow dominated on this day, transporting nitrogen emissions from Secunda to Elandsfontein (Figure 38 and Figure 39). Secunda is also at a sufficient distance from Elandsfontein (40km), to allow for the formation of O_3 during transit, hence O_3 concentrations are not diminished during the NO_x and SO_2 concentration peaks.

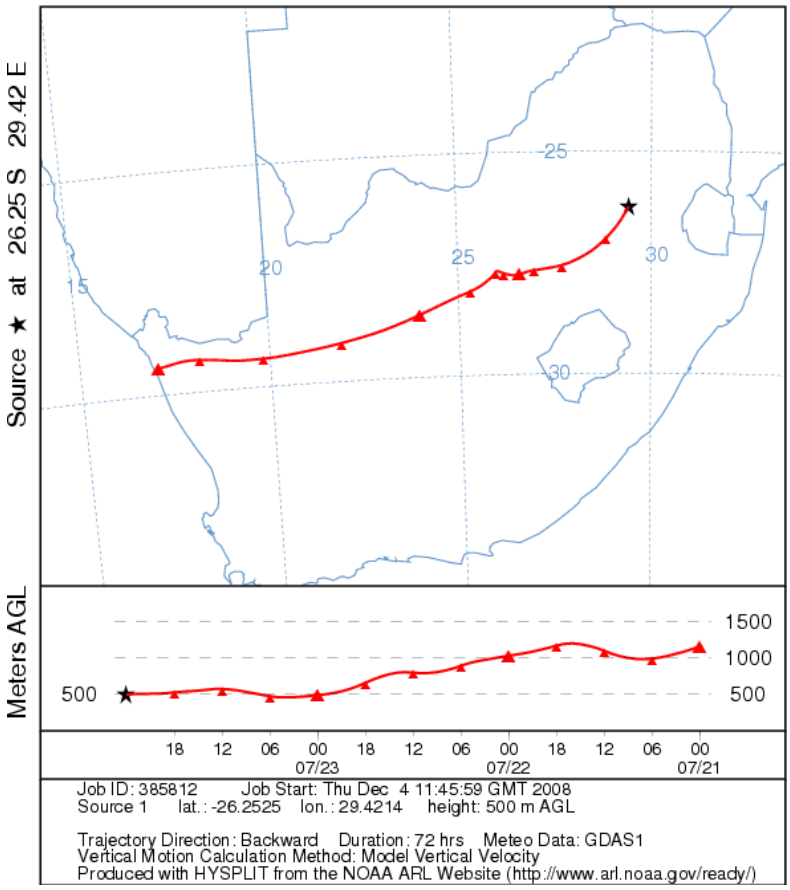


Figure 38. Three-day back trajectory from Elandsfontein starting at 22:00 on 24 July 2005.

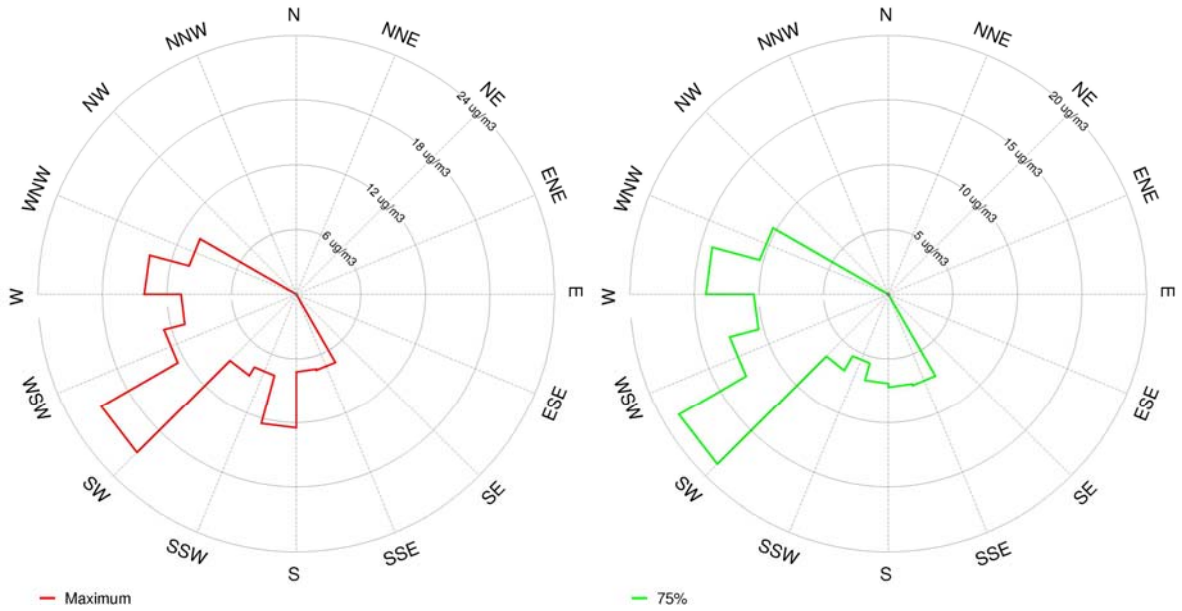


Figure 39. Pollution roses indicating maximum NO_3 concentrations (left) and 75th percentile NO_3 concentrations (right) at Elandsfontein for 11 April 2005.

5.3 Deposition

The calculated rates of dry deposition using the inferential model are directly proportional to the pollutant concentration (Equation 12). Due to the variable v_d values from literature (Table 1) the expected uncertainties in the dry deposition flux estimates when utilising the inferential model are between 30% and 50% (Blanchard *et al*., 1996). To evaluate the uncertainty in the depositional flux values, the depositional fluxes are calculated using the minimum, average and maximum v_d values. A similar approach was adopted by Lowman (2003) during a nitrogen deposition study on the Highveld.

5.3.1 Seasonal deposition patterns

Monthly dry deposition fluxes at Elandsfontein differ greatly for the three nitrogen species in question (Figure 40), just as the concentrations differ in the seasonal variation profile (Figure 12). NO dry deposition rates are much higher in winter, peaking in June, when concentrations are at their highest. The monthly depositional flux values for NO indicate a similar trend when either the average, minimum or maximum v_d values are used (Figure 41). The maximum v_d value however, indicates flux rates that are 10 times higher than the

rates calculated with the average v_d value. This huge variation highlights just how uncertain the depositional flux values may be.

Dry deposition rates of NO_2 are highly variable throughout the year. Particularly high rates occur during March, which correlates with the March NO_2 concentration peak identified in the recorded hourly data (Figure 10). The same variable seasonal profile occurs when either the average, minimum or maximum v_d values are used in the calculations (Figure 41). In comparison with using the average v_d value in the flux calculations, the maximum v_d value produces flux values that only differ by a factor of five. The uncertainty in the depositional flux values in this case is less than for NO, however the length of the whiskers still indicate much variation related to the v_d values.

NO_3 rates of dry deposition peak quite considerably during late winter, as a result biomass burning at this time, resulting in accumulation and fallout to the surface. The August NO_3 deposition rate peak is considerably high in comparison with the NO and NO_2 deposition rates (when using the average v_d value). The box and whisker plot for NO_3 indicates a lot less variability for the three different v_d values, particularly when the fluxes are low (Figure 42). During winter, there is a lot more variability in the flux values when utilising the minimum, maximum and average v_d values in the calculations. When using the maximum v_d values in this case, the calculated flux values are two times greater than using the average v_d value.

Predominant winter deposition of all three species is a result of higher concentrations together with increased atmospheric stability, which prevents transport out of the region. Hesterberg *et al*. (1996) also found higher rates of NO, NO_2 and NO_3 deposition during winter as a result of higher concentrations at this time. Throughout the year, nitrogen is predominantly deposited in the form of NO_2, except during spring, when deposition in the form of NO_3 dominates. Higher spring NO_3 deposition rates were also noted by Meyers *et al*. (1991). Lowman (2003) discovered opposite patterns in seasonal dry deposition rates, with the lowest rates occurring during winter. More nitrogen species however were investigated and different seasonal v_d values for some of the species were utilised. The

winter v_d value for many of the species was lower than during the rest of the year, resulting in lower flux rates during winter.

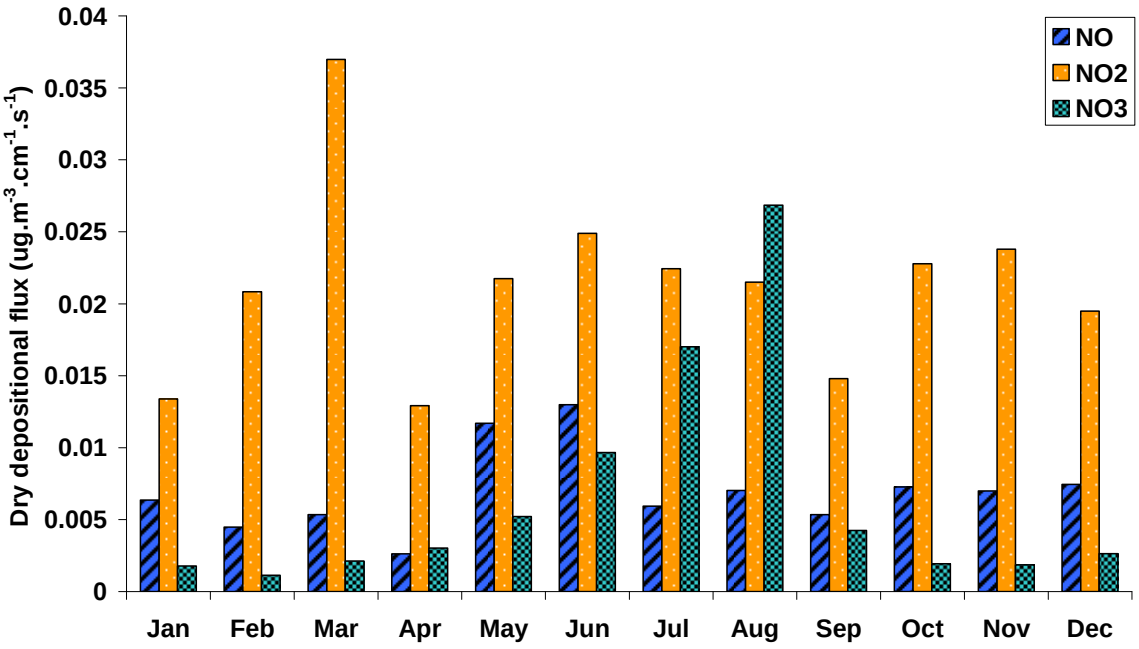


Figure 40. Mean monthly dry depositional flux values (calculated using the mean v_d values) at Elandsfontein for the period 1 April 2005 to 31 March 2006.

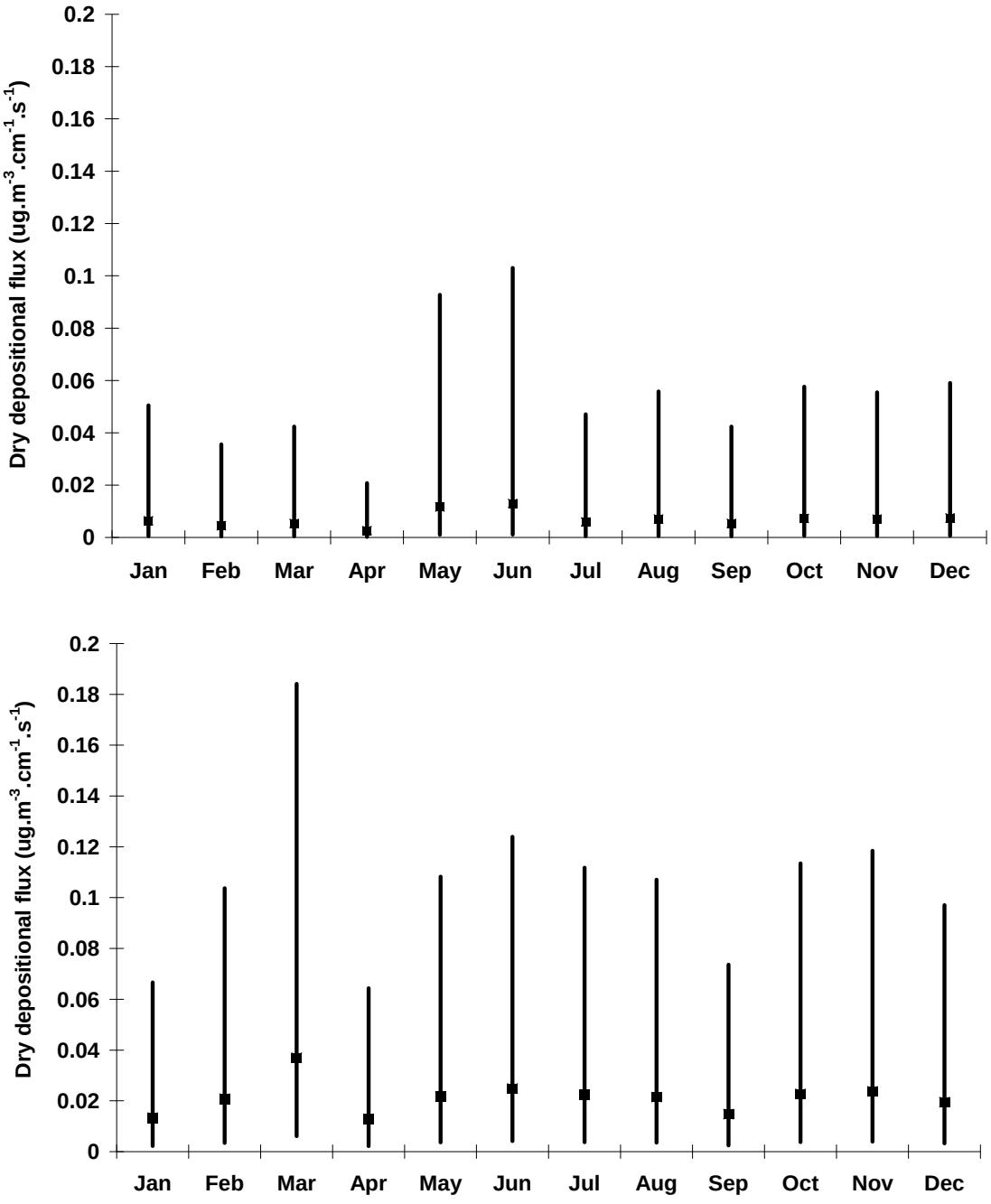


Figure 41. Box and whisker plot representing dry depositional fluxes of NO (top) and NO_2 (bottom) at Elandsfontein for the period 1 April 2005 to 31 March 2006. The boxes represent flux measurement using the average v_d value. The maximum whisker is the flux measurement using the maximum v_d value and the minimum whisker is the flux measurement using the minimum v_d value.

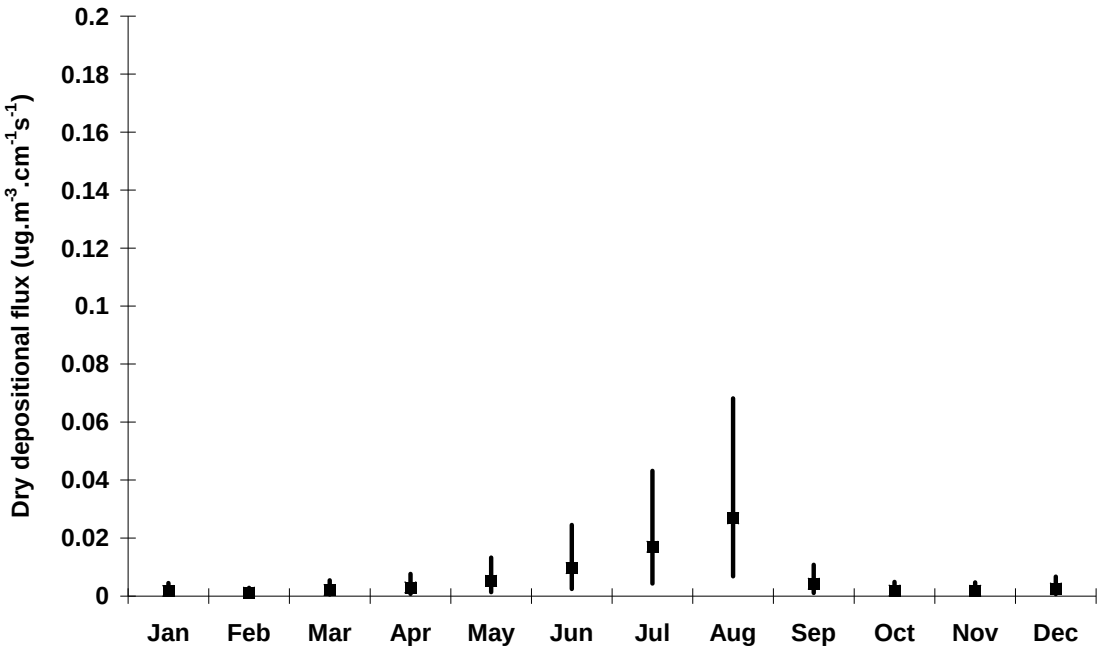


Figure 42. Box and whisker plot representing dry depositional fluxes of NO_3 at Elandsfontein for the period 1 April 2005 to 31 March 2006. The boxes represent flux measurement using the average v_d value. The maximum whisker is the flux measurement using the maximum v_d value and the minimum whisker is the flux measurement using the minimum v_d value.

5.3.2 Total deposition to the Highveld

The total amount of nitrogen deposited to the region for the entire study period provides insight into the effects of deposition in the area. From the inferential model, dry deposition rates of nitrogen for the Highveld from April 2005 to March 2006 range from 0.18 to 6.6 kg N ha^{-1} yr^{-1} (Figure 43) depending on which v_d value is utilised. These values are similar to those calculated by Mphepya (2002), where a dry deposition rate of 0.95 kg N ha^{-1} yr^{-1} was calculated. When combined with the wet deposition rates determined for Elandsfontein by Mphepya (2002), the total nitrogen deposited to the region is in the range of 2.4 to 8.8 kg N ha^{-1} yr^{-1}. These values are well below the stipulated critical load value for grasslands of 15 kg N ha^{-1} yr^{-1} (Grennfelt and Thörnelöf, 1992). Hence, such deposition in the region does not pose significant threats to the natural environment. Van Tienhoven *et al*., (1995) found similar results on the Highveld regarding sulphur, where the

rates of sulphur deposition do not exceed the critical load and do not cause any direct threats to the ecosystems in the region.

The dry deposition rates (using the minimum and average v_d values) are considerably lower than the rates of wet deposition for the Highveld region (Figure 43). When using the maximum v_d values in the deposition calculations, dry deposition exceeds wet deposition in the region considerably. Lowman's study (2003) on the Highveld provides a good comparison of wet deposition rates, as similar seasonal precipitation patterns would occur at Elandsfontein. It was found that wet deposition (7.8 kg N ha^{-1} yr^{-1}) only slightly exceeded dry deposition (7 kg N ha^{-1} yr^{-1}), which is much like the situation in this study when the average v_d value is used. Lowman also utilised v_d values that were close to the average v_d values obtained from literature. Mphepya (2002) found that the rate of wet deposition also exceeds the rate of dry deposition at Elandsfontein.

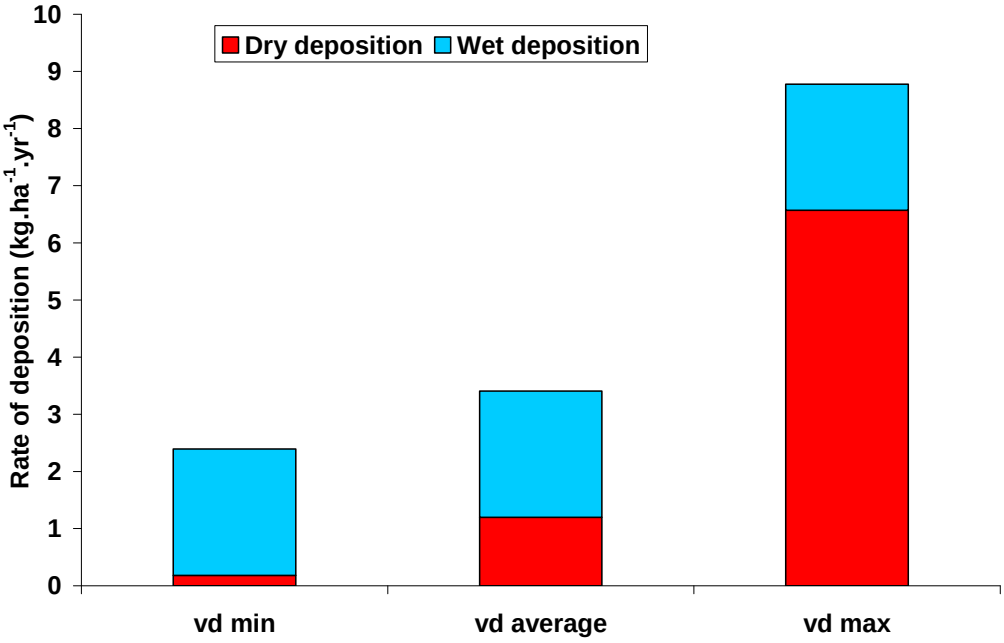


Figure 43. Annual wet and dry deposition rates at Elandsfontein. Dry deposition rates are calculated using the minimum, average and maximum v_d values from literature.

The total nitrogen deposition amounts calculated above for the Highveld region are considerably lower than those calculated during previous studies in various regions around the world. Hesterberg *et al*. (1996) calculated total deposition for an extensively managed grassland in Switzerland of 24 to 34 kg N ha^{-1} yr^{-1}. For an industrialised region in Great Britain, Stevens *et al*. (2004) also found higher deposition rates of up to 35 kg N ha^{-1} yr^{-1}. During a study in San Francisco related to urban smog, deposition to a sensitive grassland area was between 10 and 15 kg N ha^{-1} yr^{-1} (Weiss, 1999). Fenn *et al*. (2003) found nitrogen deposition rates downwind of major urban and agricultural sources in the western United States between 30 and 90 kg N ha^{-1} yr^{-1}. Background rural levels of 1 to 4 kg N ha^{-1} yr^{-1} were also calculated. For the Highveld, Lowman (2003) calculated higher total nitrogen deposition amounts of up to 25 kg N ha^{-1} yr^{-1}. This value however takes into consideration the influence of cloud droplet deposition as well as wet and dry deposition

Although the deposition values from all of the previous studies considered are much higher than the calculated values for the Highveld, it needs to be noted that the rates of deposition of nitrogen that are calculated in this study only include the species NO, NO_2 and NO_3. NH_3 however is also a very important compound in nitrogen deposition. Lowman (2003) found NH_3 to be the most significant contributor to dry deposition on the Highveld (accounting for ~60% of the total dry deposition). Hesterberg *et al*. (1996) and Stevens *et al*. (2004) also found that between 60 and 70% of the calculated dry deposition of nitrogen to grassland areas in Switzerland and Great Britain respectively was attributed to NH_3. Due to technological reasons there is a lack of NH_3 concentration data from Elandsfontein during the study period, thus NH_3 could not be included in the deposition calculations.

When incorporating the NH_3 deposition values from Lowman (2003) of 4.3 kg N ha^{-1} yr^{-1} (as a baseline for NH_3 deposition on the Highveld), the resultant range in dry deposition values at Elandsfontein is between 4.5 and 10.9 kg N ha^{-1} yr^{-1}. If the wet deposition rates are also included, the total nitrogen deposition is between 6.7 and 13.1 kg N ha^{-1} yr^{-1}. These values are still below the critical load value for grasslands, indicating no significant threats to local ecosystems. These values are also closer to the ranges calculated during previous

nitrogen studies on both the Highveld and globally, providing a more accurate interpretation of total nitrogen deposition to the region.

According to Eskom's annual reports for 2005 and 2006, the total amount of nitrogen emitted from power station sources in this region for the period April 2005 to March 2006 was ~ 209 000 tons. Using the calculated total deposition values, between 4% and 14% of this total emitted nitrogen is deposited to the surface via wet and dry deposition processes. It is assumed that the remaining nitrogen (between 86% and 96%) remains in the atmosphere and is advected out of the region (Figure 44).

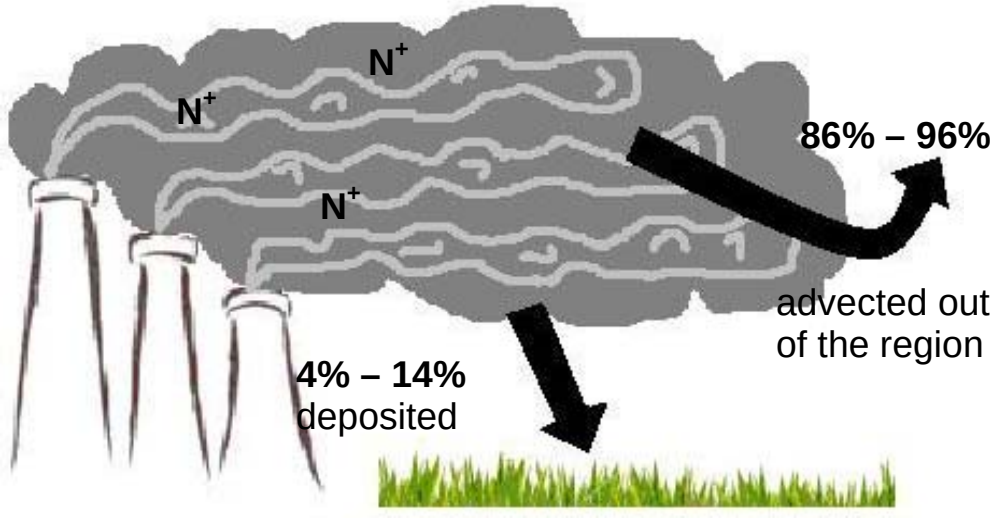


Figure 44. Percentage of nitrogen deposited during April 2005 to March 2006 based on inferential model calculations using the minimum, average and maximum v_d values from literature.

Although the amount of nitrogen deposited is below the critical load, the percentage of nitrogen that remains in the atmosphere and is advected out of the region is significant. This increase in atmospheric nitrogen causes a positive balance in the atmospheric nitrogen budget. Such an increase results in questions as to what impact this added nitrogen has on the troposphere and may begin to confirm the nitrogen 'hotspot' detected by satellite instruments such as GOME (Global Ozone Monitoring Experiment) and SCIAMACHY (SCanning Imaging Absorption spectroMeter for Atmospheric CHartographY) .

The seasonal and annual depositional flux values that are calculated are very useful in analysing deposition to the Highveld. These values however are only a first step approximation of the depositional flux to the region. For a more in-depth, accurate analysis, hourly meteorological variables and diurnal calculations may aid in providing a higher time resolution of flux values. This is important as there are significant differences in the daytime and night time depositional flux values. Accurate calculation of v_d values at Elandsfontein would also aid in determining more precise flux measurements. The inclusion of other nitrogen species (such as NH_3) in future campaigns would help improve the accuracy of such calculations.

****

NO to NO_2 conversion rates calculated in this chapter are highly variable as they are based on assumptions that all the nitrogen comes from one specific source and that the rate is uniform for every hour that an air mass transports downwind. These conversion rates range from 11% to 59% per hour. Rates of dry deposition are generally higher during the winter months when the concentrations of nitrogen species are higher due to stable atmospheric conditions and no rain. On the Highveld, the total nitrogen deposited to the region is in the range of 6.7 to 13.1 kg N ha^{-1} yr^{-1}. Less than 15% of emitted industrial nitrogen in the region is deposited to the surface.

CHAPTER 6: CONCLUSIONS

The natural nitrogen balance has been disrupted via anthropogenic activities. On the Highveld, increased atmospheric concentrations of NO, NO_2 and NO_3 have lead to a positive nitrogen balance as more of these molecules remain in the atmosphere than are deposited to the surface.

Ideally situated in the heart of the industrialised Highveld, Elandsfontein monitoring site provides the perfect location to monitor industrial nitrogen emissions in the region. The main findings with regard to the temporal variations in nitrogen concentrations are:

- NO and NO_2 concentrations are higher during winter as a result of stable atmospheric conditions, which limit the amount of upward mixing. Prevalent westerly and north-westerly airflow during winter also transport NO_x directly from the power station sources that are in close proximity to the monitoring site in the westerly sector.

- NO_3 concentrations remain low throughout the year, peaking during winter. This winter peak is a result of no rainfall as well as increased atmospheric stability leading to accumulation of particles in the atmosphere. A very distinct concentration peak occurs during July and August as a result of biomass burning in the region.

- O_3 concentrations peak during winter as a result of higher NO_2 concentrations. Biomass burning contributes to higher O_3 concentrations during August.

- Diurnally, NO and NO_2 concentrations are lower at night and peak at midday. This is a result of surface inversions which develop at night, preventing the downward dispersion of tall-stack emissions at this time. The daytime peak in NO and NO_2 (along with a coinciding peak in SO_2) confirm that the emissions monitored at Elandsfontein are predominantly of industrial origin and do not originate from motor vehicles or domestic coal fires in the region.

- NO_3 concentrations are higher at night and lower during the day. This is because the nitrate radical is rapidly photolysed during the day and nitrates cannot be produced.

- Seasonally, wind direction patterns change as a result of changing synoptic conditions. North-westerly airflow dominates during winter, whilst easterly winds are more frequent during summer.

- For the whole year, the highest NO and NO_2 concentrations are associated with westerly and north-north-westerly airflow, which transports emissions from Kendal, Kriel and Matla power stations.

- NO_3 concentrations are highest in association with winds from the south-west, which transport emissions directly from Secunda.

The rates of conversion of NO to NO_2 are highly variable and are based on the assumptions that all the NO and NO_2 originates from one specific source; that the rate of conversion is uniform for every hour that the air mass transports down wind; and that the atmospheric chemistry is conducive to NO_2 formation. The rates are also related to atmospheric stability, dispersion and time of day. Furthermore, rates of conversion differ for ambient conditions compared to conditions within a plume. Utilising various case studies, the conversion rate results are:

- Rates of conversion of NO to NO_2 range from 11% to 59% per hour.

- As a comparison, the rates of conversion from Kendal monitoring site (2km downwind of Kendal power station) range from 66% to 94% per hour. These rates are a lot higher than those calculated at Elandsfontein because the rates decrease exponentially with time, with more rapid rates of conversion occurring initially and slowing down as the air mass travels further from the source.

- The rates of NO to NO_3 are not calculated in this study, as any night time peaks in NO_3 concentration are not related to industrial emissions. This is because industrial plumes are trapped above the inversion layer at night (when NO_3 forms). Any peaks

during the night can be attributed to aged industrial plumes or plumes from non-industrial NO_x sources that are close to the surface.

Atmospheric nitrogen species are eventually deposited to the surface via dry and wet deposition. Using the inferential model, the depositional characteristics of nitrogen on the Highveld are:

- Rates of dry deposition of NO, NO_2 and NO_3 are generally higher during winter as a result of increased concentrations together with atmospheric stability, which prevents transport out of the region.

- Throughout the year, nitrogen is predominantly deposited in the form of NO_2 except during spring, when deposition in the form of NO_3 dominates.

- NO, NO_2 and NO_3 depositional flux values are highly uncertain as a result of the large variations in the depositional velocity (v_d) values.

- The total amount of nitrogen deposited to the Mpumalanga Highveld region is in the range of 6.7 to 13.1 kg N ha^{-1} yr^{-1}, which is below the stipulated critical load value for grasslands of 15 kg N ha^{-1} yr^{-1}. Such deposition therefore does not pose significant threats to the natural environment on the Highveld.

- Rates of wet deposition are much higher than rates of dry deposition on the Highveld, when utilising the minimum and average v_d values in the dry deposition calculations.

- Using emissions data from Eskom's annual report, it is found that between 4% and 14% of the total industrially emitted nitrogen on the Highveld is deposited to the surface via wet and dry deposition. The remainder of which remains in the atmosphere and is advected out of the region.

Although the amount of nitrogen that is deposited does not pose major threats to the natural environment on the Highveld, the amount of anthropogenic nitrogen that remains in the

atmosphere is substantial. This increase in atmospheric nitrogen causes a positive balance in the atmospheric nitrogen budget. Such increases in atmospheric nitrogen may provide insight and begin to confirm the nitrogen ‘hotspot’ detected by satellite instruments.

****

CHAPTER 7: REFERENCES

Acker, K., Möller, D. and Wieprecht, W., 2004: Atmospheric concentration variations of gaseous and particulate nitrate at different sites in Europe, Abstracts of the European Aerosol Conference 2004, S1049 – S1050.

Aneja, V.P., Roelle, P.A., Murray, G.C., Southerland, J., Erisman, J.W., Fowler, D., Asman, W.A.H. and Patni, N., 2001: Atmospheric nitrogen compounds II: emissions, transport, transformation, deposition and assessment, *Atmospheric Environment*, 35, 1903 – 1911.

Appel, B.R., Tokiwa, Y. and Haik, M., 1981: Sampling of nitrates in ambient air, *Atmospheric Environment*, 15, 283 – 289.

Asman, W.A.H., Sutton, M.A. and Schjorring, J.K. 1998: Ammonia: emission, atmospheric transport and deposition, *New Phytologist*, 139, 27 – 48.

Atkinson, R., 2000: Atmospheric Chemistry of VOCs and NO_x, *Atmospheric Environment*, 34, 2063 – 2101.

Augustin, S., Bolte, A., Holzhausen, M. and Wolff, B., 2005: Exceedance of critical loads of nitrogen and sulphur and its relation to forest conditions, *European Journal of Forest Research*, 124, 289 – 300, doi: 10.1007/s10342-005-0095-1.

Baumgardner, R.E., Lavery, T.F., Rogers, C.M. and Isil, S.S., 2002: Estimates of the Atmospheric Deposition of Sulfur and Nitrogen Species: Clean Air Status and Trends Network, 1990-2000, *Environmental Science and Technology*, 36, 2614 – 2629.

Beirle, S., 2004: Estimating source strengths and lifetime of Nitrogen Oxides from satellite data, PhD thesis, University of Heidelberg, Germany.

Benner, C.L., Eatough, D.J., Eatough, N.L. and Bhardwaja, P., 1991: Comparison of annular denuder and filter pack collection of HNO_3 (g), HNO_2 (g), SO_2 (g) and particulate phase nitrate, nitrite and sulfate in the south-west desert, *Atmospheric Environment*, 25A (8), 1537 – 1545.

Blanchard, C.L., Michaels, H., Tannenbaum, S., 1996: *Regional estimates of acid deposition in fluxes in California 1985 - 1994*, Californian Air Resources Board, Sacramento.

Bradshaw, J., Davis, D., Grodzinsky, G., Smyth, S., Newell, R., Sandholm, S. and Liu, S., 2000: Observed distributions of nitrogen oxides in the remote free troposphere from the NASA Global Tropospheric Experiment Program, *Reviews of Geophysics*, 38 (1), 61 – 116.

Brook, J.R., Di-Giovanni, F., Cakmak, S. and Meyers, T.P., 1997: Estimation of dry deposition velocity using inferential models and site specific meteorology -- Uncertainty due to siting of meteorological towers, *Atmospheric Environment*, 31 (23), 3911 – 3919.

Brown, S.S., Stark, H., Ryerson, T.B., Williams, E.J., Nicks Jr., D.K., Trainer, M., Fehsenfeld, F.C. and Ravishankara, A.R., 2003a: Nitrogen oxides in the nocturnal boundary layer: Simultaneous measurements of NO_3, N_2O_5, NO_2, NO and O_3, *Journal of Geophysical Research*, 108 (D9), doi:10.1029/2002JD002917.

Brown, T.L., LeMay, H.E., Bursten, B.E. and Burdge, J.R., 2003: *Chemistry: The Central Science*, Pearson Education Inc., USA, 364 – 382.

Brunner, D., Staehelin, J. and Jeker, D., 1998: Large-scale nitrogen oxide plumes in the tropopause region and implications for ozone, *Science*, 282, 1305–1309.

Bull, K.R., 1991: The Critical Loads/Levels Approach to Gaseous Pollutant Emission Control, *Environmental Pollution*, 69, 105 – 123.

Cardoso, A.A., Liu, H. and Dasgupta, P.K., 1997: Fluorometric fiber optic drop sensor for atmospheric hydrogen sulphide, *Talanta*, 44, 1099 – 1106.

Chan, C.K. and Chan, M.N., 2004: New Directions: Polymorphic transformation of ammonium nitrate in atmospheric aerosols, *Atmospheric Environment*, 38, 1387 – 1388, doi:10.1016/j.atmosenv.2003.12.009.

Clarke, J.F., Edgarton, E.S. and Martin B.E., 1997: Dry deposition calculations for the Clean Air Status and Trends Network, *Atmospheric Environment*, 31 (21), 3667 – 3678.

Cocks, A.T. and Fletcher, I.S., 1989: Major factors influencing gas-phase chemistry in power plant plumes during long range transport - II. Release time and dispersion rate for dispersion into an 'urban' ambient atmosphere, *Atmospheric Environment*, 23 (12), 2801 - 2812.

Coe, H. and Gallagher, M.W., 1992: Measurements of dry deposition of NO, to a Dutch heathland using the eddy-correlation technique, *Q. J. R. Meteorol. SOC.*, 118, 167 – 786.

Colls, J., 2002: Air Pollution, Taylor and Francis, USA, 224 -266.

Cosijn, C. and Tyson, P.D., 1996: Stable discontinuities in the atmosphere over South Africa, *South African Journal of Science*, 92 (8), 381 – 386.

Curtius, J., 2006: Nucleation of atmospheric aerosol particles, *Comptes Rendus Physique*, 7, 1027 – 1045, doi:10.1016/j.crhy.2006.10.018.

Damm, C.J., Lucas, D., Sawyer, R.F. and Coshland, C.P., 2001: Excimer laser fragmentation - Fluorescence spectroscopy as a method for monitoring ammonium nitrate and ammonium sulfate particles, *Chemosphere*, 42, 655 – 661.

Dassios, K.G. and Pandis, S.P., 1999: The mass accommodation coefficient of ammonium nitrate aerosol, *Atmospheric Environment*, 33, 2993 – 3003.

Dore, A.J., Vieno, M., Tang, Y.S., Dragosits, U., Dosio, A., Weston, K.J. and Sutton, M.A., 2007: Modelling the atmospheric transport and deposition of sulphur and nitrogen over the United Kingdom and assessment of the influence of SO_2 emissions from international shipping, *Atmospheric Environment*, 41, 2355 – 2367, doi:10.1016/j.atmosenv.2006.11.013.

Duyzer, J.H., Meyer, G.M. and van Aalst, R.M., 1983: Measurement of dry deposition velocities of NO, NO_2 and O_3 and the influence of chemical reactions, *Atmospheric Environment*, 17 (10), 2117 – 2120.

Fenger, J., 2002: Urban air quality, in J. Austin, P. Brimblecombe and W. Surges (eds.), *Air Pollution for the 21st Century*, Elsevier Science Ltd., Oxford, 1 – 54.

Fenn, M. E., Haeuber, R., Tonnesen, G.S., Baron, J.S., Grossman-Clarke, S., Hope, D., Jaffe, D.A., Copeland, S., Geiser, L., Rueth, H.M. and Sickman J.O., 2003: Nitrogen Emissions, Deposition and Monitoring in the Western United States, *BioScience*, 53 (4), 391 – 403.

Forrest, J., Garber, R.W. and Newman, L., 1981: Conversion rates in power plant plumes based on filter pack data: The coal-fired Cumberland plume, *Atmospheric Environment*, 15, 10-11, 2271 – 2282.

Fowler, D., Flechard, C., Skiba, U., Coyle, M. and Cape, J.N., 1998: The atmospheric budget of oxidized nitrogen and its role in ozone formation and deposition, *New Phytologist*, 139, 11-23.

Freiman, M.T. and Piketh, S.J., 2003: Air transport into and out of the industrial Highveld region of South Africa, *Journal of Applied Meteorology*, 42, 994 – 1002.

Galloway, J.N., Levy II, H. and Kasibhatla, P.S., 1994: Year 2020: Consequences of Population Growth and Development on Deposition of Oxidized Nitrogen, *Ambio*, 23 (2), 120 – 123.

Galloway, J.N., 1998: The global nitrogen cycle: changes and consequences, *Environmental Pollution*, 102 (S1), 15 – 24.

Gao, Y., 2002: Atmospheric nitrogen deposition in Barnegat Bay, *Atmospheric Environment*, 36, 5783 – 5794.

Garstang, M., Tyson, P.D., Swap, R., Edwards, M., Kållberg, P., and Lindesay, J.A., 1996: Horizontal and vertical transport of air over southern Africa, *Journal of Geophysical Research*, 101 (D19), 23 721 – 23 736.

Gertler, A.W., Miller, D.F., Lamb, D. and Katz, U., 1984: Studies of sulphur dioxide and nitrogen dioxide reactions in haze and cloud. In: Durham, J.L. (Ed.), Teasley, J.I. (Series, Ed.), *Chemistry of Particles, Fogs and Rain*, Acid Precipitation Series, Butterworth, Boston, Vol. 2, 131 – 160.

Gomez-Moreno, F.J., Núñez, L., Plaza, J., Alonso, D., Pujadas, M. and Artiñano, B., 2007: Annual evolution and generation mechanisms of particulate nitrate in Madrid, *Atmospheric Environment*, 41, 394 – 406, doi:10.1016/j.atmosenv.2006.07.040.

Grennfelt, P. and Thörnelöf, E., 1992: *Critical loads for nitrogen*, Report from a workshop held at Lokeberg, Sweden, 6-10 April 1992, Nordic Council of Ministers, Nord 41.

Hanson, P.J. and Lindberg, S.E., 1991: Dry deposition of reactive nitrogen compounds: a review of leaf, canopy and non-foliar measurements, *Atmospheric Environment*, 25A (8), 1615 – 1634.

Harrison, R., Park, S.S., Ondov, J., Buckley, T., Kim, S.R. and Jayanty, R.K.M., 2004: Highly time resolved fine particle nitrate measurements at the Baltimore Supersite, *Atmospheric Environment*, 38, 5321 – 5332, doi:10.1016/j.atmosenv.2004.03.075.

Held, G., Snyman, G.M., and Scheifinger, H., 1993: Seasonal variations and trends of atmospheric particulates on the South African Highveld, *The Clean Air Journal*, 8 (8), 4 – 11.

Held, G., Gore, B.J., Surridge, A.D., Tosen, G.R., Turner, C.R. and Walmsley, R.D. (Eds.), 1996: Air Pollution and its Impacts on the South African Highveld, Environmental Scientific Association, Cleveland, South Africa.

Hesterberg, R.,Blatter, A., Fahrni, M., Rossetti., M., Neftel, A., Eugster, W., and Wanner, H., 1996: Deposition of nitrogen containing compounds to an extensively managed grassland in central Switzerland, *Environmental Pollution*, 91 (1), 21 – 34.

Heubert, B.J., Luke, W.T., Delany, A.C. and Brost, R.A., 1988: Measurements of concentrations and dry surface fluxes of atmospheric nitrates in the presence of ammonia, *Journal of Geophysical Research*, 93, D6, 7127 – 7136.

Hewitt, C.N., 2001: The atmospheric chemistry of sulphur and nitrogen in power station plumes, *Atmospheric Environment*, 35, 1155 – 1170.

Holland, E. A., Dentener, F.J., Braswell, B.H. and Sulzman, J.M., 1999: Contemporary and pre-industrial global reactive nitrogen budgets, *Biogeochemistry*, 46, 7 – 43.

Horowitz, L.W. and Jacob, D.J., 1999: Global impact of fossil fuel combustion on atmospheric NO_x, *Journal of Geophysical Research*, 104 (D19), 23 823 – 23 840.

Horri, C.V., Munger, J.W., Wofsy, S.C., Zahniser, Nelson, D. and Mcmanus, J.B., 2006: Atmospheric reactive nitrogen concentration and flux budgets at a north eastern U.S. forest site, Agricultural and Forest Meteorology, 136, 159 – 174, doi:10.1016/j.agrformet.2006.03.005.

Horvath, L., Nagy, Z. and Weidinger, T., 1998: Estimation of dry deposition velocities of nitric oxide, sulphur dioxide and ozone by gradient method above short vegetation during the Tract campaign, *Atmospheric Environment*, 32 (7), 1317 – 1322.

Hov, O., Isaksen, I.S.A., 1981: Generation of secondary pollutants in a power plant plume: a model study. *Atmospheric Environment*, 15, 2367 – 2376.

Igbafe, A. I., 2007: Resolving the atmospheric sulphur budget over the Elandsfontein area of the Mpumalanga Highveld, PhD Thesis, University of the Witwatersrand, Johannesburg, South Africa.

IDAF, 2004: *The DEBITS Programme*, http://medias.obs-mip.fr/idaf/program/debits Website accessed: 10 April 2006.

Jacob, D.J., Heikes, B.G., Fan, S.M., Logan, J.A., Mauzerall, D.L., Bradshaw, J.D., Singh, H.B., Gregory, G.L., Talbot, R.W., Blake, D.R. and Sachse, G.W., 1996: Origin of ozone and NO_x in the tropical troposphere: A photochemical analysis of aircraft observations over the South Atlantic basin, *Journal of Geophysical Research,* 101 (D19), 24 235 – 24 250.

Jacob, D.J., 2000: Heterogeneous chemistry and tropospheric ozone, *Atmospheric Environment*, 34, 2131 – 2159.

Kadowaki, S., 1977: Size distribution and chemical composition of atmospheric particulate nitrate in the Nagoya area, *Atmospheric Environment*, 11, 671 – 675.

Kai, Z., Yuesi, W., Tianxue, W., Yousef, M. and Frank, M., 2007: Properties of nitrate, sulfate and ammonium in typical polluted atmospheric aerosols (PM10) in Beijing, *Atmospheric Research*, 84, 67 – 77, doi:10.1016/j.atmosres.2006.05.004.

Krupa, S.V., 2003: Effects of atmospheric ammonia (NH_3) on terrestrial vegetation: a review, *Environmental Pollution*, 124, 179 – 221, doi:10.1016/S0269-7491(02)00434-7.

Lange, L., Hoor, P., Helas, G., Fischer, H., Brunner, D., Scheeren, B., Williams, J., Wong, S., Wohlfrom, K., Arnold, F., Strom, J., Krejci, R., Lelieveld, J. and Andreae, M.O., 2001: Detection of lightning-produced NO in the midlatitude upper troposphere during STREAM 1998, *Journal of Geophysical Research*, 106 (D21), 27 777 – 27 785.

Lee, D.S., Köhler, I., Grobler, E., Rohrer, F., Sausen, R., Gallardo-Klenner, L., Olivier, J.G.J., Dentener F.J. and Bouwman, A.F., 1997: Estimations of global NO_x emissions and their uncertainties, *Atmospheric Environment*, 31, 1735 – 1749.

Leue, C., Wenig, M., Wagner, T., Klimm, O., Platt, U. and Jähne, B., 2001: Quantitative analysis of NO_x from Global Ozone Monitoring Experiment satellite image sequences, *Journal of Geophysical Research*, 106 (D6), 5493 – 5505.

Levine, J.S., Winstead , E.L., Parsons, D.A.B., Scholes, M.C., Scholes, R.J., Cofer III, W.R., Cahoon, D.R. and Sebacher, D.I., 1996: Biogenic soil emissions of nitric oxide (NO) and nitrous oxide (N_2O) from savannas in South Africa: The impact of wetting and burning, *Journal of Geophysical Research*, 101 (D19), 23 689 – 23 697.

Long, R.W. and McClenny, W.A., 2006: Laboratory and Field Evaluation of Instrumentation for the Semicontinuous Determination of Particulate Nitrate (and Other Water-Soluble Particulate Components), *Journal of Air and Waste Management Association*, 56, 294 – 305.

Lowman, G. R. P., 2003: *Deposition of Nitrogen to Grassland Versus Forested Areas in the Vicinity of Sabie, Mpumalanga*, South Africa, MSc dissertation, University of the Witwatersrand, Johannesburg, South Africa.

Marner, B.B. and Harrison, R.M., 2004: A spatially refined monitoring based study of atmospheric nitrogen deposition, *Atmospheric Environment*, 38, 5045 – 5056, doi:10.1016/j.atmosenv.2004.06.016.

Matsumoto, K. and Tanaka, H., 1996: Formation and dissociation of atmospheric particulate nitrate and chloride: An approach based on phase equilibrium, *Atmospheric Environment*, 30 (4), 639 – 648.

Mauzerall, D.L., Sultan, B., Kim, N. and Bradford, D.F., 2005: NO_x emissions from large point sources: variability in ozone production, resulting health damages and economic costs, *Atmospheric Environment*, 39, 2851 – 2866.

Meyers, T.P., Hicks, B.B., Hosker, R.P., Womack, J.D. and Satterfield, L.C., 1991: Dry deposition inferential measurement techniques—II. Seasonal and annual deposition rates of sulfur and nitrate, *Atmospheric Environment*, 25A (10), 2361 – 2370.

Mphepya, J.N., 2002: *Atmospheric Deposition Characteristics of Sulphur and Nitrogen Compounds in South Africa*, PhD Thesis, Potchefstroomse Universiteit vir Christelike Hoer Onderwys, Potchefstroom, South Africa.

Mphepya, J.N., Pienaar, J.J., Galy-Lacaux, C., Held, G. and Turner, C.R., 2004: Precipitation chemistry in semi-arid areas of southern Africa: a case study of a rural and industrial site, *Journal of Atmospheric Chemistry*, 47, 1–24.

Munger, J.W., Fan, S.M., Bakwin, P.S., Goulden, M.L., Goltstein, A.H., Colman, A.S. and Wofsy, S.C., 1998: Regional budgets for nitrogen oxides from continental sources: variations of rates for oxidation and deposition with season and distance from source regions, *Journal of Geophysical Research*, 103, 8355 – 8368.

Murphy, D.M., Fahey, D.W., Proffitt, M.H., Liu, S.C., Chan, K.R., Eubank, C.S., Kawa, S.R. and Kelly, K.K., 1993: Reactive Nitrogen and Its Correlation With Ozone in the Lower Stratosphere and Upper Troposphere, *Journal of Geophysical Research*, 98 (D5), 8751 – 8773.

Olivier, J.G.J., Bouwman, A.F., Van der Hoek, K.W. and Berdowski, J.J.M., 1998: Global air emission inventories for anthropogenic sources of NO_x, NH_3 and N_2O in 1990, *Environmental Pollution*, 102 (S1), 135 – 148.

Nilsson, S. and Grennfelt, P., 1988: *Critical Loads for Sulphur and Nitrogen.* Report from a workshop held at Skokloster, Sweden, 19-24 March 1988. NORD miljorapport, 15, Nordic Council of Ministers, Copenhagen, 225 – 268.

Orel, A.E. and Seinfeld, J.H., 1977: Nitrate Formation in Atmospheric Aerosols, *Environmental Science and Technology*, 11 (10), 1000 – 1007.

Peiró-Garcia, J. and Nebot-Gil, I., 2003: *Ab Initio* Study of the Mechanism of the Atmospheric Reaction: $NO_2 + O_3 \rightarrow NO_3 + O_2$, *Journal of Computational Chemistry*, 24, 1657 – 1663.

Reason, C.J.C., Engelbrecht, F., Landman, W.A., Lutjeharms, J.R.E., Piketh, S., Rautenbach, C.J. and Hewitson, B.C., 2006: A review of South African research in atmospheric science and physical oceanography during 2000 – 2005, *South African Journal of Science*, 102, 35 – 45.

Rupprecht and Patashnick Co., Inc., 2003: *Operating Manual: Series 8400N Ambient Particulate Nitrate Monitor*, Albany, New York, USA, 1-1 – 1-5.

Russell, K.M., Galloway, J.N., Macko, S.A., Moody, J.L. and Scudlark, J.R., 1998: Sources of nitrogen to Chesapeake Bay region, *Atmospheric Environment*, 32 (14), 2453 – 2465.

Ryerson, T.B., Buhr, M.P., Frost, G.J., Glodan, P.D., Holloway, J.S., Hübler, G., Jobson, B.T., Kuster, W.C., McKeen, S.A., Parrish, D.D., Roberts, J.M., Sueper, D.T., Trainer, M., Williams, J. and Fehsenfeld, F.C., 1998: Emissions lifetimes and ozone formation in power plant plumes, *Journal of Geophysical Research*, 103 (D17), 22 569 – 22 583.

Ryerson, T.B., Trainer, M., Holloway, J.S., Parrish, D.D., Huey, L.G., Sueper, D.T., Frost, G.J., Donnelly, S.G., Schauffler, S., Atlas, E.L., Kuster, W.C., Goldan, P.D., Hubler, G., Meagher, J.F. and Fehsenfeld, 2001: Observations of Ozone Formation in Power Plant Plumes and Implications for Ozone Control Strategies, *Science*, 292, 719 – 722.

Savage, N.H., Law, K.S., Pyle, J.A., Richter, A., Nüß, H. and Burrows, J.P., 2004: Using GOME NO_2 satellite data to examine regional differences in TOMCAT model performance, *Atmospheric Chemistry and Physics*, 4, 1895 – 1912.

Scheifinger, H. and Held, G., 1997: Aerosol Behaviour on the South African Highveld, *Atmospheric Environment*, 31 (21), 3497 – 3509.

Schmidt, M., Thoni, L., Waldner, P. and Thimonier, A., 2005: Total deposition of nitrogen on Swiss long-term forest ecosystem research (LWF) plots: comparison of the throughfall and the inferential method, *Atmospheric Environment*, 39, 1079 – 1091.

Schultz, M.G., Jacob, J.D., Mang, Y., Logan, J.A., Atlas, E.L., Blake, D.R., Blake, N.J., Bradshaw, J.D., Browell, E.V., Fenn, M.A., Flocke, F., Gregory, G.L., Heikes, B.G., Sachse, G.W., Sandholm, S.T., Shetter, R.E., Singh, H.B. and Talbot, R.W., 1999: On the origin of tropospheric ozone over the tropical South Pacific, *Journal of Geophysical Research*, 104 (D5), 5829 – 5843.

Seinfeld, J.H. and Pandis, S.N., 1998: *Atmospheric Chemistry and Physics: From Air Pollution to Climate Change*, Wiley, New York, 67, 74 – 75, 97 – 105, 175 – 176, 282 – 284, 355, 440 – 443, 958 – 959, 997 – 1000, 1030 – 1031, 1045, 1057 – 1065.

Stein, A.F. and Lamb, D., 2003: Empirical evidence for the low- and high-NO_x photochemical regimes of sulfate and nitrate formation, *Atmospheric Environment*, 37, 3615 – 1625.

Stevens, C. J., Dise, N. B., Mountford, J.O. and Cowing, D.J., 2004: Impact of Nitrogen Deposition on the Species Richness of Grasslands, *Science*, 303, 5665, 1876 – 1879.

Stolzenburg, M.R. and Herring, S.V., 2000: Method for the Automated Measurement of Fine Particle Nitrate in the Atmosphere, *Environmental Science and Technology*, 34 (5), 907 – 914.

Terblanche, A.P.S., Danford, I.K. and Nel, C.M.E., 1993: Household energy use in South Africa, air pollution and human health, *Journal of Energy in South Africa*, 54 – 57.

Thermo Environmental Instruments, 2000: Instruction manual: *Model 17C Chemiluminescence NH_3 Analyser*, Franklin, Massachusetts, 1-1 – 1-3.

Tie, X., Emmons, L., Horowitz, L., Brasseur, G., Ridley, B., Atlas, E., Stround, C., Hess, P., Klonecki, A., Madronich, S., Talbot, R. and Dibb, J., 2003: Effect of sulfate aerosol on tropospheric NO_x and ozone budgets: Model simulations and TOPSE evidence, *Journal of Geophysical Research*, 108 (D4), 8364, doi:10.1029/2001JD001508.

Toenges-Schuller, N., Stein, O., Rohrer, F., Wahner, A., Richter, A., Burrows, J.P., Beirle, S., Wagner, T., Platt, U. and Elvidge, C.D., 2006: Global distribution pattern of anthropogenic nitrogen oxide emissions: Correlation analysis of satellite measurements and model calculations, *Journal of Geophysical Research*, 111 (D05312), doi:10.1029/2005JD006068.

Tyson, P.D., Preston-Whtye, R.A. and Diab, R.D., 1976: Towards an Inversion Climatology of southern Africa: Part I, Surface Inversions, *South African Geographical Journal*, 58 (2), 151 – 164.

Tyson, P.D., Garstang, M., Swap, R., Kållberg, P. and Edwards, M., 1996a: An Air Transport Climatology for Subtropical southern Africa, *International Journal of Climatology*, 16, 265 – 291.

Tyson, P.D., Garstang, M. and Swap, R., 1996b: Large-Scale Recirculation of Air over Southern Africa, *Journal of Applied Meteorology*, 35, 2218 – 2235.

Tyson, P.D., Gasse, F., Bergonzini, L. and D'Abreton, P., 1997: Aerosols, Atmospheric Transmissivity and Hydrological Modelling of Climatic Change over Africa South of the Equator, *International Journal of Climatology*, 17 (13-15), 1651 – 1665.

Tyson, P.D. and Preston-Whyte, R.A., 2000: *The Weather and Climate of Southern Africa*, Oxford University Press, Southern Africa, 285 – 304.

Van Tienhoven, A.M., Olbrich, K.A., Skoroszewskp, R., Taljaard, J. and Zunckel, M., 1995: Application of the Critical Loads Approach in South Africa, *Water, Soil and Air Pollution*, 85, 2577 – 2582.

Warneck, P., 1988: *Chemistry of the Natural Atmosphere*, International Geophysics Series, 41, 340 – 341, 454 – 483,

Watt, S.A., Wagner-Riddle, C., Edwards, G. and Vet, R.J., 2004: Evaluating a flux-gradient approach for flux and deposition velocity of nitrogen dioxide over short-grass surfaces, *Atmospheric Environment*, 38, 2619 – 2626.

Wayne, R.P., Barnes, I., Biggs, P., Burrows, G.P., Canosa-Mas, C.E., Hjorth, J., Le Bras, G., Moortgat, G.K., Perner, D., Poulet, G., Restelli, G. and Sidebottom, H., 1991: The Nitrate Radical: Chemistry, Physics and the Atmosphere, *Atmospheric Environment*, 25A (1), 1 – 203.

Webb, A.H. and Hunter, G.C., 1998: Power-station contributions to local concentrations of NO_2 at ground level, *Environmental Pollution*, 102 (S1), 283 – 288.

Weiss, S.B., 1999: Cars, Cows, and Checkerspot Butterflies: Nitrogen Deposition and Management of Nutrient- Poor Grasslands for a Threatened Species, *Conservation Biology*, 13, 6, 1476 – 1486.

Wenig, M., Spichtinger, N., Stohl, A., Held, G., Beirle, S., Wagner, T., J¨ahne, B., and Platt, U., 2003: Intercontinental transport of nitrogen oxide pollution plumes, *Atmospheric Chemistry and Physics,* 3, 387 – 393.

Wesely, M.L., Eastman, J.A., Stedman, D.H. and Yalvac, E.D., 1982: An eddy correlation measurement of NO_2 flux to vegetation and comparison to O_3 flux, *Atmospheric Environment*, 16 (4), 815 – 820.

Wesley, M.L. and Hicks, B.B., 2000: A review on the current status of knowledge on dry deposition, *Atmospheric Environment*, 34, 2261 – 2282.

White, W.H., 1977: $NO_x – O_3$ Photochemistry in Power Plant Plumes: Comparison of Theory with Observation, *Environmental Science and Technology*, 11 (10), 995 – 1000.

Widory, D., 2007: Nitrogen isotopes: Tracers of origin and processes affecting PM10 in the atmosphere of Paris, *Atmospheric Environment*, doi:10.1016/j.atmosenv.2006.11.009, in press.

Yang, H., Hsieh, L. and Cheng, S., 2005: Determination of atmospheric nitrate particulate size distribution and dry deposition velocity for three distinct areas, *Chemosphere*, 60, 1447 – 1453, doi:10.1016/j.chemosphere.2005.01.067.

Yeatman, S.G., Spokes, L.J. and Jickells, T.D., 2001: Comparisons of coarse-mode aerosol nitrate and ammonium at two polluted coastal sites, *Atmospheric Environment*, 35, 1321 – 1335.

Zapletal, M., 1998: Atmospheric deposition of nitrogen compounds in the Czech Republic, *Environmental Pollution*, 102 (S1), 305 – 311.

Zunckel, M., Turner, C.R. and Wells, R.B., 1996: Dry Deposition of sulphur on the Mpumalanga Highveld: a pilot study using the inferential method, *South African Journal of Science*, 92, 485 – 491.

Zunckel, M., Venjonoka, K., Pienaar, J.J., Brunke, E-G., Pretorius, O., Koosialee, A., Raghunandan, A. and van Tienhoven, A.M., 2004: Surface ozone over southern Africa: synthesis of monitoring results during the Cross border Air Pollution Impact Assessment project, *Atmospheric Environment*, 38, 6139 – 6147.